Joining of Engineering Ceramics to Metals

Thesis by
Moustafa Mohamed Aboughadir

Submitted to the University of Hertfordshire in partial fulfilment of the requirement of the degree of Doctor of Philosophy (PhD)

Date
02/2023

DECLARATION STATEMENT

I certify that the work submitted is my own and that any material derived or quoted from the published or unpublished work of other persons has been duly acknowledged (ref. UPR AS/C/6.1, Appendix I, Section 2 – Section on cheating and plagiarism)

Student Full Name: Moustafa Mohamed Mohamed Moustafa Aboughadir

Student Registration Number: 14010514

Signed: ***Moustafa Aboughadir***
Date: 12/09/2023

ABSTRACT

In this research, successful joining of Al_2O_3 to Al_2O_3 was achieved through novel brazing methods involving the Ti-Al, Ti-Al-Ni, and Ti-Al-Fe systems. Subsequently, the Ti-Al-Ni-based braze was employed to join Al_2O_3 and Ti6Al4V alloy. Additionally, the study demonstrated the feasibility of using a commercially available Pd-40wt%Ni braze and a novel Ni-14wt%Zr braze for effectively joining Al_2O_3 to Ti6Al4V alloy. Furthermore, successful bonding of small components of Al_2O_3 and Ti6Al4V alloy was achieved using a commercial Ti-15wt%Ni-15wt%Cu braze. However, this method faced challenges when applied to larger samples with dimensions of 25 mm x 25 mm and a thickness of 4 mm. The project investigates brazing as method of joining, using a braze that can withstand high temperature application as well as, accommodate the difference in coefficient of thermal expansion (CTE) between the braze and the ceramic-metal. Aluminium Oxide (Al_2O_3) were used to bond with both Titanium (Ti) and Ti6Al4V alloy. Thus, it allows the understanding of both reactive and non-reactive systems of bonding. Moreover, a titanium aluminide (TiAl) braze was used in the latter case. TiAl braze seems to be amongst the best options with regards to high temperature restriction. The braze seems to have poor ductility at room temperature which means that it can have poor resistance to force and stress. Further investigations such as SEM and EDAX were used to identify the reactions. When nickel was used as a braze, LM, a strong bond was developed, leading to investigating Ni element further. Wettability results show that enough addition of Ni or Fe to TiAl braze can enhance the joint. SEM results shows that nickel dissolves into the substrate with no interfacial compounds noticed. This dissolution is causing damage to the interface of the ceramic. Fe shows identical results to Ni. Four braze systems were used to bond metal to ceramic (Al_2O_3 / Ti6Al4V), two of which are commercial – Pd-Ni (PALNI) and Ti-Cu-Ni (TICUNI) – whilst the other two were novel and developed by this project – Ti-Al28%-Ni3.6% and Ni-Zr14% (weight-percentage). Analysis from SEM and EDAX showed that Palni and NiZr were most efficient in terms of wetting, flowability, and strength. Three braze systems: Ti-Al28%-Ni3.6%, Pd-Ni40%, and Ni-Zr134% were heat-treated at 450°C for 500hrs post-brazing. While other braze systems had either formed brittle phases or broken at handling, Pd-40Ni and Ni-14Zr braze systems showed good bonding results. Metal-to-ceramic brazed with Palni or Ni-14Zr were tested for single lap shear test. Furthermore, initial brazing hardness was then compared to heat-treated hardness using nano-indentation. In addition to hardness, results for

toughness and young’s modulus were obtained. The comparison of before and after heat treatment, has showed that no further chemical reaction took place, suggesting a reliable joint for industrial use.

TABLE OF CONTENTS

LIST OF FIGURES

LIST OF TABLES

LIST OF EQUATIONS

GLOSSARY

CTE	Coefficient of thermal expansion
Lv	Liquid-Vapour
SEM	Scanned Electron Microsopy
Sv	Solid-Vapour
Sl	Solid-Liquid
SLO	Single lap offset
W_a	Work of Adhesion

1 Introduction

1.1 *Project Background*

Although metals are widely used in almost every aspect of the material industry, they have weak oxidation and corrosion resistance. Moreover, metals lose effectiveness and strength as temperatures increase, at about $0.6T_m$, limiting their high-temperature capabilities - some fail at <700 °C, making high-temperature application problematic [1]–[3]. Even though some metals like Niobium and Tantalum can maintain their strength at a higher temperature, they oxidize. High-temperature applications tend to exceed temperatures of about 1000°C meaning metals are not suited for such applications on their own. Ceramics, on the other hand, can retain their strength at temperatures as high as 2000°C and have proven oxidation resistance; nonetheless, ceramics are brittle. Therefore, introducing the possibility of joining metal to ceramic could solve these problems that occur at high temperatures. The application of such materials is extensively used in many different sectors, for example, in the defence and aerospace industry. The desired bonded materials like Aluminium Oxide, Silicon Carbide, and Silicon Nitride can be used in missiles where they need to be bonded to the metal body. Generally, this process needs to avoid oxidation. Potentially, in missiles, the bonded materials can be used in the head. Some applications tend to bond both materials using bolts; however, ceramics would fail quicker due to the presence of holes which can encourage crack initiation. The joined materials are also used in engine blades due to the high-temperature application. In supersonic aircraft, where carbon fibre is likely to be used, the bonding materials can coat the carbon fibre to prevent oxidation. There is also a need for this process in manufacturing cutting tools. It is proven that when a ceramic-metal combination is used, strength, fatigue resistance, creep and oxidation resistance can be improved.

The challenge is to accomplish a very stable metal-to-ceramic joint. Ceramics have interesting characteristics; however, they cause an obstacle in the joint fabrication [4]. Ceramics are known to have chemical inertness. Therefore, not all metal joining methods can be used. There are different techniques of bonding metal to ceramic, like diffusion bonding, mechanical fastening

as aforementioned, soldering, and brazing. Nevertheless, brazing is the most widely used method due to its simplicity and low cost [5]. Brazing is a process where two materials are joined together with a molten filler metal.

High temperature is often needed to achieve a desirable and a higher quality bond. Reactive metals have been used as a bonding medium [6]. The properties and the structure of the interface are determined by the chemical events that appear at the interface. Usually, bond formation begins once there is a chemical reaction between the ceramic and the metal [7]. However, when brittle reaction layers form at the interface, this might result in premature failure caused by impact or very low stresses [7].

The mechanical strength of the joined material is not assured even after joint formation. Ceramics and metals each have their own properties, and the difference in these properties complicates the process of joining the materials without a significant change in the strength and flexibility. The coefficient of thermal expansion (CTE) mismatch is found to be one of the major elements that influence the reliability of the joint as well as the different structure of the interface bond. During the process of cooling down, the CTE mismatch and the altered mechanical responses of ceramics and metals produce thermal residual stresses. It was found in [7], [8] that this can cause a weak joint strength.

Ceramic substrate used in this project is Al_2O_3, since it is widely used in the ceramic systems. The metal systems selected are Titanium and Ti6Al4V alloy. Titanium is used in the aerospace industry and is a light metal. For the new set of experiments, the investigations will start by joining Alumina to Alumina using a TiAl based braze. In this project, the filler metal used is based on the Ti-Al, NiAl, Al-Ni-Ti, and Al-Fe-Ti systems. The composition that was investigated is in the form of (Ti, X)Al, X= Ni or Fe.

After two sets of experiments, a new behaviour was observed; Nickel-rich areas found near to the interface with alumina. From that point, it was decided to examine four different braze systems (Ti-3.6Ni-28Al, Ti-15Ni-15Cu, Pd-40Ni, Ni-14Zr) at various temperatures. Two of these

were developed in this project: Ti-Ni-Al and Ni-Zr. The other two are commercial: Ti-Cu-Ni and Pd-Ni.

Some brittle phases appear to have an influence when joining via Ti-15Cu-15Ni [9]. These brittle phases appeared to have formed between the Ti6Al4V and alumina substrate. Previously, when Ti-Ni-Al was used to bond alumina to alumina it looked as though it was weakening the alumina substrate, giving really good results for wettability compared to just Ti-Al. When this system was utilized to join Ti6Al4V to alumina, it either broke at handling or did not form any bond at all. Knowing that, Ti-Ni-Al, wets the alumina really well, when fracture analysis was done it seems to have weak flowability. It remains unknown whether this problem has occurred in the past, since there not much information mentioned the literature.

On the other side, as well as brittle phases that were observed forming, $CuTi_2$ and $NiTi_2$ with Cu dissolved in Ni, and there has been information that, Ti-15% Cu-15% Ni system, lacks flowability. It was also observed that the latter system seems to also wet alumina well, lacking flowability.

The other two systems have formed a really sound bond in terms of wetting and mechanical strength. In the case of the Ni-Zr14%, aluminium from the Ti6Al4V substrate seem to form alpha + beta + $NiTi_2$. However, as mentioned earlier not enough information has been documented on this system. Even though the Pd-Ni, had high CTE compared to both substrates. The joint was considerably sound. In both systems, the interaction from the braze and alumina allowed the braze to cover the alumina. Pd-Ni joined samples were lower in strength compared to Ni-Zr. On both occasions, the substrate broke rather than the braze, suggesting a really strong bond or thermal stresses from the difference in the CTE, make the alumina break before the braze.

All systems used in the third set of experiments were heat treated at 450°C for 500 hours. To understand the dissolving behaviour at extreme conditions. The samples don't seem to have changed much after 500 hrs of treatment at 450°C from the original brazing treatment.

Suggesting that there will be no interactions occurring at a more realistic time scale. Which can give an indication of strong joint, if bonding takes place. The temperature was set low, since above 600°C corrosion might start occurring at the titanium substrate. However, it looks as though the nickel is dissolving in the substrate. This suggests that perhaps nickel requires more time to diffuse, which is the case when samples were left for extended time, in this case 500 hrs.

Most of these brazes have not been reviewed in matter of joining metal-to-ceramic. Some were not reviewed at all. Usually, high temperature brazed joints suffer from defects or are very weak to consider industrial use, due to the coefficient of thermal expansion mismatch. Parameters such as brazing temperature, were determined via phase diagrams relevant to each system.

During the course of this project, only metallic foils were used as a braze. On one occasion, LM powder was used. For further investigations, different techniques were used to determine vital factors. In the case of characterisation: optical microscopy, contact angle, SEM and EDAX were used. To determine the mechanical strength of joints: single lap shear test and nano-indentation (hardness, reduced modulus, young's modulus, etc.) were carried out.

1.2 *Aims and Objectives*

The project aims to develop new techniques for bonding metals to ceramics. Furthermore, this project will be looking at concepts to understand reactive and the non-reactive systems. The main focus will be to join titanium alloys to two ceramic systems, aluminium oxide and silicon carbide.

The objectives of the project are:

- Understand how characteristics like wetting and fluidity affect the quality of brazes with some consideration on the ductility of the braze.

- Undertake brazing to join titanium to aluminium oxide using Ti-Al foil with and without third element addition (nickel) as well as nickel-based brazes to understand the effect of Ni and Fe addition.
- Undertake brazing to join titanium to aluminium oxide using the commercial braze systems Ti-15Ni-15Cu, Pd-40Ni, and novel Ni-14Zr braze system to further understand the distinct behaviour of Ni in a brazing system.
- Conduct relevant tests to examine the bond integrity and strength and understand the effect of any interfacial reactions.

2 Literature Review: Joining Processes

2.1 *Brazing*

Brazing is a process where joining of two materials takes place by the use of a molten filler metal. The procedure is carried out at temperatures above the melting point of the molten filler metals but below the melting point of the base metal or even both materials to be joined. The reason behind setting the brazing temperature above the melting point of the filler metal is to ensure the molten filler metal to flow in the gap between the two substrates to form a sound metallurgical bond as it cools down.

Brazing, ideally, requires an interlayer that will melt and flow on top of the substrates. At that point, reaction and wetting occurs between the interlayer and the substrate producing a strong bond. To assure this, it demands that the interlayer withstands capillary attraction at high temperature. That way it will prevent the braze from flowing out.

Brazing is usually heavily considered when taking strength and durability as essential conditions. That is mainly because of the usage of the filler metal as well as heating the whole area at the same time. Generally, brazing is used when the joint is not temporary, and when joining for the purpose of high temperature application.

2.1.1 Active Metal Brazing

The origins of brazing were the use of brass as a joining element; however, recently various alloys have been researched to be used when joining metal-to-ceramic or ceramic-to-ceramic. Unlike welding, in brazing the substrates will not melt. Hence, brazing is more advantageous in the joining process. Conveniently, brazing can be used to join dissimilar materials over welding because of metallurgical inconsistencies [10].

Joints can be achieved by two possible methods:

(i). Direct brazing: this procedure is widely used, this process relies on active elements in the filler alloys, for example Titanium.

(ii). Indirect brazing: during this brazing process, the surface of the ceramic substrate is metallised.

2.1.2 Combustion Reaction

This method of joining relies solely on operating at a lower temperature, and for ceramics and intermetallic to form. Usually, the low operating temperature is set to be lower than the melting point and for short duration relying on exothermic reactions [11]. Miyamoto et al. [12] has used the combustion reaction procedure to join metal-to-ceramic. The procedure involves the use of a thin layer of reactive powders, to be placed between the metal and ceramic substrate while applying pressure at the same time. Heating leads to the ignition of exothermic reaction and to melting of the braze. The topic of joining Ti-Al_2O_3 and Al_2O_3-Al_2O_3 has not been widely discussed. Hence, the review addresses some of the identified systems together with some general information on brazing and braze behaviour.

2.1.3 Brazing Systems

2.1.3.1 The Ag-Cu Brazing System

Al_2O_3 is a well-known ceramic; bonding to Titanium has been widely researched as a mechanism for joining it to metal. It is mentioned in [13], [14] that the reason behind using aluminium oxide is the fact it has proven mechanical strength as well as low thermal and electrical conductivity. Yet, the application of the ceramic is limited without joining it to metal as aforementioned. Howlader et al. [15] and Kinsho et al. [16] suggested that bonding Al_2O_3 to Ti6Al4V is desirable in different areas that include the use of vacuum ducts, semiconductors, satellites, missiles, and rockets. The methods of bonding alumina to metals vary and involves techniques like diffusion welding and brazing. Diffusion welding is usually used for both similar and dissimilar materials. However, according to [17]–[20] brazing is the recommended technique of joining Al_2O_3 ceramic. Nonetheless, due to the complexity of the wetting ability in ceramics, brazing alumina becomes challenging. As a result, metallization at the surface of the alumina is needed to enhance the wetting of alumina. However, Barrena [21] has discussed

that metallising the surface demonstrated some problems and disadvantages. This contributed to the technique of direct brazing that proposes an active element as a filler metal. The filler metal was suggested to be either Ti or Zr. As discussed in [18], Ti is not easy to produce as a filler metal and leads to reduction in the fluidity.

Cao et al. [22] have presented the use of Ag-Cu eutectic filler metal in brazing Al_2O_3 to Ti6Al4V. They argued that using a Cu interlayer can improve the CTE mismatch. The braze was produced by sintering at a high temperature from powders that contained less than 0.1% impurities (0.009% CaO, 0.053% SiO_2, 0.007% MgO, and 0.0023% Fe_2O_3) Their project investigated the microstructure at the bonded interface, including the mechanical properties of the joint.

The brazing was carried out in a high vacuum heating apparatus keeping a vacuum pressure of 5 x 10^{-4} Pa. The heating rate was 20 °C/min up to 500 °C from room temperature, then 10 °C/min from 500 °C up to the brazing temperature. They varied the brazing temperature from 800 to 950 °C; dwelling was also between 5 to 60 minutes. After dwelling the assembly was cooled down at 5 °C/min from brazing temperature to room temperature. To assure there is adequate contact at the brazing process, they used a 500g of stainless-steel weight, but the area of the specimen they used in the brazing process was not given. Following brazing, SEM and EDS were used to characterise the microstructure of the brazed samples. Also, an Instron 1186 machine was used for shear strength tests. The tests were carried out at a constant speed of 0.5mm/min.

It was observed that brazing for 10 min at 825 °C, phases such as α-β Ti, Ti_2Cu, TiCu, Ti_3Cu_4 appeared at the interface with the alloy. In addition, the Ti_4(Cu, Al)O phase was shown at the braze/Al_2O_3 interface. Increasing the temperature of brazing increased the thickness of the Ti-Cu interfacial layers. Which is presumably due to increasing reaction between the braze and titanium.

Figure 1 shows the formation of layered structures (A, B, C, and D) because of the interdiffusion between Ti and Cu at the Ti_6Al_4V/braze interface [22]. Layer 1 contained needle-like β-Ti holding Cu. Moreover, there was distribution between the dark α-Ti and β-Ti. Table 1 [22] shows the composition of the different layers shown in figure 1.

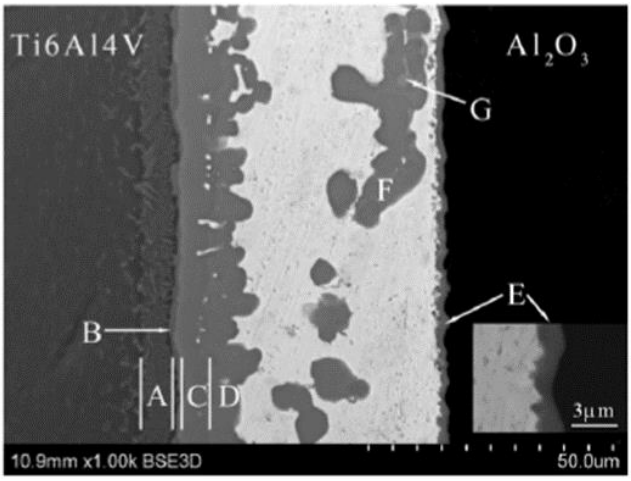

Figure 1 Microstructure of Al_2O_3/AgCu/Ti_6Al_4V joint brazed at 825 °C for 60 min [22]**.**

Table 1 Composition analysis of the different elements of the joint [22]

Region	Composition (at.%)					Phase
	Ti	Cu	Al	Ag	O	
A	87.5	8.1	4.4	–	–	α–β Ti
B	66.5	30.9	2.6	–	–	Ti_2Cu
C	46.1	49.8	3.2	0.9	–	TiCu
D	42.7	52.6	2.3	2.4	–	Ti_3Cu_4
E	55.2	17.8	11.3	0.9	14.8	$Ti_4(Cu,Al)_2O$
F	43.8	51.7	1.8	2.7	–	Ti_3Cu_4
G	39.3	56.5	1.3	2.9	–	Ti_2Cu_3

To compare the shear strength, Cao et al. [22] have plotted the different brazing parameters as seen in figure 2 (a) and (b).

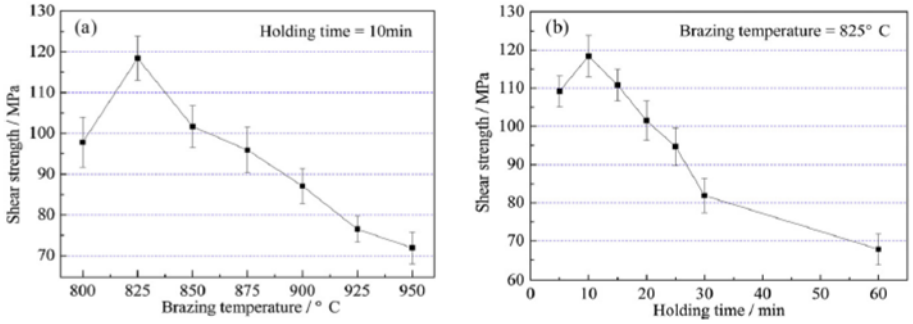

Figure 2 Effect of brazing parameters on the shear strength of Al_2O_3/Ti_6Al_4V joint. (a) brazing temperature (b) holding time [22]**.**

As shown in figure 2, at a temperature of 825 °C and a holding time of 10min gave the highest shear strength, which consisted of α-β Ti, Ti_2Cu, TiCu, Ti_3Cu_4 phases while joints bonded at 950°C has Ti-Cu intermetallic domination and increase in interfacial layers. They also found that when they inserted a Cu foil between Ag-Cu foils the shear strength increased, in addition to an impressive change in the microstructure. Hence, it can be said that using Ag-Cu foils as well as similar parameters can result in a reliable metal/ceramic joint. Nonetheless, due to the purpose of high temperature applications, Ag-Cu foils are not the favoured interlayers.

2.1.3.2 The Ti-Al Brazing System

As a result of interest in high-temperature applications, Martin et al. [23] refuted the use of Ag-Cu base and proposed that a braze based on the Ti-Al system is preferable for the high temperature applications. Their investigation focused on joining alumina to alumina and also considered joining SiC and Si_3N_4. The Ti-Al system forms intermetallic compounds which have been advanced for high-temperature construction use. Therefore, the Ti-Al system becomes favourable when choosing a braze for high-temperature applications due to its proven ductility, oxidation resistance, and mechanical strength as demonstrated in [23]. Martin et al. [23] have tried to find the perfect brazing temperature, where they used parameters of 1200 and up to 1500 °C. During brazing, they varied the weight composition of Ti-Al to achieve different Ti-Al phases. They reported that the Ti-Al intermetallics start to form just below 1000 °C. However, the temperature range reaction is dependent on the ceramic reaction. No interaction was

observed between alumina and the braze, but it was noticed that there was an interaction between the braze and both Silicon Carbide and Silicon nitride. Due to the high chemical stability of Al_2O_3, the formed Ti-Al phases were like in the Ti-Al phase diagram.

On the other hand, Ti_3SiC_2 MAX-phase and metallic Aluminium were discovered in the DTA-sample of SiC as well as phases like $TiSi_2$, TiN, AlN, and Al_3Ti for Si_3Ni_4. DTA samples were produced differently, using ceramic powder. The XRD characterisation in Figure 3, shows that Ti-Al intermetallics might have formed without interaction with Al_2O_3. Phase combinations of TiAl + Ti_2Al and TiAl+Ti_3Al were reported. This can be due to the quick heating up and/or short time at the maximum temperature, which can cause kinetic imbalance. For SiC, the XRD shows the formation of the MAX-phase, Ti_3SiC_2. This MAX phase has desirable characteristics such as stable mechanical and high-temperature behaviour. XRD illustrates the formation of nitrides in Si_3N_4, probably from Ti and Al. Titanium Silicide, $TiSi_2$, is also formed showing that from the Al40-Ti60 original composition there is Titanium aluminide left. Finally, it was observed that the decomposition of the Silicon Nitride led to the formation of elemental Silicon. Although it is unlikely for Si_3N_4 to decompose at such temperature, the authors do not comment on this. Chemical reactions can result in an interlayer on the ceramic surface that might improve the wettability of TiAl. Martin et al. [23] were also interested to know if during the formation of Titanium aluminide, a liquid phase, or solid-state interaction would provide the best joining characteristics. They operated a low-temperature experiment, at 1300 °C, in which they found that the formation of TiAl intermetallides did not bond with the ceramic. However, reliable bonding was observed at 1400 °C for both SiC and Si_3Ni_4, and bonding was achieved at 1450 °C for Al_2O_3 samples.

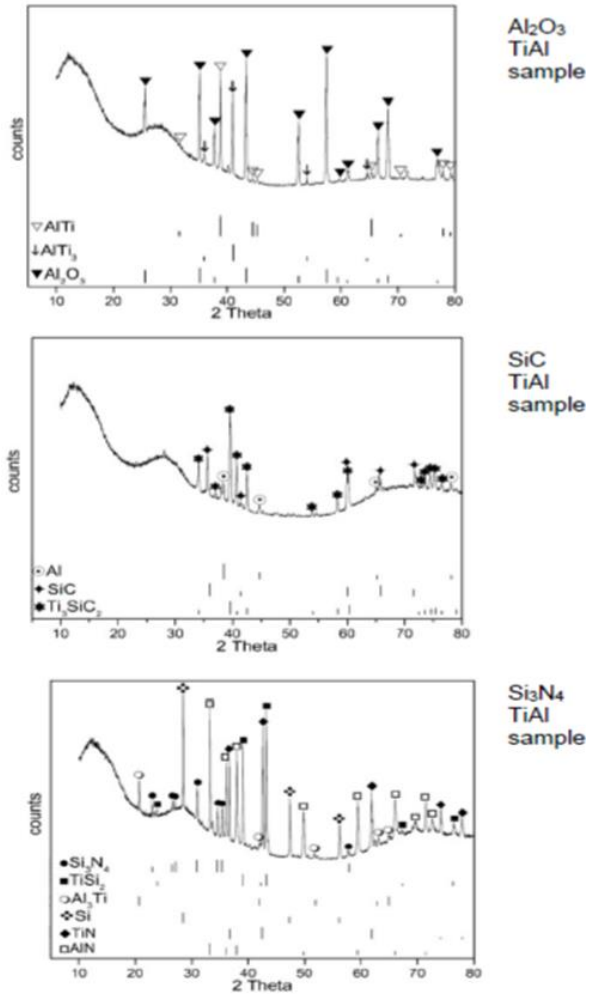

Figure 3 XRD patterns of the Al40-Ti60 samples after DTA up to 1500°C together with different ceramic powders, final phase formation is clearly shown [23]

2.1.3.3 The Nickel-based Brazing Systems

Lourdin et al. [24] have investigated the mechanical properties of a solid-state bonded nickel-alumina interface. The investigation was carried through different bonding parameters such as time, temperature, pressure and the purity of alumina. In their report, they used two different types of polycrystalline alumina, A99 standard and high purity, used as sintered. To prohibit the growth of alumina grains on sintering they added MgO in both types of alumina. The nickel braze had the following composition: Cu<0.01, Si=0.14, C=0.051, Mn=0.08, Fe=0.98, Co<0.01, and Ni balance. Some researchers [25], [26] found the Ni-Al_2O_3 to have strong mechanical properties, while others found it weak [27], [28]. In both scenarios, the investigation showed that the existence of a nickel aluminate spinel determined the mechanical properties achieved.

In [24] they used an assembly of Al_2O_3-Ni-Al_2O_3, where they used dynamic vacuum while the temperature varied between 1050 and 1410°C, as well as an applied pressure between 2 to 21 MPa. The heating and the cooling rate was 150°C/hr from the room temperature to the bonding temperature and 200°C/hr to room temperature respectively.

It was concluded that the use of pressure led to the highest possible contact area between both materials. This would attain a strong Ni-Al_2O_3 bond through a solid-state bonding technique. There was no direct chemical reaction between nickel and alumina, however, on the Alumina side, Magnesium Silicate and Magnesium spinel were observed, while on the Nickel side, Nickel Silicide was formed. These foundings are assumptions were drawn through two investigations: the diffraction patterns and data from ASTM with patterns of sodium magneisum silicate lattice parameters. Hence, assuming that $MgAl_2O_3$ is the compound present. They showed that both the nature and the amount of the interfacial phases are related to the mechanical properties of the bond. It was reported that both Magnesium spinel and Nickel Silicide had led to adhesive failures while Magnesium Silicate led to cohesive failure. After time was increased to 1 hour, Nickel silicide and Magnesium silicate formations were found.

Another similar investigation, by Hattali et al. [29] was concerned about the residual stress of the bonded Ni-Al_2O_3. Furthermore, they attempted to join alumina-alumina and alumina-nickel alloy using solid-state bonding under hot pressing. They used nickel metallic foil sheets and used similar heating and cooling rates to Lourdin [24]. However, the bonding temperature was 1150 °C. After comparing the results of FEM calculations with traditional XRD and Vickers Indentation Fracture experiments; it was observed that the highest tensile stress concentration occurred at the edge of the boundary. Moreover, the CTE mismatch between Al_2O_3 and Ni-base alloy has weakened the joints in comparison with the Al_2O_3-Al_2O_3 samples which exhibited the same bonding parameters.

Another favoured ceramic is Silicon Carbide due to its ability to be used up to temperatures of 1400-1600°C. Applications of SiC not only include electronics but they also involve in mechanical equipment that is used in the chemical industry [30].

Owing to its strong reactivity with a variety of metals leading to brittle silicides, it becomes problematic to bond SiC to metals. Thus, Hattali et al. [31] have studied the formation metal-ceramic joints using the solid-state bonding method. They attempted to bond Silicon Carbide to Ni-based superalloy using metallic foils of Ni and Ag. When nickel reacts with Silicon, they result in silicides. Therefore, Hattali et al. [31] have claimed that a coating of $Ni_{0.93}B_{0.07}$ can be used due to the proven improvement of the mechanical properties of silicides from the usage of Boron. It is also mentioned in their work that silver can be used as a diffusion barrier when coated. Nevertheless, they did not indicate the melting temperature of the $Ni_{0.93}B_{0.07}$ coating. Accordingly, Hattali et al. [31] used three different techniques in their investigation, as presented below in Table 2.

Table 2 Experimental conditions for the joining of Silicon Carbide with different metallic foils (Ni, Ag) and coatings ($Ni_{0.93}$, $B_{0.07}$ and Ag) [31]

	Temperature (°C)	Pressure (MPa)	Time (h)	e_{foil} (µm)	$e_{coating}$ (µm)	Vacuum (Pa)
SiC/Ni0.93B0.07/Ni-HAYNES® 214™	1100	16	1	200	2	10^{-3}
SiC/Ag/HAYNES® 214™	910	6	1	200	0	10^{-3}
SiC/Ag/HAYNES® 214™	910	6	1	-	2	10^{-3}

Using Ni0.93 B0.07 coating was not enough to prevent silicide formation at high residual stress. However, the silver coating prevented SiC reaction with Ni. Nonetheless, Ni can diffuse through the Ag coating if the coating thickness is sufficiently high. A reliable thickness of <50 µm is assumed to be sufficient to restrain a catastrophic reaction at 900 °C [31]. They explained that a foil thickness of approximately 200 µm improved the mechanical shear resistance which allows industrial use for over 10,000 hours at 700 °C.

The investigation reportedly solved the problem of the strong reaction between SiC and metals. Furthermore, it has also improved the wettability of the SiC surface. Nonetheless, it does not provide a favourable high-temperature application, where the use of the bonded materials might be restricted between 600 and 900 °C.

2.1.3.4 The Ti-Si Brazing System

Li et al. [32] have used Ti-Si braze to accommodate for the CTE mismatch between titanium and silicon, high-temperature application, good wettability and good adhesion. They prepared 22Ti-78Si (wt%) eutectic braze using arc-melting technique [32]. It is apparent from Fig. 4 that the braze and SiC had bonded well. Neither porosity nor microvoids were found at the interface. Usually such an interface contains some structural defects, but this was not apparent in the work by Li et al. [32]. Also, it was not clear if any interface or interlayer had been formed between the braze and SiC.

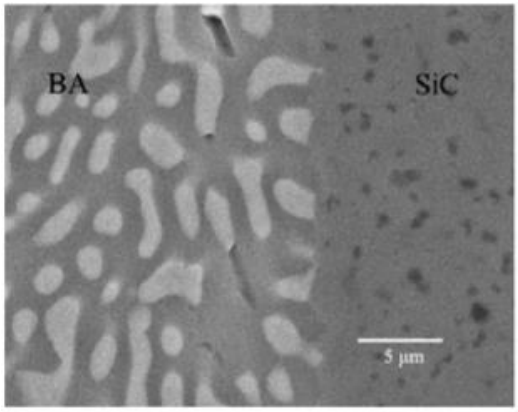

Figure 4 Backscattered electron image of the Braze/SiC interface (BA: Brazing Alloy) [32]

The experiment was conducted in vacuum ($6x10^{-3}$) at a temperature of 1400 °C (for 10 minutes) at a heating rate of 10 °C/min. The SiC on the braze side showed a good contact angle of 25°. The other results from the wettability experiment are presented in Table 3.

Table 3 Wettability experiment for the braze/SiC [32]

T_S(°C)	T_L(°C)	Contact angle (degree)	CTE×10^{-6}/°C (RT~1000°C)	Bending strength (Mpa)	Remarks
1342	1371	25	6.5	218	Good adhesion was obtained, and no fracture occurred at the interface

From the XRD analysis [32], both TiC and Ti_5Si_3 were formed at the interface of the braze/SiC. This formation was caused by reaction between Ti and SiC, since TiC is formed at the interface of the braze/SiC it has encouraged the wetting and the bonding of the braze.

Thus, 22Ti-78Si(wt%) can be described as a favourable braze for the purpose of joining SiC, due to the appropriate CTE between SiC and the braze. As aforementioned, a suitable CTE, that accommodates for both materials to be bonded, will decrease the thermal stress between the braze and the material.

2.1.3.5 The Ni-Zr Brazing System

Nickel Zirconium is used commercially to improve ductility and creep strength of superalloys, nickel-based. In addition, this system is used to aid with producing nickel and cobalt-based superalloys, where zirconium is the additive. In an investigation carried out by Okamoto et al. [33] 41.2% and 43% at. Zr samples were annealed and cooled down at furnace. Annealing temperatures were at 700, 800, and 1000°C. This was to examine the homogeneity of $Ni_{10}Zr_7$, by X-ray diffraction and metallographic studies [34]. Which indicated that the homogeneity was very narrow, and it was unlikely that a two-phase field would get wider.

Another X-ray diffraction and metallographic studies were carried out by Kosorukova et al. [35], for a reinvestigation of the phase equilibria of the Ni-Zr system. As well as their good mechanical properties, this system is interesting because of the high thermo-chemical stability within Ni-Zr. Depending on the condition, they can be used as a base for superalloys [35].

Tao et al. [36] carried out an investigation on the mechanical properties and the interdiffusion behaviour of the Ni-Zr intermetallic compounds. Specifically, compounds that are formed at the interdiffusion interface zone of Ni-Zr within a temperature range of 865° - 955°C were investigated. The intermetallic compounds observed at the diffusion zones of Ni-Zr where eight: Ni5Zr, Ni_7Zr_2, Ni_3Zr, $Ni_{21}Zr_8$, $Ni_{10}Zr_7$, $Ni_{11}Zr_9$, NiZr, and $NiZr_2$ [36]. It was found that when the

concentration of Zr, increases the Young's modulus decreases, mentioning that a highest value of 250.21 GPa was registered for Ni_5Zr, while $NiZr_2$ had the lowest value of 76.82 GPa. Furthermore, the highest hardness value registered at this investigation was 10.17 GPa for $Ni_{10}Zr_7$ and the lowest was 5.56 GPa for $NiZr_2$, with no correlation to the concentration of Zr [36].

Lei et al. [37] used laminated foils of Ni/Zr/Ni to successfully bond cast Al0.3CoCrFeNi to itself. The joining was achieved through transient liquid phase bonding. The following was concluded from their research [37]:

i. At bonding temperatures higher than 1140°C, a composite microstructure was formed at the joint interface. This microstructure contains an FCC (face centre cubic structure) phase ingrained into the brittle matrix of Ni_7Zr_2.
ii. Indications of a semi-coherent phase with low strain energy was generated at the interface. This is thought to be due a lattice mismatch between the Ni_7Zr_2 matrix and the FCC phase.
iii. At 1140°C, a eutectic reaction between the interdendritic Al0.3CoCrFeNi and Zr has caused the grain boundaries and interdendritic are of the Al0.3CoCrFeNi substrate to go into liquid state. Hence, increasing the dissolution of the Al0.3CoCrFeNi substrate at the joint centre line.
iv. Bonding at 1160°C for 30 min, has shown a maximum shear strength of 247 MPa. The joint had a balanced soft FCC and brittle Ni_7Zr_2. Furthermore, a fracture was seen at that joint.

2.1.3.6 The Ti-Cr-V Brazing System

Canonico et al. [38] have investigated the use of Ti - 25%Cr - 21%V alloy to bond alumina, where the alloy has been proven to wet and flow at surface of the alumina. However, this composition has not been reviewed on metal-to-ceramic joining. This alloy was chosen since titanium and zirconium are reactive elements. These elements are expected to react with oxide ceramics, due to the free energy formed for oxides and carbides. Canoinco et al. [38] has

carried out flowability tests, the results where that Ti - 25%Cr - 21%V has flowed almost 63.5mm on nonmetallics. Their investigation showed that the pores were filled by the alloy. This can indicate that the joints produced by this alloy are strong, due to the interlocking mechanism [38]. When a lower Cr composition was tested, it showed that the alloy was not flowing. However, they were more ductile and could be rolled into sheets [38]. Other alloys were also experimented and convincingly used, like Ti-Zr-Ge, Ti-Zr-Ta, and Ti-Zr-Nb. Joining dissimilar materials has also been investigated, such as tantalum/alumina, tantalum/graphite, graphite/alumina, and graphite/molybdenum. They all showed excellent wetting and flowing, however, due to the difference in the thermal expansion between the materials, the materials suffered dimensional changes after the joining procedure. Nonetheless, graphite/molybdenum has been joined at higher temperatures as well as in different environments and have been joined successfully [38].

2.1.3.7 The Pd-Ni Brazing System

Asthana et al. [39] has investigated joining ZrB_2 – SiC (ZSC) and ZrB_2 – SCS-9a SiC fibers (ZSS) using Pd – based brazes. PdNi which has a composition consisted of 60% Pd and 40% Ni T_L = 1237°C, has shown either weak joints (wetting) or cracks. They heated the samples to above the T_L by 15-20 K. Cracks found in the experiment are arguably due to residual thermal stress. ZSC and ZSS joints that were brazed using Palni, has displayed weak joints; ZSC joints were not examined due to them breaking before examination and ZSS joints were partially bonded but also cracked, however, they were polished. Furthermore, there was no evidence of dissolution of Pd or Ni at ZSS joints, but there was very little diffusion of Si into the braze. This braze is a commercial braze, however not enough information has been published about it.

2.1.3.8 The Ti-Ni-Cu Brazing System

This is another class of commercial brazes, which are becoming extremely important due to their super-elasticity and high corrosion resistance [40]–[45]. Yang et al. [9] have joined $Ti_{50}Ni_{50}$SMA (shaper memory alloy) using Ti – 15Cu – 15Ni and pure Cu by infrared brazing.

The matrix and the angular phase are usually the two initial phases at the joint. The angular phase, known also as dispersed phase, is often surrounded by a matrix phase. When the brazing time increases, the angular phase disappears leaving the matrix phase only. At the same time, line scan demonstration shows that due to increasing the brazing time, the homogeneity of the chemical composition of the braze can be identified [9].

According to [9], at 960 °C for 30s, it is apparent that no interfacial reaction phase can be detected between $Ti_{50}Ni_{50}$ metal substrate and the alloying braze. Nonetheless, Cu from the braze seems to alloy the base metal, in addition to a seemingly stoichiometry related to $Ti_{50}(Ni,Cu)_{50}$.

The vital difference between the angular and the matrix phase is the amount of Cu in $Ti_2(Ni,Cu)$; the angular phase is very close to $Ti_2(Ni,Cu)$ [9]. The matrix phase contains lower amounts of Cu. At the Ti_2Ni phase, the Cu atoms have an intendency to replace the Ni atoms, hence, the $Ti_2(Ni,Cu)$ phase is formed at brazing.

Ti and Cu, both will diffuse into $Ti_{50}Ni_{50}$ from the alloy. On the other side, Ni will diffuse into the alloy from Ti50Ni50. This is due to high gradient concentration of the brazing alloys. The Ti – 15Cu – 15Ni system is in weight composition, converting it into atomic: 74.8Ti–12.1 Cu–13.1Ni.

The interdiffusion of the molten braze and the $Ti_{50}Ni_{50}$ substrate occurs together at higher temperature, hence the angular phase decreases as the brazing temperature increases. At temperatures exceeding 1000 °C, Cu consumption at the molten braze is higher. Hence, decreasing the amount of angular phase with more Cu element. At 1050°C and for 30 s, the angular phase has greatly vanished, in addition to a high decrease in the width of the $Ti_2(Ni,Cu)$ matrix. When the $Ti_2(Ni,Cu)$ phase is reduced, this resulted in deficiency of Ti at the braze. Similarly for investigations brazed at 1100 °C for 30 s.

The joints were fractured after bending them, this resulted in a crack propagating along the braze. The bending test schematic diagram can be seen in figure 5 below. The existence of brittle Ti_2(Ni,Cu) matrix is expected to have been the reason behind this observation. Unlike Ti50Ni50/Cu/Ti50Ni50, the Ti(Ni, Cu) was not noticed at $Ti_{50}Ni_{50}$/Ticuni/Ti50Ni50 after infrared brazing. Nonetheless, Ti_2(Ni,Cu) was noted at samples brazed at 1150 °C. Increasing the time and temperature was not enough in diminishing the extensive brittle presence of Ti_2(Ni,Cu), that has affected the completion of the bending test. Longer brazing time has proved that less TiNiCu phase exist at the joint, but more Ti(Ni,Cu). The existence of TiNiCu phase has affected the shape memory of the joint, however, the Ti(Ni,Cu) has kept the shape memory behavior, but also alloyed the joint with large amounts of Cu.

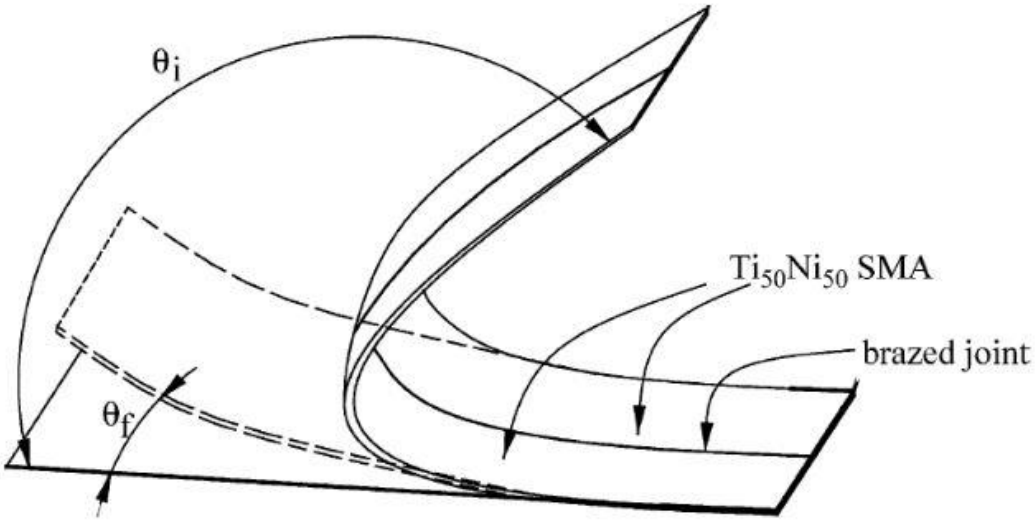

Figure 5 The bending test schematic diagram [9]

The aforementioned braze systems, have all showed the tendency to react with Ti. Moreover, little information has been mentioned regarding specific brazes used within this project. However, information collected some of them fall in hand with what has been already investigated or reported in the results and discussion section.

Commercial brazes such as, Ti-15Ni-15Cu and Pd-40Ni, have not been used yet for metal-to-ceramic joining. Furthermore, the information found on Pd-40Ni was not very promising and showed little potential. Nonetheless, in this project the results seem very promising. This has been discussed thoroughly at section 4.4.3. It is understood that the flowability of the braze to

fill the pores found in the ceramic substrate is arguably the prime reason for these promising results.

However, in the case of Ti-15Ni-15Cu, results collected, falls in line with literature review. The formation of some brittle phases was detrimental in obtaining a joint between Titanium and Alumina substrates. Those phases were observed using a similar joining substrate, explaining that these phase are occurring either from the braze – Ti-substrate or the braze solely.

2.2 *Diffusion Bonding*

Diffusion bonding is a term that is used to describe solid-state and liquid-phase welding. The process is dependent on the interdiffusion of atoms across the interface. In order to minimise the damaging oxidation within the faying surfaces, the bonding procedure mainly occurs either in vacuum or in an inert atmosphere for instance argon or nitrogen. The bonding procedure can sometimes be conducted in air, that is in the case of oxides that are thermodynamically unstable at the bonding temperature. In other words, where oxidation is unlikely to occur [10].

Diffusion bonding is similar to brazing in terms of procedure and using foil or coating to accommodate between the faying surface and the materials to be joined; brazing, unlike diffusion bonding, is mainly used for high temperature applications as aforementioned. Hence, brazing is the favoured joining process in this project. Moreover, from the literature it is assumed that diffusion bonding is classified into Solid State and Transient Liquid Phase diffusion bonding.

2.2.1 Solid-State bonding

In this process, normally, there is pressure applied on the parts to be joined during dwelling at a considerably high temperature. Occasionally, depending on the joints to be produced, a metallic interlayer is deployed between substrates. However, it is not meant for that interlayer to melt, rather it is to support the process by mitigating the possibility of voids at bond interface.

The fact that this process does not necessarily require an interlayer to be used, it provides variety of options to join different materials. It is also capable of producing joints with the least number of microstructural flaws. Nonetheless, the excessive existence of oxides at the interface is a vital factor of having a weak joint.

The following are important elements to ensure production of a strong joint is produced:

i. Before the joining procedure, substrates are polished and ultrasonically cleaned. This is to assure that no contamination is present at the substrates.
ii. Full contact during the joining process at the interface between substrates.
iii. Adequate time during the process to make sure diffusion is taking place at the interface, and that is to reduce the possibility of microstructural inconsistency, hence providing a strong bond at the interface

.

Chemical interaction at the contact area cause adhesion between dissimilar materials. Metals have higher energy atoms at the surface, compared with other materials. In metal-to-ceramic joining, the metal substrate energy acts as a powerful factor in reducing the chemical interactions that are responsible of lowering the surface energy [46]. During solid state joining, the chemical reactions that appear along with the new phases forming at the interface, is what determines the strength of the joint. The procedure parameters: joining temperature, dwelling time, force applied, and chemical composition are all factors that drive these reactions.
In the case of joining without using an interlayer, the joining process does usually fail or results in a weak joint. Usually this is due to the difference in CTE that occurs during cooling down process, resulting from residual thermal stresses.

Krugers et al. [47], [48] tried to join silicon carbide to steel, using the following parameters: 800-1000°C and 24 hours dwelling time. It is shown that, using a metal interlayer was the only route for joining. The reason behind this interlayer was the mediator to the huge difference of CTE in the substrates. Hence, the residual thermal stresses that usually occur when there is a mismatch in the CTE, is not occurring after an interlayer is deployed. The joint had an average

of 30 MPa lap-shear (strength). Further analysis (FEA) to understand the thermal stress, has presented a clear thermal stress reduction at the metal-to-ceramic interface. Moreover, silicides and other rejected phases are all decisive factors for the strength of the joints. Suganama et al. [48] has investigated joining iron-to-silicon nitride, without using an interlayer, at 1200°C and dwelling time of 30 minutes, which resulted in a weak joint. This was due to the formation of Fe5Si3, iron silicide.

Vegter and Den Ouden [49] investigated solid state diffusion bonding of Zirconia to Silicon nitride using an interlayer of Ni. This technique is where the surface of two materials is pressed together during a specific time at an elevated temperature until the formation of a bond [49]. At temperatures between 1000 °C and 1100 °C, they used a heating rate of 25 °C/min to 50° C and then 5 °C/min up to the bonding temperature that was varied between 1000 °C and 1100 °C. The cooling rate was 10 °C down to room temperature.

They reported decomposition of Si_3N_4 at the Si_3N_4-Ni interface forming free Silicon and Nitrogen. The free Silicon had diffused into the nickel; however, nitrogen atoms combine again to molecular nitrogen. The molecular nitrogen either escaped to the surroundings or formed pores on the interface, and sometimes both. No reaction was noticed at the interface of ZrO_2-Ni. Neither the bonding pressure nor the thickness of the interlayer could improve or influence the bond strength. Following the optimal experiment conditions, the mechanical lap shear strength of the bond was 57 MPa. The Si_3N_4-Ni interface has shown to have a weak reliability due to the consistent occurrence of failure. Therefore, this suggests that a Ni interlayer might not be the favoured interlayer to the Si_3N_4 system.

2.2.2 Transient Liquid Phase (TLP) & Partial Transient Liquid Phase (PTLP) bonding

Transient liquid phase is normally a joining method for metal-to-metal joints by using a metallic interlayer, usually thin to hold different chemical elements [50]. The procedure starts when the interlayer is completely melted, solidifying takes place after wetting the substrate. This is due

to inter-diffusion occurring from the substrate. The region containing solidified joint, is mainly made of an initial solid solution. That way, the brittle phases at the interface can be eliminated. Unlike brazing and solid-state diffusion bonding, where these brittle phases are formed. This bonding technique can employ alloy systems which are peritectic and eutectic, lowering the liquidus temperature whilst alloying [51].

Oxide removal is a vital stage, named “pre-stage”, which is ignored predominantly despite of its importance. The oxide film is disrupted by the existence of the liquid phase, and after a joint between metal-and-metal occurs on one reported occasion at least, the volume of inter-diffusion and penetration of the oxide at the substrate interface changed [51].

Nakoa et al. [52] has investigated a potential joining of MA 956, which is Fe based, to itself, using a IM 7 filler metal, also Fe based. The outcome of the investigation is a successful joint at 1290°C, dwelling for 36 mins. The results of these joints did not show any micro-voids at the interface, as well as elongation results were similar to that of the metal substrate before treatment. Not only the elongation values, but also the tensile strength at room temperature. Sound joints were formed at 1290°C, showing that the TLP process can be used in other applications than low temperature. Nonetheless, in the latter case, it was mainly because of the the interlayer’s liquidus temperature which is 1143°C.

An alternative of the TLP process is known as Partial Transient Liquid Phase (PTLP). This bonding procedure has been investigated to accommodate for metal-to-ceramic and ceramic-to-ceramic bonding. The process of joining using this technique, involves employing a multilayer filler metal. This multilayer metal is made of a low temperature thin insert outerlayer and a thick base of a refractory ductile metal [53]. This is to compensate for the CTE mismatch, hence melting the outer layer, whilst the ductile layer remains.

Usually, a liquid is formed by this process, by exceeding the melting temperature of the outerlayer. Another possibility is, the reaction occurring between the outer and the base layer of the multilayer which might produce a molten phase at that temperature. Therefore, liquid will

wet the solid surface of the substrate, inter-diffusing at the substrate turning it to a strong refractory material. The homogeneity of the outerlayer while joining, makes it viable to develop joints that can have similar operational temperatures to the joining temperature [54].

Joining silicon nitride to itself using CuTi/Pd/CuTi, has been investigated by Paulasto et al. [54]. The process tried temperatures of 950 and 1050°C with applied pressure of 50kPa and dwelling for 10 to 240 mins. They concluded that using systems involving a eutectic system or a low liquidus temperature are more likely to form transient liquid phases. Hence, choosing a multiylayer that tends to melt and cause a reaction between the outerlayer and the base layer. To make sure the transient liquid phases formed are favourable.

Another investigation including the joining of silicon nitride to itself has been published by Zheng et al. [55], however, Ti/Cu/Ni and Ti/Ni multilayer has been used this time. The temperatures used were 1050°C using a 0.1 MPa pressure force and dwelling for 60 minutes at 1120°C dwelling for 30 minutes. To evaluate the joint strength, a four-point bend test was carried out. Their results showed that using the multi-interlayer of Ti/Cu/Ni had better results to that of Ti/Ni. This behaviour was mainly due to Ni-Ti compounds being formed which were evidently brittle. For that reason, it is vital to study and understand any reactions appearing at the interface, as well as their radical impact on the joint overall.

To conclude, these two processes can produce metal-to-ceramic and ceramic-to-ceramic joints. Nonetheless, there is a lack of research in comparison to metal-to-metal joining. TLP/PTLP processes differ slightly from brazing in terms of joining metal-to-ceramic bonding. The vital difference is the occurrence of the TLP/PTLP isothermally. At constant temperature, the inter-diffusion causes the interlayer to melt and solidify with the substrate. Brittle phases are not a common issue with regards to TLP/PTLP, unlike brazing. No work has been published on joining alumina to titanium using TLP or PTLP procedure.

2.3 *Soldering*

Soldering is different from brazing in terms of joining interlayer melting temperatures which is below 450°C. Hence, it is not suited for high temperature applications.

This process is dependent on low melting points, and metals with high atomic weight. An example is Pb-Sn which melts at approximately 200°C. In addition to their low temperature, the Pb-Sn system contains very expensive elements which make them extremely disadvantageous, also for their poor creep strength. Furthermore, the toxicity of Pb is leading to investigations on alternatives. These points has pushed researches to investigate other systems, such as Tin-Gold which melts at almost 220°C [10], [56]–[59].

2.4 *Mechanical Joining*

This joining process is the classic of joining, which depends on attaching a solid part to another solid part, without any heat use. Usually rivets, bolts, or nails supports the joint. To assure the joints are placed tight and compressed enough, they rely on tensile residual stress. Unlike other joining methods, this method does not require any heat, however, requires external force through interlocking or/and physical. Hence, there are no chemical reactions occurring, which makes this process advantageous for assembling or disassembling joined parts. Moreover, this method of joining becomes a strong option for applications that need constant maintenance. For that reason, in space shuttles, the tiles (heat resistance) are mechanically joined, for replacement and/or inspection after and/or before missions.

Additionally, the problem with this process is the fact of relying on drilling holes; this tends to weaken ceramics. Hence, the joints are often weak or develop premature failure, due to weak stress concentration at joint interface [10], [56]–[59].

2.5 *Adhesive Bonding*

This technique of joining relies on a material that can withhold substrates together due to attachment forces. Adhesive bonding is usually carried out at room temperature, additionally the hardening can occur at room temperature or in some cases requires further treatment. Hardening during this process of bonding is usually called curing. The component of the adhesive is commonly polymeric mixtures. This procedure is normally rapid in producing joints that are commonly strong. Nonetheless, they have low melting temperatures of 300°C, hence it becomes disadvantageous and not very practical to most metals/ceramic [10], [56]–[58].

For strong joints, chemical reactions between polymer molecules and substrate must occur. Due to the lack of partial arrangement between polymer molecules results in poor occupation at the substrate. To insure sound chemical bond at the interface, covalent or ionic bonding is expected. Surfaces that are not chemically reactive are not expected to bond. Moreover, adhesive bonding produce joints that are quickly reactive to environmental aspects like moisture and sunlight.

Various adhesive options are now available commercially. Epoxy resins, are one of them, considered strong thermosetting adhesives. On the other side, polyurethane is usually better than epoxy in terms of strength and toughness at low temperature. They are also available in many grade options. Additionally, acrylics and cyano-acrylics can be used for joining metals, plastics and rubbers, at a various temperature range. As long as, joints that are bonded adhesively, are not prone to high temperature range and other environmental factors, this process can be used to join metal-to-ceramic.

2.6 *Wettability*

The Young's contact angle value, θ_Y, is known as a unique characteristic of liquid, solid, and a vapour system [60]. The Young relationships are fundamental equations that best describe the wetting conditions [61]:

Equation 1 Young 's contact angle relationship equation

$$\sigma_{SV} = \sigma_{SL} + \sigma_{LV} \mathrm{Cos}\theta$$

where Sv, Lv, and Sl presents the equilibrium, at the triple line, of the solid-vapor, liquid-vapor, and solid-liquid interfacial tensions via the contact angle θ, and the work of adhesion, also known as the Young-Dupre equation:

Equation 2 Young-Dupree equation

$$W_a = \sigma_{SV} + \sigma_{LV} - \sigma_{SL} = \sigma_{LV}(1 + \mathrm{Cos}\theta)$$

Generally, there are three fundamental wetting types that are recognised: non-reactive, reactive, and dissolutive wetting.

2.6.1 Non-reactive wetting

Non-reactive wetting is an infrequently used method that can explain high-temperature applications, and it only happen if specific conditions are met. No doubt, non-reactive wetting can occur, given that the interaction of the three interfacial tensions sets up a low-contact angle (as estimated by equation 1), considering that no chemical reactions arise between the solid and liquid phase, and that the solid and the liquid phases are equally immiscible, and the liquid phase reaches chemical equilibrium with the solid [61]. The conditions mentioned can be met using a low temperature that does not tolerate a very rapid exchange of atoms diffusing between the liquid and the solid phase.

2.6.2 Reactive wetting

Reactive wetting on the other hand is defined when chemical reactions appear at the solid-liquid interface, along with a new nature that can subsequently modify the wetting behaviour of the system completely. This is done through the formation of new phases at the interface that often carry different wetting characteristics. There has been a lot of debate regarding the role that the free energy of reaction can have on the final contact angle [61]. If reaction occurs, then

the formation of repetitive layers of certain reaction products should determine the final equilibrium structure. Depending on the chemistry of the system and the kinetics of the triple line, these reactions can form a new compound. This formation of new compounds by heterogeneous nucleation at the solid-liquid interface can only happen when a specific amount of supersaturation in the liquid phase is reached [61]. However, that is dependent on the presence of insignificant elements, which include the active elements utilized in brazing such as Ti, Cr, Al, and V, within the liquid phase that can give rise to interfacial reactions whose kind and quantity are dependent on the activity of these elements activity during the experimental procedure. Specifically, this is more likely to happen after the triple line velocity is considered low [62]. After the formation of a repetitive layer of a new compound at the liquid-solid interface, solid-state diffusion must be used to transfer the atoms required to provide the interaction, as well as reducing the rate of the substrate dissolution considerably.

2.6.3 Dissolutive wetting

Excessive atom mobility at temperatures indicates that there will be a possible partial dissolution process happening through the molten matrix before a similar solid and liquid state chemical reaction of the distributed sources occur. Over time, the liquid solution will have an alteration in state considering there might be a stall in the expected reaction. This though creates a negative effect since there are undesired changes to the surface and the setup of a dynamic condition through the behaviour of the contact angle and other parameters such as volume and height of the drop. Hence, the liquid-solid interface does not lie flat on a plane anymore, however an indentation forms below the drop with a virtually spherical profile, as seen in Figure 6, which will be to some degree perturbed. As a result, Equation 1, the Young equation, referring to rigid, homogenised, non-deformable topographies, is not valid anymore, because the triple line equilibrium should conjointly consider the vertical elements of the surface tension vectors.

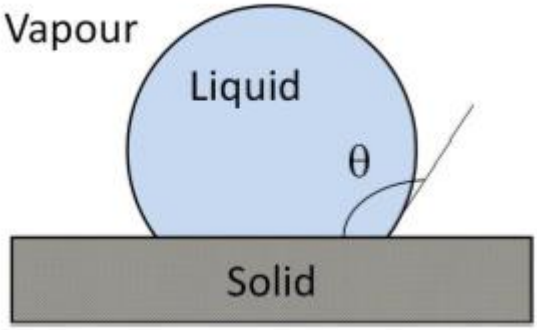

Figure 6 Definition of the equilibrium contact angle [60]**.**

2.6.4 Summary on wettability

Passerone et al. [61] have presented a survey explaining the vital interaction phenomena that occurs at the solid–liquid interfaces within the metal-ceramic systems at high temperatures. They used experimental and theoretical points in their review. The following was concluded [28]:

i. Different phenomena such as: reaction, dissolution of the ceramic in the liquid phase, new phases formed at the solid-liquid interface, and also the fast drop being spread along the substrate surface; these competitive phenomena determine the contact angle result as well as determines the formation of interfacial dissolution, at high temperature.

ii. One of the main reasons ultra-high temperature ceramic (UHTC) substrates have poor wetting by liquid alloys is the formation or the existence of surface layers such as, oxides. Using additives such as active metals or very low oxygen partial pressures can get rid of oxides.

iii. Utilization of phase diagrams to firstly interpret the progress of the system and secondly to restrain the substrate dissolution.

iv. Experiments like sessile-drop can be useful to evaluate the critical characteristics of new phase diagrams, for example, isothermal transitions, and the formation of compounds, etc..

2.7 *Effect of Third Element Addition*

There is interest in adding third element to the braze, whether it be Ni or Fe. A number of researchers have reported addition of a third element can enhance the strength of the joint. Shu et al. [63] have mentioned that Ni forms NiTi due to the difficulty of its existence near TiAl, therefore it will not react with Ti or Al only. On the other hand, both Fe and Co are more likely to occupy the Al element of the TiAl compound. This work lacks proof of work, where their work is not illustrated by contact angle for example, to explain the reaction in depth. Furthermore, this can lead to improving the ductility of TiAl, by the means of enhancing the electronic structures and elastic properties at the same time. Fe showed an apparent improvement on the ductility of TiAl alloy. Adding 3 at.% Fe has enhanced the fracture strain of TiAl alloy from 17.3% to 19.1%. Furthermore, TiAl-3Fe has an average strength of 354 MPa which is higher than the alloy TiAl. Hence, it is proven that Fe can potentially improve the ductility as well as the strength of TiAl alloy. In another paper Shu eta al. [64] investigated the addition of Mn, Co and also Fe, and reported that Fe can enhance the strength of TiB_2/TiAl, yet might affect the ductility. It has been mentioned in their work that there is potential in solving the problem of weak strength in the TiAl alloy without affecting the ductility.

2.8 *Summary of Literature Review*

Most metal-to-ceramic joining procedures and advances has been outlined. Giving specific attention to relevant techniques to this project, such as brazing and solid-state diffusion bonding.

The vital part of any dissimilar joining technique is usually the CTE difference, which in reward affects the interfacial microstructure. Hence, the properties of the braze and the substrate is extremely important i.e., the bonding interface. Phases and their morphology and quantity is key factors of deciding the reliability of brazed joints.

Various techniques have been investigated to understand the compounds and phases formed by joining metallic components to aluminium oxide. These chemical reactions can develop

strong interfacial bond. The most suitable techniques are active metal brazing and diffusion bonding (often suitable). Metal-to-ceramic joints are known to be used commercially, specifically in defence and aerospace industry. Hence, this joining process needs to be researched extensively and thoroughly.

Basic metal-to-ceramic joints has been generally achieved. However, these joints are not normally viable due to constraints. Some of the constraints are joining metal-to-ceramic on a large scale, due to larger residual stresses. In addition to having slightly low operation temperature of 500°C. Therefore, this has not utilized the main properties of ceramics, high temperature.

Techniques in this section has their own advantages and disadvantages. One simple and common process is active metal brazing. This process can produce strong metal-to-ceramic joints. Nonetheless, wetting and joining results are not compatible. Making the selection of bonding interlayer and parameters very vital to obtain productive results. Another common process, diffusion bonding is a feasible joining technique. When solid-state phase occurs, it can provide applications with high temperature operation. Nevertheless, the processing of this technique is difficult. The process involves surface preparation, pressure applying and high temperature.

More research needs to be carried out on joining of metal-to-ceramic. This area of research needs to be improved and developed. Mainly, improving current procedures to enhance the properties and performance of the joints. Hoping that this research project can contribute to the metal-to-ceramic joining techniques. The novel and commercial braze systems in this proposed research has not been reviewed for high temperature application. In the following sections the novel Ti(Ni),Al and Ni-14Zr braze systems, and commercial Ti-15Ni-15Cu and Pd-40Ni braze systems will be examined and analysed. This will provide an understanding of Ni behaviour at Al_2O_3 interface in four different braze systems. Furthermore, promote potential use for the novel and/or commercial braze systems in industry.

3 Methodology

In this chapter the samples preparation and bonding methods will be explained. As well as the methods of joints, phases, surface morphology characterization; in addition to some fracture analysis.

All joining techniques in this project was done under certain conditions and had parameters set depending on the braze used. Variety of braze systems were used across this project. The optimised experimental procedure is typically as follows:

1. Search for braze systems relevant to project scope
2. Outline phases from phase diagram
3. Choose composition of braze
4. Carry out brazing procedure
5. Cut samples (if joint is successful)
6. Prepare samples for metallurgical examination
7. Understand and analyse phases occurring

After exploring different braze systems, through literature survey and experiments, Ni was the most interesting element. Nickel was most of the time observed close to the alumina substrate. Hence, the four-composition chosen had Ni element in all of them. Two braze compositions were developed in the course of this project: Ti-Al28wt%-Ni3.6wt% and Ni-Zr14%. The other two braze systems chosen are commercially available: Pd-Ni40wt% and Ti-Cu15wt%-Ni15wt%.

Initially, SEM and EDAX are used to understand the behaviour of the braze with the titanium and alumina substrate. After the microstructure examination using SEM, the identification process of new phases or element distribution is carried out using EDAX.

The four braze systems that were agreed upon, were heat treated at 450°C for 500 hours in a conventional furnace. The temperature and duration set for this experiment is because oxidation of Ti can start at ≈600°C, regarding the duration, the time set in this post-brazing procedure will exceed the operating parameters at industry. Hence, this is mainly to put joints

under conditions similar to real life projects, even more extreme conditions. All brazed samples were compared before and after the aforementioned heat treatment.

Braze compositions agreed upon, were prepared for shear test, the procedure is mentioned in 3.4. For third element addition shear test results refer to 3.4. Joints that were broken at handling, before shear test or after shear test are all set for fracture analysis.

In regard to measuring the strength of the joints, there is not much information mentioned with reference to International Standards, concerning metal to ceramic. The mechanical test experiment regarding ceramic-to-ceramic was done in accordance with ASTM D1002-05 [65] using universal testing machine SINTEC D/10. For later results concerning metal-to-ceramic Tinius Olsen 50ST was used with accordance to ASTM D1002-05. Regarding the latter, a fixture was produced for the purpose of single lap shear test, refer to Figure 14. Nonetheless, this standard is used for Metal-to-metal bonded using adhesive. This test was conducted for both sets 2 and 3.

Further investigation like contact angle measurements were conducted on samples prepared at set 2. However, no contact angle measurements were carried out for set 3 samples, rather nano-indentation to obtain hardness, toughness and young's modulus. Roughness is an important parameter for obtaining mechanical properties, however, measuring roughness can induce cracks to the Al2O3 substrate, which can affect the joining process later on. These nano-indentations were carried out on braze systems that eventually produced joints. Two set for indentations were obtained for a single system, before and after long heat treatment.

Three sets are mentioned in this chapter, each set of experiments include had its own procedure. However, same assembly technique is used throughout the project, refer to 3.2.

3.1 *Bonding technique*

3.1.1 Set 1

Bonding aluminium Oxide was the main focus of this project, while some Silicon Carbide-to-Titanium experiments were conducted to start with. The layout was similar to that used in [23], using Al-Ti foils as an interlayer. Both SiC and Al_2O_3 were cut to fit on top of the Titanium and later to sit in it, therefore they were approximately 6mm x 5mm x 4mm. Titanium cylindrical discs with 12.8mm dia and a thickness of 5.2 mm, the cylindrical discs were milled approximately 10 mm. For SiC, it was bonded straight to Ti, the Silicon Carbide being placed on top of Titanium and then they are both placed in the furnace. A schematic diagram of the bonding mechanism can be seen in figure 7. SiC experiments were at brazing temperatures of 1450, 1400, and 1350°C. The heating rate was not controlled, neither was the cooling rate. There was dwelling at the brazing temperature for 10 minutes. The experimental procedure for Al_2O_3-Ti involved cutting both Aluminium and Titanium foil. The weight composition was varied to achieve desirable chemical reaction - hence, the foil was mainly cut into three sets. The Al_2O_3 discs used in this project has a purity of 99.8%. LM powder braze was used later on to bond Al_2O_3/Ti, run 14. The LM braze is a powder made of Ni Balance, 3% Fe, 7% Cr, 4.5% Si, and 3.1% B. Run 11 was an investigation on the interface of alumina with Ti-Al foil, therefore no Titanium bonding was intended. On the other hand, run 10 was to investigate how alumina looks after heating up whilst neither adding Titanium nor foil. The brazing temperature was 1450 °C with 10 min/K heating rate and 30 minutes dwelling time. Runs 12, 13, 14 had same brazing parameters; the only difference was dwelling for 1 hour. Table 4 shows the specification of the brazing procedure. It was doubtful if there was more Titanium than Aluminium in the process of bonding Aluminium Oxide to Titanium, hence a layer of Aluminium foil was added to cover the surface of the Titanium before the brazing process. After this stage, the normal brazing procedure was carried out. The cooling temperature, however, was not controlled. After brazing, the samples were cut through the cross-section area.

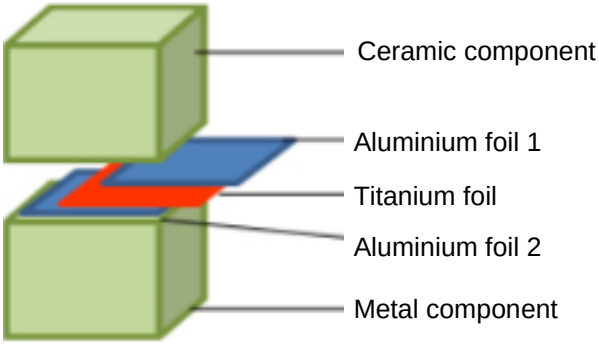

Figure 7 Schematic diagram of bonding mechanism

All brazing runs were carried out in a Carbolite STF 15/180 a high temperature tube furnace with maximum temperature of 1500 °C. Argon was flown through the alumina tube to help protect the samples from oxidation.

Table 4 Testing specification for set 1

Run	Temperature (°C)	Dwelling time (min)	Heating rate (°C/min)	Cooling rate (°C/min)	Braze	Type of braze	Weight of braze (g)
1	1400	10	10	~5	-	-	-
2	1350	5	10	~5	-	-	-
3	1300	5	10	~5	-	-	-
4	1450	30	10	~5	Ti-Al	Foil	0.0222
5	1450	30	10	~5	Ti-Al	Foil	0.01482
6	1450	30	10	~5	Ti-Al	Foil	0.01452
7	1450	30	10	~5	Ti-Al	Foil	0.0185
8	1450	30	10	~5	Ti-Al	Foil	0.0161
9	1450	30	10	~5	Ti-Al	Foil	0.0177
10	1450	30	10	~5	-	-	-
11	1450	30	10	~5	Ti-Al	Foil	0.0185
12	1450	60	10	~5	Ti-Al	Foil	0.02
13	1450	60	10	~5	Ti-Al	Powder	0.02
14	1450	60	10	~5	LM	Powder	0.02

3.1.2 Set 2

The main aim at the second set of experiments was to examine the effect of third element addition to a TiAl based braze. Two alumina discs were joined using brazing alloys of various compositions, of a 0.2g total weight of foil. The brazing compositions are presented in Table 5.

The brazing temperature was set at 1500°C, at a heating rate of 10°C/min, and dwelling time of 1 hour. As with pervious treatments, the cooling rate was not controlled. Figure 8 is an illustration of the schematic diagram of the new set of treatments.

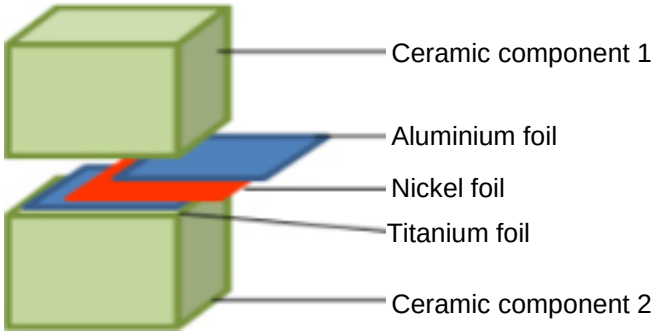

Figure 8 Schematic diagram of set 2 bonding mechanism

Similar brazing equipment were used throughout this set as well.

Table 5 Testing specification for set 2

Run	Braze (wt%)	Type of braze	Temperature (°C)	Dwelling time (min)	Heating rate (°C/min)	Cooling rate (°C/min)
1	Ti-7.2Ni-28Al	Foil	1500	60	10	~5
2	Ti-7.2Fe-28Al	Foil	1500	60	10	~5
3	Ti-3.6Ni-28Al	Foil	1500	60	10	~5
4	Ti-36Al	Foil	1500	60	10	~5

3.1.3 Set 3

This set of experiments examined two braze systems that were developed in the course of this project, Ti-3.6Ni-28Al and Ni-14Zr. Only four systems were used for further analysis; two of which are commercial (Pd-40Ni and Ti-15Ni-15Cu). Commercial names for systems used are PALNI (Pd-40Ni) and TICUNI (Ti-15Ni-15Cu). For consistency the same mechanism was used during these set of experiments. However, the metal substrate used during this set was

Ti6Al4V, purchased from Thames stockholders. For preliminary joints, buttons were used similar to set 2, refer to 3.2. Shear test samples are explained in 3.4. Foil weights were not measured for this set. It was more concerning to make sure the weighed foil would sit in the titanium button with alumina on top of it. Same with preparations for single lap shear test. It was made sure that the overlapped area are covered, 12.5mm x 25mm. Table 6 below shows the composition and range of temperatures used during this set.

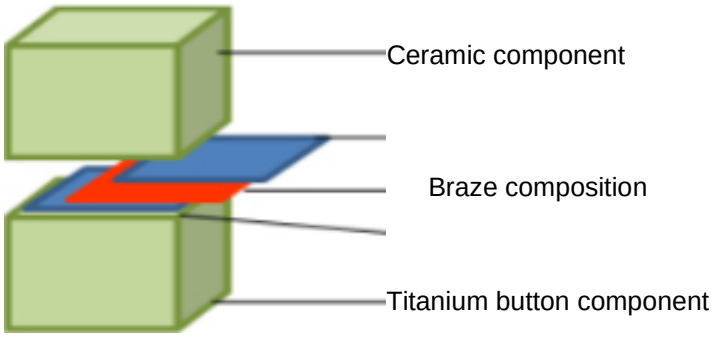

Figure 9 Schematic diagram of set 3 bonding mechanisms.

Similar brazing equipment were used throughout this set as well. Even though different braze systems were examined, the agreed upon systems were used for further analysis – SEM, EDAX, and Shear Test.

Table 6 Testing specification for set 3

Run	Braze (wt%)	Type of braze	Temperature (°C)	Dwelling time (min)	Heating rate (°C/min)	Cooling rate (°C/min)
1	Ti-3.6Ni-28Al	Foil	1500	60	10	~5
2	Ti-15Ni-15Cu	Foil	1200	60	10	~5
3	Pd-40Ni	Foil	1350	60	10	~5
4	48Ti-42Cr-10V	Foil	1460	60	10	~5
5	48Ti-48Cr-4V	Foil	1490	60	10	~5

6	54Ti-25Cr-21V	Foil	1490	60	10	~5
7	60Ti-20Zr-20Ni	Foil	1050	60	10	~5
8	56Zr-28V-16Ti	Foil	1350	60	10	~5
9	60Ti-20Zr-20Ni	Foil	1300	60	10	~5
10	Ni-14Zr	Foil	1350	60	10	~5
MF1	Ti-3.6Ni-28Al	Foil	1500	60	10	~5
MF2	Pd-40Ni	Foil	1500	60	10	~5
MF3	Ti-15Ni-15Cu	Foil	1500	60	10	~5
MF4	Ni-14Zr	Foil	1500	60	10	~5

MF runs stands for Muffle furnace, representing samples that were placed in a conventional furnace for heat treatment at 450°C for 500 hours.

3.2 *Assembly*

The assembly of the SiC/Ti is shown in the figure 10 where the SiC sample is placed on top of the Ti. A braze was used in the Al_2O_3/Ti samples – using two types of assembly as shown in figure 11. The first assembly for Al_2O_3/Ti samples is placing the Al_2O_3 on top of Ti using Aluminium and Titanium foil, figure 11. This layout was hard to place inside the furnace without the foil or the Al_2O_3 samples moving, due to the samples not being either pressed or forced together. It was thus decided that the Titanium samples were going to be milled for Al_2O_3 to sit inside it, to insure that the titanium would remain on top of the alumina, figure 12.

(a) 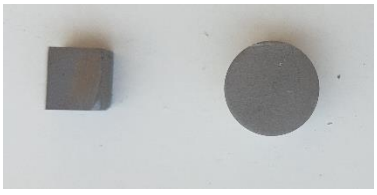 (b) 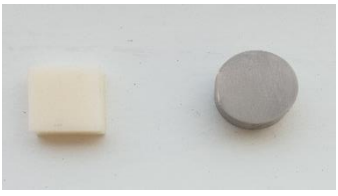

Figure 10 (a) SiC sample along with Titanium (b) Al_2O_3 along with Titanium

(a) 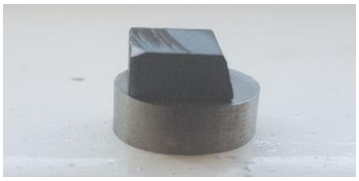 (b) 

Figure 11 (a) procedure of bonding SiC/Ti (b) procedure of bonding Al_2O_3/Ti

Figure 12 Titanium used for bonding

3.3 *Contact angle*

As for the contact angle measurements, alloys were prepared by arc melting before tests. Test parameters were as follows:

- Temperature: 1500°C
- Atmosphere: Ar + 5% H2 + Zr
- Dwelling time: 30 min

Metal/ceramic couples were introduced into the preheated furnace by a magnetically operated push rod only after the temperature had reached equilibrium; in the same way, after the tests had been completed, the samples were extracted from the hot part of the experimental chamber.

3.4 *Shear test*

The mechanical strength measured refers to single lap offset test in compression at room temperature adapted from ASTM D905-08; using a universal testing machine SINTEC D/10), for the first run of samples. Moreover, for the second run the machine used is Tinius Olsen 50ST.

All joined samples were machined down to 5mm x 5mm x 8mm shear test samples. In order to ensure greater accuracy three samples were tested for each joining condition.

A designed fixture was used such that sample movement was prevented during testing and that shear force was applied to the bond line and either side of bond line (see Fig 13 & 14). A computer assisted Instron tensile testing machine was used with a cross-head speed of 0.5 mm/minute.

Figure 13 shows the schematic diagram of the shear test samples. A similar furnace was used; as for brazing by applying the same brazing parameters. Tungsten Carbide was used as a weight to keep samples in position during brazing treatment. Regarding samples from set 3, a steel clamp was used to make sure substrates were positioned in a lap joint whilst inserting them in the furnace.

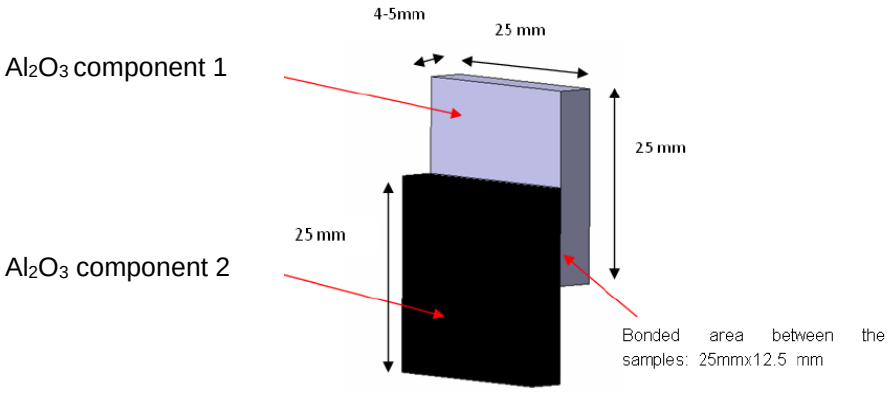

Figure 13 Schematic diagram of shear test for set 2 samples

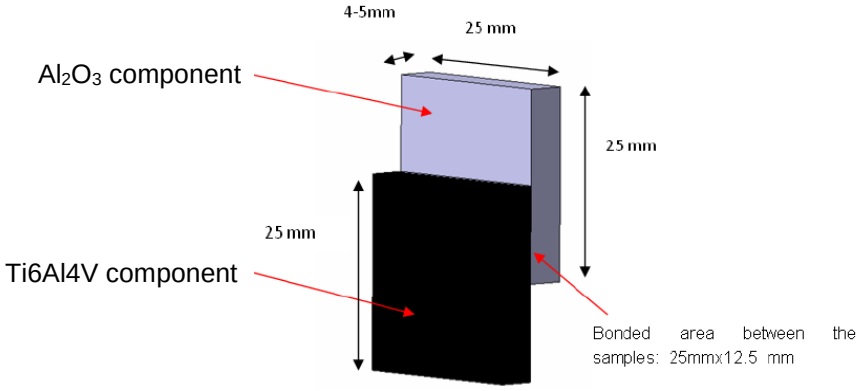

Figure 14 Schematic diagram of shear test for set 3 samples

For the second run of experiments, Tinius Olsen 50ST was used with a fixture purposely produced to obtain lap shear test results. Below is figure 15 representing the lap shear test

procedure for samples produced at set 3. As a start the rigs are placed in idle position ready to start shearing (a), the equipment start pulling the rig to shear the sample as seen in (b). Samples are placed in position (c), using a steel clamp and alumina on between titanium substrate and clamp to ensure no reaction occurs at brazing temperature.

(a) Fixture in idle position

(b) Fixture in shear position

(c) Fixture from inside

(d) Steel clamp to make sure substrates are in overlapped for lap shear test

Figure 15 Lap shear test for set 3

3.5 *Nano-indentation*

The measurements are performed using a Diamond Berko-vich indenter on Micromaterials Nanotest Vantage (nano-indentation platform 3) machine. Indentation parameters were:

- 50 indentations
- Three identified layers (only two layers in one 42ccasion)
- 10x10 grid matrix
- Indent spacing of 100 µm
- Load of 50mN and 10 s of load holding time
- Dwelling of 20s and 5 s for unloading

These measurements are conducted to identify the hardness and the H3/E2, H and E representing hardness and elastic modulus respectively. The following equation was used to calculate the elastic modulus:

Equation 3 Elastic modulus equation

$$E = \frac{1 - v_s^2}{\frac{1}{E_r} - \frac{1 - v_i^2}{E_i}}$$

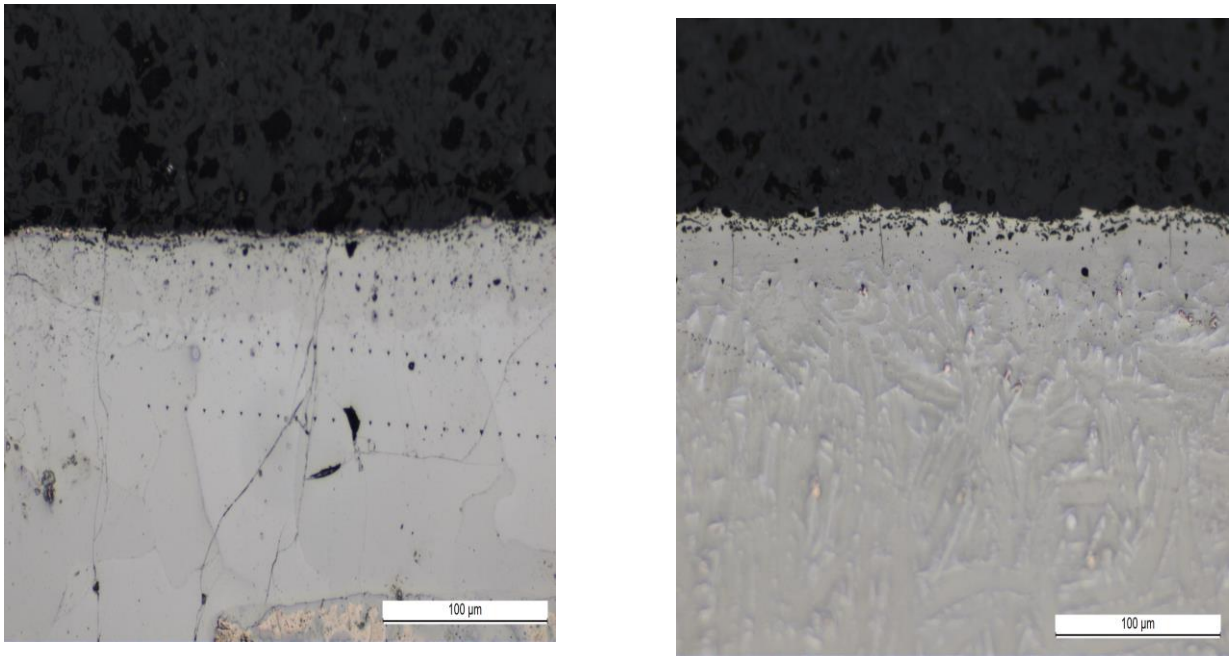

Figure 16 Images of indentation for Pd-40Ni (right) and Ni-14Zr (left)

In figure 16, random images of indentations to show layers. Three layers in most cases were chosen to give an insight of any differences occurring in any of the obtained results. Results includes:

- Hardness, H (Gpa)
- Reduced Modulus, E_r (Gpa)
- Young's Modulus (Gpa)
- Elastic Recovery Parameter
- Plastic Work (nJ)
- Elastic Work (nJ)
- Plasticity Index
- H/ E_r
- H^3/ E_r^2 (Gpa)

Each layer represents the relevant position of the braze. In the case of the top layer, the braze is just under the alumina interface. Middle layer, the braze with probably some reaction from the Ti6Al4V substrate. However, the bottom layer is mainly the Ti6Al4V substrate. In one case, Ni-Zr system braze was thick enough to carry out two rows of indents on them. Hence two layers were chosen. The top one being under the alumina interface, and the bottom one being the Ti6Al4V substrate.

3.6 *Metallography and metallographic preparation*

The alumina samples were first cut (cross-section) with a diamond cut-off wheel while Titanium were cut (cross-section) using a resin bonded Aluminium Oxide cut-off wheel. After cutting, the samples were mounted using hot (conductive) mount. This step is to prepare samples for SEM and EDAx analysis.

The samples were then mounted in a conductive mount. They were then ground using P180, 400, 800, and 1200 silicon carbide paper and polished by progressively using diamond polishing fluid of 9µm, 3µm and 1µm polish. To remove contamination, samples were cleaned using soapy water in ultrasonic bath, then cleaned with cloth and isopropanol. A drier was used to dry samples and get ready for next stage of polishing as well as for examination. Etching samples was not needed in the process of preparation for metallographic examintaion, since new phase were visible through SEM and light microscopy.

The samples were then examined using light microscopy (Leica DFC295) which was connected to a Leica Application Suite V4 program. Scanning electron microscopy (SEM) was also performed using a JEOL JCM-5700.

3.6.1 Scanning Electron microscopy

Scanning electron microscopy (SEM), it is a microscope that forms an image utilizing electrons instead of light, producing high resolution images. One of many advantages in comparison to

conventional microscopes, is having a large depth-of-field, allowing focus on a large scale of one sample.

SEM used was JEOL JCM-5700 for microstructure and interfacial analysis. Unlike Titanium, Alumina needed to be coated with gold (thin layer coating). The coating procedure was carried out a vacuum coating.

3.6.2 Energy Dispersive Spectroscopy (EDAX)

Energy dispersive spectroscopy provided by EDAX, was used for phase identification and concentration. All analysis were ZAF corrected. The alteration in elemental composition is a vital analytical tool for interface topography characterization and evaluation. This helps to understand the bonding process and also has a significant impact on the mechanical properties of the bonding. In order to display the distribution of elements, X-ray mapping was carried out to map and present the ceramic-joint interface.

4 Results and discussion

As stated in the literature review, brazes based on the Ti-Al system can potentially be used for metal-ceramic and ceramic-ceramic joints. However, it is unclear as to whether pressure is required in order to create a sound bond. In order to understand the characteristics of the interfacial bond between the bonding materials, Ti-SiC, Ti-Al_2O_3, and Al_2O_3- Al_2O_3 joints were created. Further analysis to understand what type of reactions are occurring will be conducted in the future.

4.1 *Joining of Al_2O_3-to-Ti*

4.1.1 Ti-Al Braze System

In regard to the tests between Aluminium Oxide and Titanium, there were initially a bond between one of the samples, but the joint was later broken. As for the broken bond with Aluminium Oxide, this might be due to the insufficient amount of Aluminium foil in the Ti-Al braze. As aforementioned in the methodology, the cooling rate was not controlled, and therefore this might have had a role in the failure to achieve a bond between Aluminium Oxide and Titanium. There is evidence of foil melting on the surface of the titanium as seen from figure 17.

Figure 17 Foil melting on titanium

As more titanium reacts with aluminium, the high titanium containing aluminides start to form. Another factor for the unsuccessful bonding may be due to the lack of pressure applied in the testing process to make sure there was enough contact between both materials. However, it was previously shown [23] that pressure is not required to achieve a bond. Martin et al. [23]

had not used pressure, yet they achieved a bond despite bonding Aluminium Oxide to Aluminium Oxide via the use of Ti-Al based braze.

At 1450 °C pure Titanium will not melt, however due to the melting of Aluminium it forces Titanium to melt as well. From the phase diagram in figure 18 it can be seen that Aluminium starts to react, with Titanium to initially form low-melting aluminides. TiAl melting temperature is approximately 1420 °C. Hence, the concept is to make use of this molten state at that stage and when it cools down it will solidify, achieving a bond as it is cooling down.

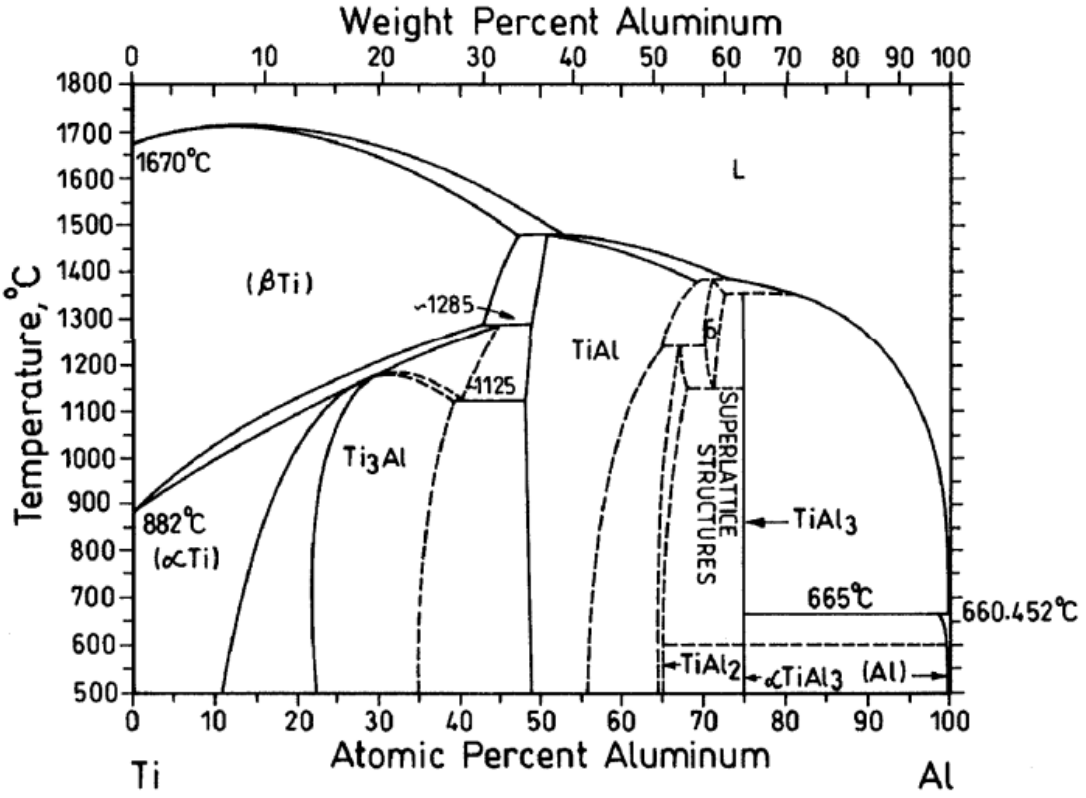

Figure 18 Ti-Al binary phase diagram [66]

Although it is apparent from figure 19 that there is Aluminide forming at the interface with Titanium, a number of voids can be seen which makes the joint unreliable. Therefore, even if Titanium had bonded with Aluminium Oxide, the joint would be relatively weak. At the interface with Titanium, Titanium Aluminide has melted, but it has not bonded very well onto the Titanium. Again, most probably if a joint occurred between Al_2O_3 and Ti it would have broken off. As it

can be seen at the layer at the top, effectively there's not much holding on between Aluminium Oxide and Titanium. Hence, this can be an indication that there is not enough material.

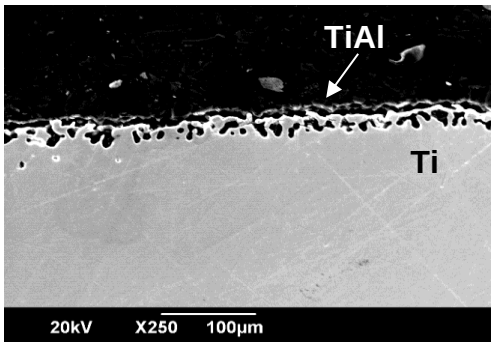

Figure 19 Titanium interface (SEM)

When only foil was placed on Alumina, and later was put into the furnace and subjected to both light microscopy and SEM it showed that Ti-Al braze is not fluid enough. Nonetheless, it can be seen from figure 20 that some Titanium Aluminides have formed. Additionally, some voids can also be seen, suggesting an unreliable joint. For that reason, it has been proposed that an Aluminium foil would cover the interface of Titanium, be placed in the furnace with same brazing parameters and technique, and then add the Ti-Al braze and Alumina sample, and again the same procedure for brazing. The idea was to ensure there is enough Aluminium to form a bond and to potentially produce Titanium aluminides. Initially there was a bond, however, whilst cutting the samples for microscopic analysis, the bond was later broken. Further analysis will also be carried to analyse any reactions and to comment on the strength of the joint.

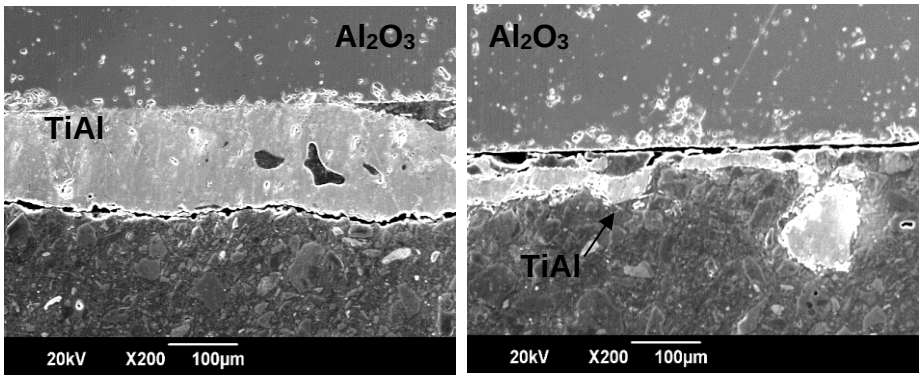

Figure 20 TiAl forming on Aluminium Oxide

4.1.2 LM25 (ready-made powder Ni-based braze)

When nickel was used as a braze, it appeared to have good fluidity, on the other hand Ti-Al braze appears to have poor fluidity which may be the cause of unsuccessful joints. In addition, it appears that LM braze is more fluid than the Ti-Al. Nevertheless, it is still unknown whether the joint is reliable and if the occurring reactions might have a high melting point.

As seen from figure 21, the nickel braze seems to have bonded both materials very well, and as mentioned above this might be due to good fluidity of this braze. Furthermore, additional analysis will be conducted to understand what type of reactions occurred, as well as if the bond has good mechanical strength.

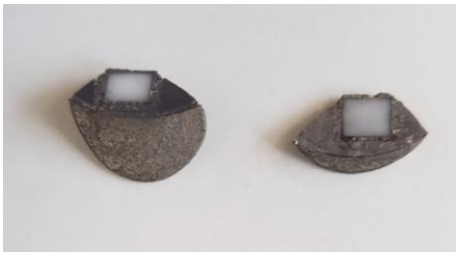

Figure 21 Al_2O_3/Ni/Ti

Figure 22 below is element mapping analysis, showing the interfacial reaction between Ni and Al_2O_3 which was also later on observed during Ti(Ni), Al brazing. Dissolution of Al_2O_3 is occurring resulting in an interfacial bond. After cutting samples to view the cross-section, the braze indicates very good flowability. The mapping also indicates what has been later on observed in all cases where Ni-based braze system were used. This braze is the main reason behind the development of later brazes. The promising and phenomena of Ni towards the Alumina substrate.

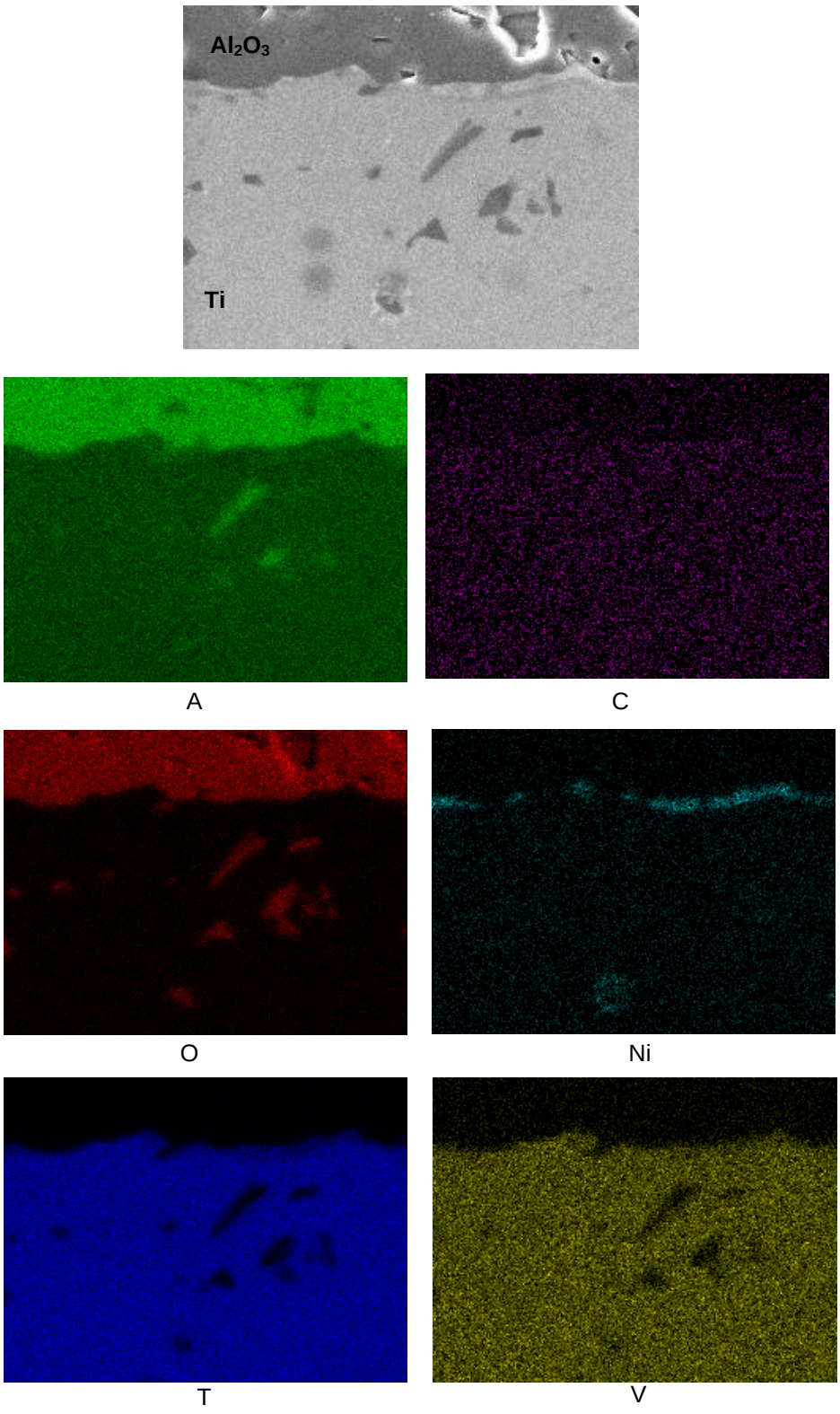

Figure 22 Mapping analysis of LM braze showing elements of substrates and Ni element from braze

4.2 *Joining Al_2O_3 -to- Al_2O_3*

4.2.1 Brazing of Al_2O_3- Al_2O_3 using a (Ti, X)Al Braze

Following the recent successful joining of Al_2O_3 to Al_2O_3 by Martin et al. [23] using a titanium aluminide-based braze, this part of the current investigation further examined the joining capability of a similar system by adding a third element to the braze composition. The aim of the third element addition was to investigate whether this approach would enhance the wetting between the braze and Al_2O_3 and improve the bond strength between them. The elements that were chosen as additions were nickel and iron. These were specifically selected because of their well-known interaction with aluminium to form aluminides. The braze compositions that were investigated were based around the TiAl and (TiAl + $TiAl_2$) phase fields that are present in the Ti-Al equilibrium phase diagram that is presented in Figure 18 [66] and are summarised in Table 7.

Table 7 showing the braze compositions that were used for the Ti-Al, Ti-Al-Ni and Ti-Al-Fe systems to join Al_2O_3 to Al_2O_3.

Test name	Ti		Al		Fe		Ni	
	Wt %	At %	Wt %	At %	Wt %	At %	Wt %	At %
TiAl7.2Ni_Al_2O_3	64.8	53.8	28	41.3	-	-	7.2	4.9
TiAl7.2Fe_Al_2O_3	64.8	53.7	28	41.2	7.2	5.1	-	-
TiAl_Al_2O_3	72	59.2	28	40.8	-	-	-	-
TiAl3.6Ni_Al_2O_3	68.4	56.5	28	41.1	-	-	3.6	2.4
TiAl3.6Fe_Al_2O_3	68.4	56.4	28	41.0	3.6	2.6	-	-
TiAl28.8Ni_Al_2O_3	43.2	37.1	28	42.7	-	-	28.8	20.2
Ti64Al36_Al_2O_3	64	50	36	50	-	-	-	-

Prior to undertaking brazing experiments for these systems, it was decided to conduct contact angle measurements at a temperature of 1500°C in order to investigate the effect of the third element addition on the wettability of the proposed compositions with Al_2O_3. These measurements were obtained under a flushing gas of argon with 5% hydrogen, while a zirconium “getter” was placed around the specimens to minimize the presence of oxygen in the gas. The proposed compositions were based around the Ti-50at%Al (or 64wt%Ti-36wt%Al and

referred to as Ti64-Al36) composition with either iron or nickel partially replacing aluminium. One of the compositions (TiAl28.8Ni) had higher levels of nickel at the expense of titanium as shown in Table 7. A plot of contact angle with time is presented in figure 23 and shows that all compositions had reached an equilibrium contact angle within about 100-150 seconds and that the contact angle remained virtually constant thereafter. The results are summarized in Table 8 show that the measured contact angle between the reference composition of Ti64Al36 with Al_2O_3 was 60°. From the results, it is evident that the addition of either iron or nickel led to a decrease in the contact angle between the braze and Al_2O_3. The addition of 3.6wt% nickel resulted in a decrease of the contact angle down to 48°, while a value of 50° was measured for an equivalent amount of iron. By raising the amount of either nickel or iron to 7.2wt%, the measured contact angle values dropped down to 29° and 32° respectively. The results also suggested that no further benefit occurred by extending the amount of nickel in the braze beyond 7.2%wt. These results showed that the addition of either nickel or iron led to a significant reduction in the contact angle values between the braze and Al_2O_3 and further analysis was undertaken to understand the reasons behind these observations. Since the addition of nickel had led to a greater decrease in the contact angle most of the Investigation on the third element addition to the Ti-Al system was based on this metal.

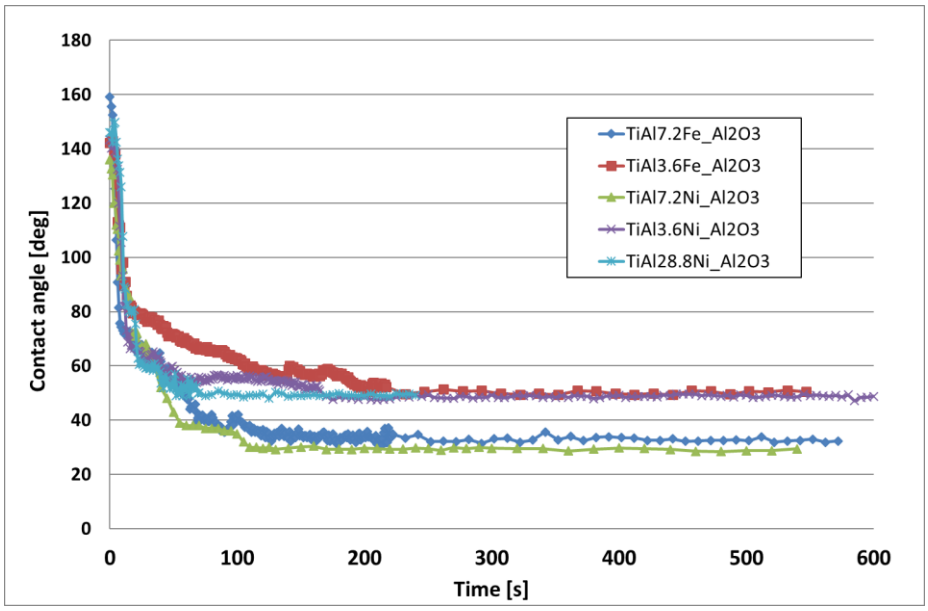

Figure 23 Plot of contact angle value vs time for the tested braze compositions

Table 8 Summary of wetting contact angle for the tested compositions.

Composition (wt%)	Contact angle
Ti64Al36_Al_2O_3	60
TiAl7.2Ni_Al_2O_3	29
TiAl7.2Fe_Al_2O_3	32
TiAl_Al_2O_3	Did not melt
TiAl3.6Ni_Al_2O_3	48
TiAl3.6Fe_Al_2O_3	50
TiAl28.8Ni_Al_2O_3	49

Examination of a TiAl7.2Ni sectioned sample in Figure 24 showed that the interface line had receded slightly with a small amount of Al_2O_3 dissolving in the braze.

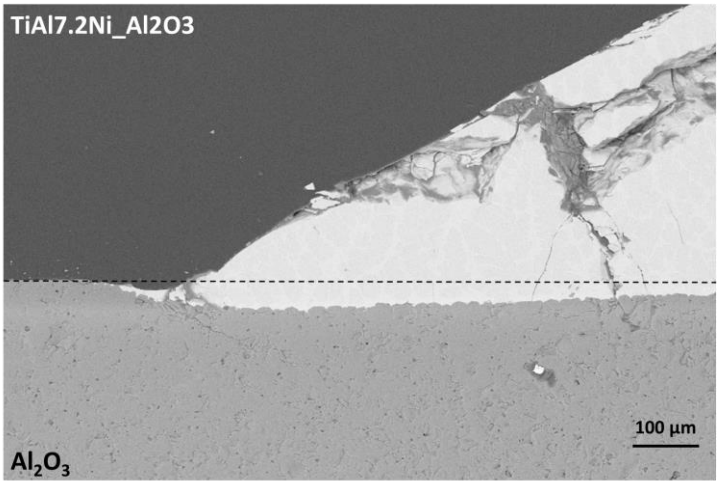

Figure 24 Micrograph showing the wetting interface between TiAl7.2Ni and Al_2O_3 with evidence of dissolution of Al_2O_3.

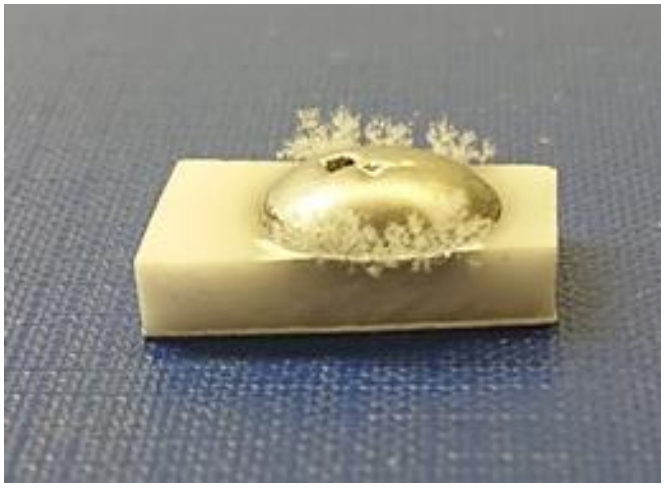

Figure 25 Micrograph showing a wider overview of the wetting angle experiments are presented in Figure 24.

From these micrographs (figure 24 & 25), it was apparent that there was formation of Al_2O_3 whiskers at the edge of some brazes. One possible source of the Al_2O_3 whiskers may be the evaporation of aluminium followed by oxidation. From chemical thermodynamics data as compiled by Turkdogan [67], the Gibb's Free energy, $\Delta G°$, of the vaporisation of aluminium from molten aluminium

$$Al(l) \rightarrow Al(g)$$

is given as

$$\Delta G° = (72{,}810 – 26.17T) \times 4.18 \text{ J/mol}$$

and

$$\Delta G° = \Delta H° - T\Delta S° = -RT \ln k$$

where $\Delta G°$ is the Free energy change for the reaction in J/mol, $\Delta H°$ is the enthalpy of the reaction in J/mol, T is the temperature in K, $\Delta S°$ is the entropy change for the reaction in J/mol.K, R is the gas constant in J/mol.K and k is the equilibrium constant and in this case is represented by k = pAl,/ aAl, where aAl is the activity of molten aluminium and pAl is the partial pressure of aluminium in atm. By assuming the activity of aluminium to be equal to 1, the partial pressure of aluminium vapour at 1500°C can be calculated to be 5.55 x 10-4 atm. Of course, in the presence of titanium and nickel within the melt, the activity of aluminium is going to be lower than 1 and its vapour pressure would also be lower. The calculation as presented can be used as an approximation and it suggests that the vapour pressure of aluminium is high enough

for a small amount of evaporation of aluminium to take place. Whisker growth normally occurs via the vapour-liquid-solid (VLS) mechanism as explained by Wagner [68], and the aluminium vapour would be expected to turn to liquid and then to oxidise to Al_2O_3 by the reaction

$$2Al(l) + 3/2\ O2(g) \rightarrow Al2O3(s)$$

and

$$\Delta G°f,Al_2O_3 = (-403{,}260 + 78.11T) \times 4.18\ J/mol = -RT\ ln\ k \text{ (where } k = aAl_2O_3 / aAl_2\ pO_{23/2})$$

The equilibrium partial pressure of oxygen for the oxidation of molten aluminium at 1500°C was calculated to be 1.75 x 10-22 atm (assuming an aluminium activity of equal to 1). However, for the contact angle measurements, a zirconium oxygen “getter” was used and the expected oxygen partial pressure in the system was expected to be dictated by the reaction

$$Zr(s) + O2(g) \rightarrow ZrO2(s)$$

where

$$\Delta G°f,ZrO2 = (-261{,}000 + 43.9T) \times 4.18\ J/mol$$

The expected oxygen partial pressure of the system has been calculated to be 2.64 x 10-23 atm, a value which is lower than that required for the oxidation of aluminium. These values suggest that the vapour pressure of oxygen in the system would not have been sufficiently high for the oxidation of Al to Al_2O_3 to take place. Therefore, the formation of the whiskers by evaporation and oxidation of aluminium is unlikely. The only other possible mechanism for Al_2O_3 whisker formation is by reaction between aluminium and Al_2O_3 to form gaseous Al2O followed by the reverse reaction

$$Al2O3(s) + 4Al \rightarrow 3Al2O(g)$$

where

$$\Delta G° = (280{,}860 – 113.51T) \times 4.18\ J/mol$$

Assuming an aluminium activity value equal to 1, the calculated partial pressure of Al_2O at 1500°C is 5.36 x 10-4 atm. Such a low partial pressure of Al_2O is suggestive of low-level interaction between Al_2O_3 and aluminium are the reverse reaction can potentially yield Al_2O_3 whiskers. The feasibility of this low-level interaction was previously confirmed by Porter et al

[69], who used mass spectrographic analysis that had shown that aluminium vapour and gaseous Al_2O were the predominant vapour/gaseous species when molten aluminium came to contact with Al_2O_3.

The reverse reaction,

$$3Al2O(g) \rightarrow 4Al(l) + Al2O3(s)$$

is most likely to occur during the cooling stage and this is likely to promote whisker growth if there is low-level supersaturation of Al_2O. The equilibrium partial pressure of Al_2O decreases as the temperature decreases; therefore, during cooling, there is supersaturation of gaseous Al_2O and this promotes Al_2O_3 whisker growth during the reverse reaction [70]. This appears to be the most likely mechanism for Al_2O_3 whisker growth and this is particularly interesting as far as wetting is concerned because it implies that the wetting is aided by the interaction between molten aluminium and Al_2O_3. Other possible causes of improved wetting via oxygen chemisorption can be discounted; while aluminium has a great affinity of oxygen, the solubility of Al_2O_3 in aluminium is extremely low and therefore oxygen chemisorption in this system would be rather limited [60]. According to Eustathopoulos [60], [71], modification of the surface chemistry of the oxide surface is possible leading to a lower oxygen to metal ratio in the oxide, but no interaction mechanisms for this to happen were given. Further support for this is provided by recent work [72] on Al/AlOx/Al tunnel junctions that are used in electronic devices; this study [72] has provided experimental evidence that there is oxygen deficiency at the interface at room temperature with the ratio between oxygen and aluminium at the oxide surface ranging between 0.8 to 1.3 (in comparison to 1.5 for Al_2O_3). The observation by Hauser [73] that an increase in the wettability of Al_2O_3 by aluminium can be achieved by reduction of the partial pressure of oxygen adds further support to the “oxygen-deficiency” mechanism since a decrease in the surface stoichiometry of Al_2O_3 is possible at lower oxygen potential. It must also be noted that the interaction between aluminium and Al_2O_3 to form the gaseous Al_2O which has a lower oxygen level is likely to lead to oxygen deficiency at the surface of Al_2O_3. Therefore, previous research suggests that some interaction between aluminium and Al_2O_3 can take place. Such interaction at higher temperatures to yield Al_2O is one possible mechanism that may enable wetting of Al_2O_3 by aluminium and this is proposed to be active for the examined samples since

this is also associated with Al_2O_3 whisker growth as observed in the present investigation. However, the contact angles between Al_2O_3 and molten aluminium as reported in the literature [71] range between 90° and 130° and such values are much higher than the values reported in the current work. The percentage amount of aluminium that was used in the proposed brazes was the same for all compositions except for the Ti-36wt%Al composition and it is important to also consider the activity of aluminium in the melt as this will affect the reaction between Al_2O_3 and aluminium,

$$Al2O3(s) + 4Al(l) \rightarrow 3Al2O(g)$$

since the activity of liquid aluminium in the melt will also be dependent on its interaction with both titanium and nickel. Theoretically, a higher aluminium activity will promote the above reaction as it will also yield a higher partial pressure of Al_2O and thus drive the reaction to the right. From this, it can be implied that the TiAl28.8Ni composition promoted a sufficiently high activity of aluminium (due to the higher content of aluminium) to drive the interaction with Al_2O_3. In samples containing lower levels of aluminium, no Al_2O_3 whiskers were formed; a lower aluminium activity value is likely at lower levels of aluminium and this may reduce the driving force for interaction with Al_2O_3. Thus, at lower levels of aluminium, other mechanisms may come into force and these need to be considered. In any case, additional mechanisms may be activated in the presence of titanium and nickel as the earlier studies on the wettability of aluminium for Al_2O_3 have reported higher contact angles. In other words, there must be alternative or additional mechanisms that lead to the higher wettability for the Ti-Al-Ni brazes that were used in the present work.

Before addressing the effect of nickel additions, a wider review of the literature was necessary to also understand the possible wetting of Al_2O_3 by titanium. The effect of small additions of titanium to aluminium on the wetting of Al_2O_3 at 1000°C was the subject of an investigation by Sui et al [74]. The results of their study [74] showed a significant drop in the contact angle from values that ranged from 118° to 141° for pure aluminium down to values ranging from 65° to 84° when 5 at% titanium had been added. By using high resolution scanning transmission electron microscopy (STEM) the authors [74] observed a small number of spots of a TiOx phase

of size between 100nm to 200nm at the interface with Al_2O_3. However, this seemed to be a rare occurrence within the sample and there was no evidence of a continuous TiOx layer. For this reason, the authors [74] suggested that the improved wetting effect was not due to formation of TiOx. Instead, they proposed that the observed effect was due to some contribution of titanium to the reaction,

$$Al2O3(s) + 4Al(l) \rightarrow 3Al2O(g)$$

However, consideration of the above reaction would suggest that the addition of titanium to the aluminium melt would lead to a drop in the activity of the latter. In addition, any interaction between Al_2O_3 and the TiOx phase would lead to reduction in the activity of Al_2O_3. Thus, based on chemical thermodynamics considerations, the addition of titanium to the aluminium melt is likely to lead to a drop in the activity of the reactants and to a decrease in the thermodynamic driving force for the above reaction. Therefore, the addition of titanium will not enhance the reaction from a purely chemical thermodynamic point of view. This does not necessarily mean that interaction between molten aluminium and Al_2O_3 is no longer feasible as there may be a different way to contribute to the interaction. It is rather possible that an additional mechanism or interaction may be active. One possible effect may be due to melting and/or dissolution of Al_2O_3 when it comes into contact with the melt. Inspection of the Al-rich corner of the isothermal cross-section of the Al-Ti-O equilibrium phase diagram [75] shown in figure 26 [74] reveals liquid formation at additions below 1.6 at% Ti, while at higher contents of titanium, there is liquid formation along with TiAl3 and Al_2O_3.

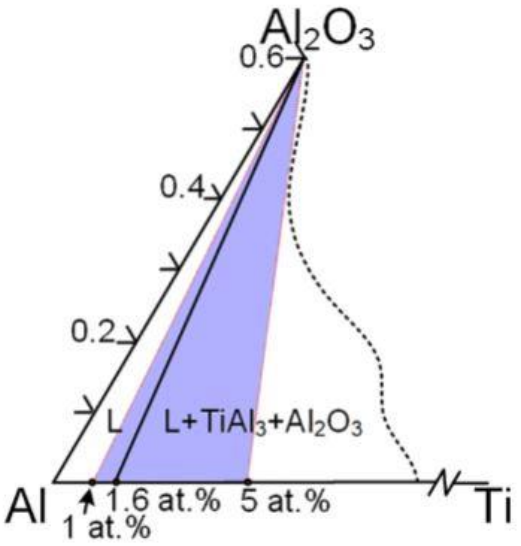

Figure 26 Al-rich corner of isothermal cross-section of Al-O-Ti ternary phase diagram at 1273 K [73]

Even though Sui et al [74] did not report any observation of $TiAl_3$, the Al-Ti-O equilibrium phase diagram shows that some dissolution of Al_2O_3 in the liquid phase can take place and this is the most likely mechanism of improvement of the wettability of Al_2O_3 in Al-Ti melts. It is therefore necessary to consider the reaction

$$Al2O3(s) \rightarrow 2[Al]melt + 3[O]melt$$

by which Al_2O_3 dissociates and dissolves in the melt. In fact, this particular reaction is unlikely to take place when Al_2O_3 is in contact with a melt that contains only aluminium because of the strong affinity of aluminium for oxygen and the low solubility of oxygen in aluminium. On the other hand, an inspection of the Ti-O equilibrium phase diagram [76] shows substantial solution of oxygen in both α-Ti and β-Ti and thus the addition of titanium is likely to enhance the wettability of Al_2O_3. According to Merlin and Eustathopoulos [77], the dissolved aluminium and oxygen can combine together to form Al_2O by the reaction:

$$2[Al]melt + [O]melt \rightarrow Al2O(g)$$

and the overall reaction can be written as:

$$Al2O3(s) + 4Al(l) \rightarrow 3Al2O(g)$$

It can thus be concluded that the “contribution” of titanium [74] is the dissolution of Al_2O_3 in the titanium-containing aluminium melt; this promotes the overall interaction between Al_2O_3 and aluminium since both become constituents of the melt.

It is also important to understand the effect of the nickel addition to the TiAl braze and previous work on the wettability of nickel with Al_2O_3 had to be considered. The wetting of Al_2O_3 by nickel has been investigated by Levi and co-workers [78], who conducted a series of sessile drop experiments at 1500°C and observed dissolution of Al and O in initially pure nickel. By using EDAX analysis in secondary electron images, it was also observed that the dissolved aluminium was segregating at the nickel surface. By further analysis in later work, Levi et al [79] proposed that the segregation of aluminium at the surface of nickel had led to a reduction in the surface Free energy of the melt. Merlin and Eustathopoulos [77] had previously shown that at temperatures between 1397°C and 1482°C in helium, the addition of aluminium to nickel (mole fraction of 0.25 aluminium) had led to a reduction of the wetting angle with Al_2O_3 to 83° in comparison to an angle of 112° for pure nickel. containing a high mole fraction (0.25) of aluminium, while there was an opposite effect at mole fractions below 0.08, but it must be stressed that these measurements were conducted at higher temperatures of 1650°C and 1750°C. SEM characterisation revealed the presence of small oxide particles close to the metallic surface. Similar observations with the work of Merlin and Eustathopoulos [77] have been reported in recent work by Valenza et al [80]. By conducting contact angle measurements and using results from earlier work [81], Gauffier et al [82] also showed that the addition of aluminium to nickel improved the wettability with Al_2O_3. Similar observations were also presented by Gauffier et al [82] who conducted contact angle measurements and use results from earlier work [81]. All of these studies have shown evidence of wetting of Al_2O_3 by nickel taking place by dissolution of Al_2O_3 in nickel. Further evidence of the possibility of such dissolution has been provided by a Ni-Al-O phase diagram that was presented by Fritscher et al [83]. The presence of aluminium in nickel either by intentional addition or from dissolution of Al_2O_3 appeared to improve the wettability of Al_2O_3 by nickel melts.

The above discussion based on results from the literature has shown mechanisms by which aluminium, titanium and nickel can, on their own, wet Al_2O_3. Furthermore, the binary systems Al-Ti and Al-Ni seem to exhibit better wettability in compared to results when these metals are applied on their own. The contact angle measurement of 29° for the TiAl7.2Ni_Al_2O_3 composition is by far the lowest that has been reported in the reviewed literature. The measured contact angle for the Ti64Al36_Al_2O_3 system was 60° and the addition of any amount of nickel led to significant decrease in the contact angle and thus to improved wetting. These results implied that the improved wetting may have been dominated by the presence of nickel. In order to further explore this hypothesis, SEM and EDAX analyses of brazed samples were undertaken.

The results of the wetting angle measurements also revealed that, similar to the effect of nickel, the addition of iron also led to improvement in the wettability for Al_2O_3. The wetting angle for the TiAl7.2Fe_Al_2O_3 sample was 32° and an angle of 50° was measured for TiA3.6Fe_Al_2O_3. This behaviour was attributed to Al_2O_3 dissolving in iron. In a recent investigation, Kang et al [84], showed that the solubility of Al_2O_3 in iron occurs in molten steel. Further investigation on this system was also carried out by SEM and EDAX analyses of brazed samples. In summary, the improved wetting of Al_2O_3 by additions of either nickel or iron to TiAl was attributed to more dissolution of Al_2O_3 in the presence of nickel and iron. Previous studies of the relevant equilibrium phase diagrams had indicated the dissolution of Al_2O_3 in both nickel and iron. By contrast, the dissolution of Al_2O_3 in aluminium and titanium is much lower owing to the greater affinity of these two metals for oxygen.

4.2.1.1 Brazing using (Ti, Ni)Al

Figure 27 shows an SEM micrograph of the interface between the braze and Al_2O_3. The formation of two phases was observed in the braze. This observation was confirmed by the results of elemental mapping shown in figure 28. The presence of a continuous phase (grey colour in figure 27), while a light grey coloured phase was also observed. The latter appeared to precipitate out within the matrix phase and to also form adjacent to the entire interface with Al_2O_3. Consideration of the results spot-analysis using EDAX as presented in figure 29

suggested that the light grey phase was Al_3NiTi_2 and this was the phase that provided the bond with Al_2O_3. It is clear that during formation of the bond by the braze, the nickel migrates to the interphase with Al_2O_3 and upon cooling, solidification takes place to form Al_3NiTi_2.

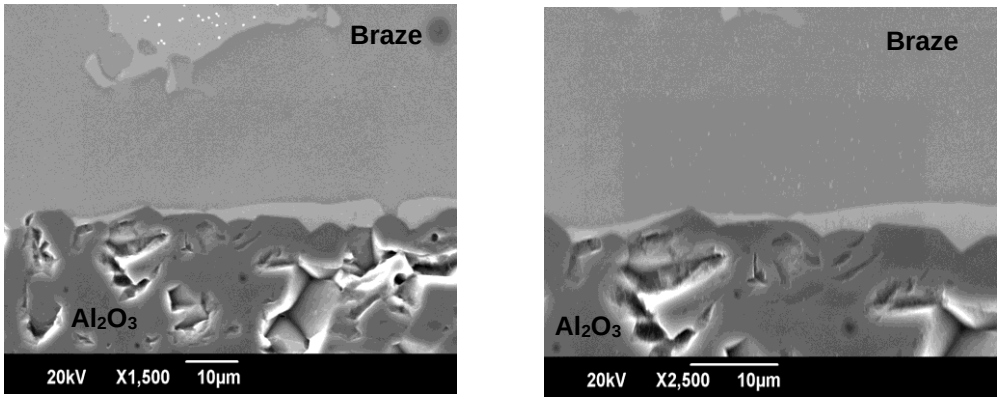

Figure 27 SEM of $(Ti_{0.92}Ni_{0.08})Al$ braze system used for joining Al_2O_3-to- Al_2O_3

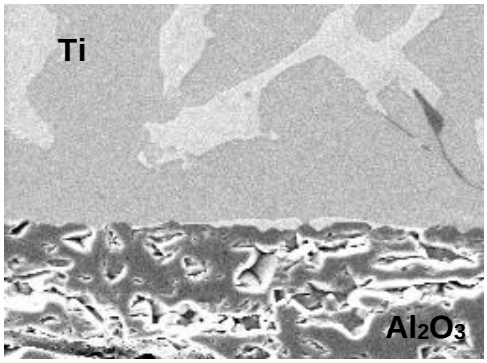

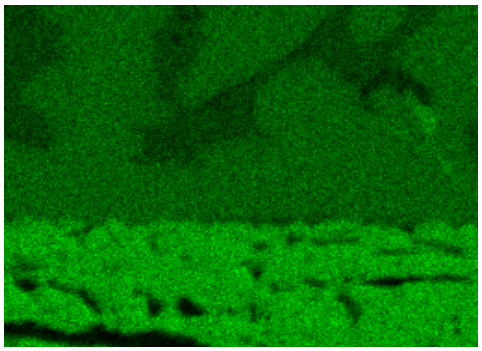

Al

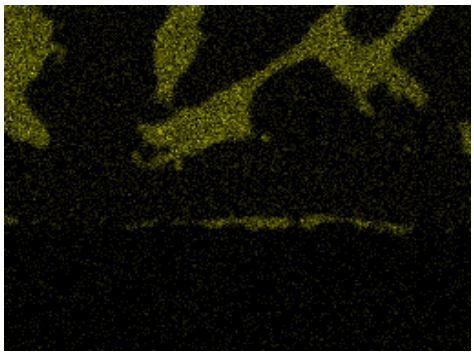

Ni

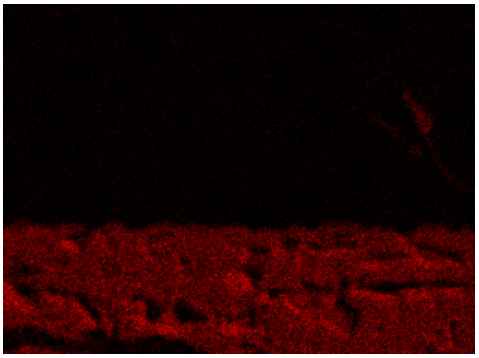

O

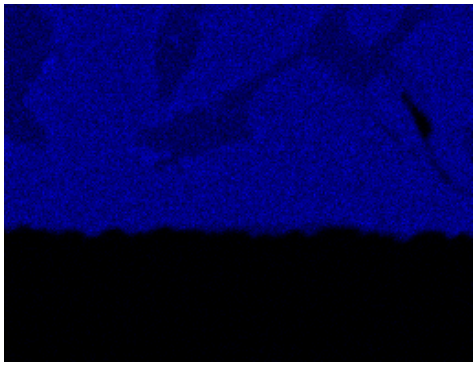

Ti

Figure 28 Mapping analysis of $(Ti_{0.92}Ni_{0.08})Al$ brazing Al_2O_3-to-Al_2O_3

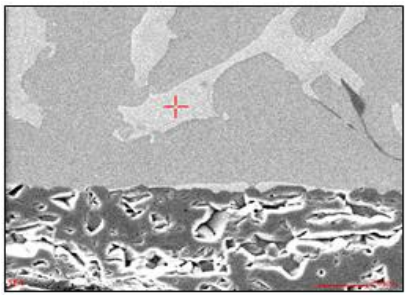

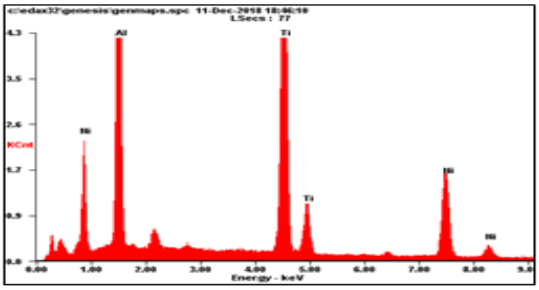

Element	*Wt%*	*At%*
AlK	35.18	50.90
TiK	39.92	32.54
NiK	24.90	16.56
Matrix	Correction	ZAF

Figure 29 EDAX result showing Al_3NiTi_2 phase.

EDAX analysis shown in figure 31 revealed that the darker grey continuous phase was TiAl with about 1% Ni dissolved in it. More Ni was observed in the bright area at the interface with alumina (figure 32). Inspection of a section of the Al-Ni-Ti equilibrium phase diagram presented in figure 30 shows that the composition used lies marginally within the $\alpha + \tau_3$ phase field (Al_3NiTi_2). The observation that the Al_3NiTi_2 phase covers the entire interface with Al_2O_3 suggested that the two phases may be chemically more compatible in relation to the TiAl-Al_2O_3 couple. In order to explore this possibilty, it was decided to undertake wetting angle measurements for some of the compositions that were investigated and the results (along with the compositions) are shown in Table 7. It is apparent the the contact angle between the braze and Al_2O_3 dropped when nickel was added to TiAl. Indeed there was a drop in the value of the contact angle from 60° for TiAl down to 29° when 7.2% of Ni was added. This is a significant drop and is likely to enhance the adhesion at the interface with Al_2O_3. In order to understand this behaviour, further SEM examination was undertaken for samples that were obtained from the wetting angle measurement experiments.

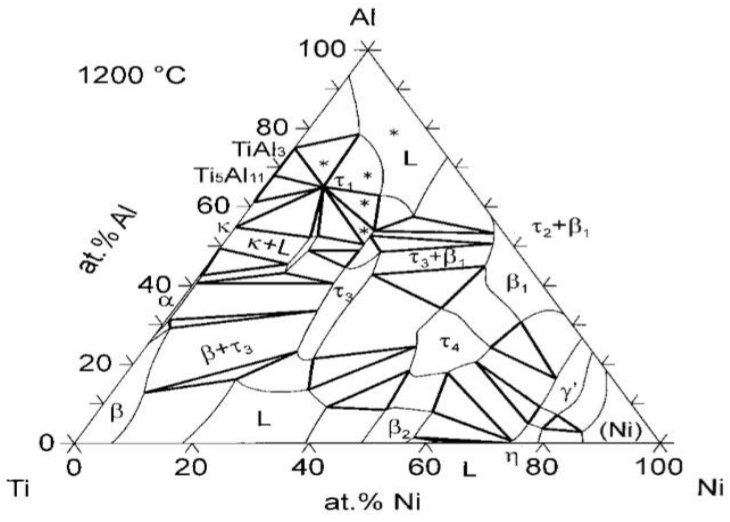

Figure 30 Al-Ni-Ti ternary phase diagram [34]

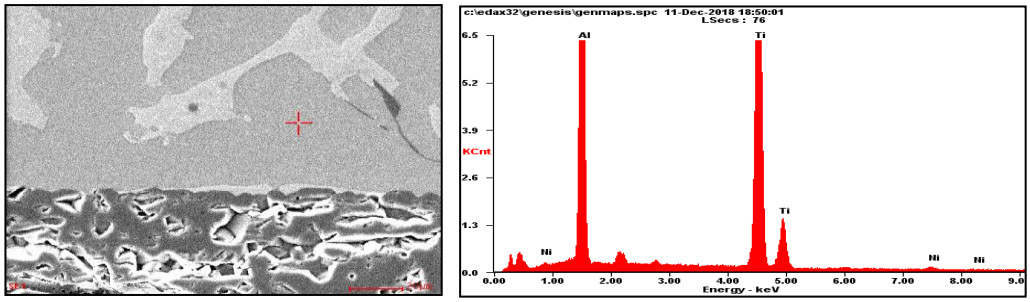

Element	Wt%	At%
AlK	42.44	56.77
TiK	56.50	42.57
NiK	01.06	00.65
Matrix	Correction	ZAF

Figure 31 EDAX result showing TiAl with few amounts of Ni (dark area)

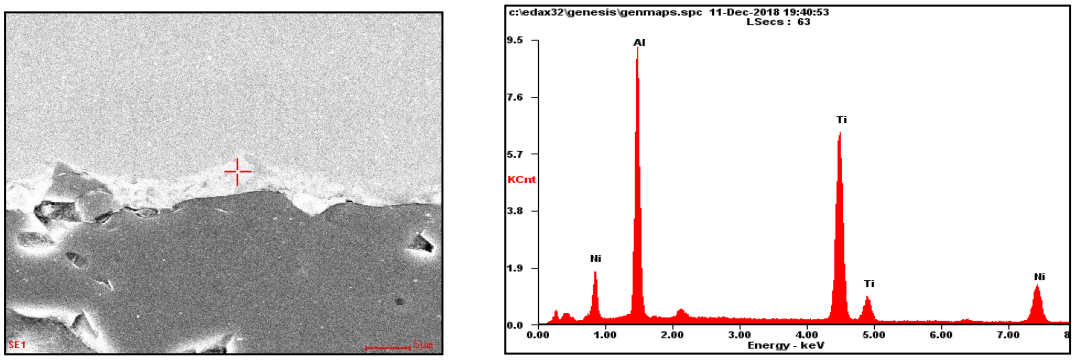

Element	Wt%	At%
AlK	36.70	52.43
TiK	40.63	32.70
NiK	22.66	14.88
Matrix	Correction	ZAF

Figure 32 EDAX of ($Ti_{0.96}Ni_{0.04}$)Al brazing Al_2O_3-to-Al_2O_3 showing high amounts of Ni element at interface with alumina

Figure 33 shows a cross-section of a sample from the contact angle measurements. The dotted line represents the original interface prior to reaching interfacial equilibrium. It appears that some interaction had taken place between the Al_2O_3 and the melt. This is rather surprising because consideration of the Gibbs free energy of formation ($\blacktriangle G^{\theta}$) of Al_2O_3 shows that it is thermodynamically more stable than the oxides of nickel and titanium. The reduction of Al_2O_3 by either nickel or titanium is unlikely. Figures 33 & 34 are illustration images of the sessile drop, the mechanism of measuring the contact angle.

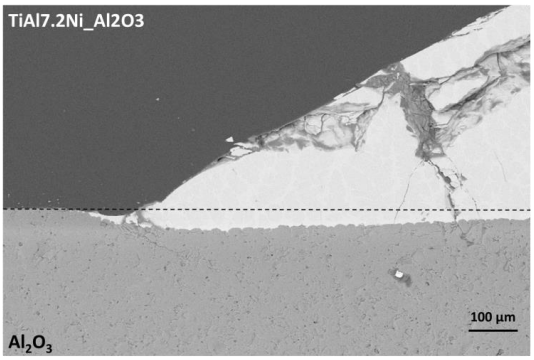

Figure 33 SEM of ($Ti_{0.92}Ni_{0.08}$)Al after contact angle measurements

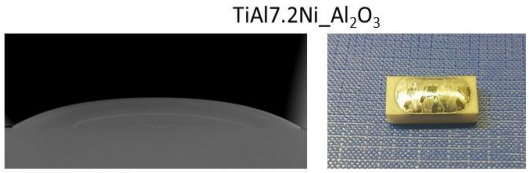

Figure 34 Illustration of sessile drop to measure contact angle of ($Ti_{0.92}Ni_{0.08}$)Al

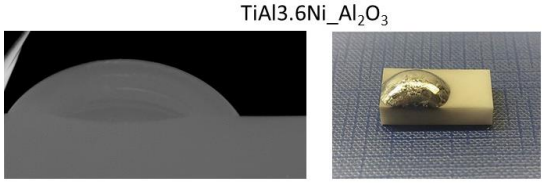

Figure 35 Illustration of sessile drop to measure contact angle of ($Ti_{0.96}Ni_{0.04}$)Al

4.2.1.1.1 SEM and EDAX analyses of Al_2O_3 brazed with (Ti,Ni)Al

Following the wetting angle measurements, brazing of Al_2O_3 to Al_2O_3 was undertaken for SEM and EDAX investigation and to also carry out lap shear tests. Figure 36 was taken from the study of Martin and Triebert [23] who used brazes based on TiAl (without third-element addition). The SEM micrograph shows the interfacial bond between the braze and Al_2O_3. The presence of TiAl (white) and Ti_3Al is evident. Parts of the Al_2O_3 interface were wetted by TiAl and some parts were wetted by Ti_3Al. The examination suggested that there was no specific interfacial preference of the two aluminides for Al_2O_3.

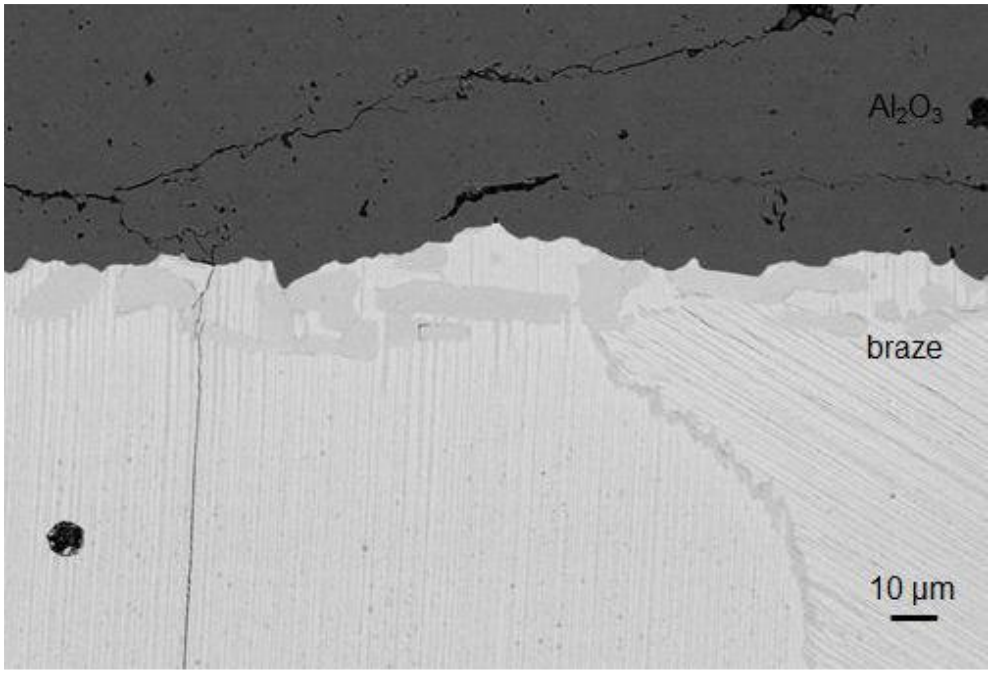

Figure 36 showing the interface between TiAl braze with Al_2O_3 [23]

Figure 37 shows an SEM micrograph of the interface between the TiAl7.2Ni braze and Al_2O_3 and presents evidence of the formation of two phases within the braze. This observation was confirmed by the results of elemental mapping shown in figure 38. The presence of a continuous matrix phase (grey colour) and a light grey coloured phase was observed. The latter of the two phases appeared to form not only within the continuous matrix phase but to also form adjacent to and in direct contact with Al_2O_3. In fact, the entire brazed Al_2O_3 surface was covered by the light grey phase. Consideration of the results of spot-analysis using EDAX as presented in figure 39 suggested that the light grey phase was the Al_3NiTi_2 phase designated in the Al-Ni-Ti equilibrium phase diagram constructed by Huneay et al [85] as τ3. These observations suggested that the τ3-Al_3NiTi_2 phase provided the bond with Al_2O_3. The EDAX analysis for the darker of the two phases in the braze is presented in figure 39 and has composition of 56.77at% Al, 42.57at% Ti and 0.65at% Ni. Evidently this phase contains only a tiny amount of nickel and is based on the TiAl phase. Inspection of the Al-Ni-Ti equilibrium phase diagram obtained by Huneay et al [85] at 900°C suggests that the braze composition that was used lied within the TiAl + Ti_3Al + τ3 phase field. However, in the present braze samples (at room temperatures), no third phase (Ti_3Al) was detected. The SEM observations show clear evidence that the phase that formed at the interface between the braze and Al_2O_3 was the nickel-containing τ3 phase. The reason for the improved wetting was therefore most likely due to the presence of the nickel-

containing τ3 phase. From the earlier discussion, it is evident that all three of the braze constituent elements have the means to interact with Al_2O_3. These three elements formed a melt at the dwelling temperature. When the melt was in contact with Al_2O_3, the three wetting mechanisms can be active. The presence of the nickel-containing τ3-Al_3NiTi_2 phase in direct contact with Al_2O_3 suggests that the solubility of Al_2O_3 in nickel may be the most active mechanism leading to improved wetting. Consideration of the Gibbs Free energy of formation of the oxides of the three constituent elements shows that aluminium has the highest attraction for oxygen; this suggests that aluminium is more likely to react with oxygen than to dissolve it. Titanium also has a high tendency to react with oxygen, while nickel has the least. For this reason, nickel which is less reactive than the other two metals can permit more solution of oxygen within it and can be expected to allow more dissolution of Al_2O_3 to take place. The contact and interaction between Al_2O_3 and nickel from the melt leads to precipitation of τ3-Al_3NiTi_2 at the braze-ceramic interface. A continuous TiAl phase with τ3-Al_3NiTi_2 particles is formed away from the interface. The lowest wetting angle (and therefore the best wetting) has been achieved in the presence of nickel with the formation of the τ3-Al_3NiTi_2 phase in contact with Al_2O_3.

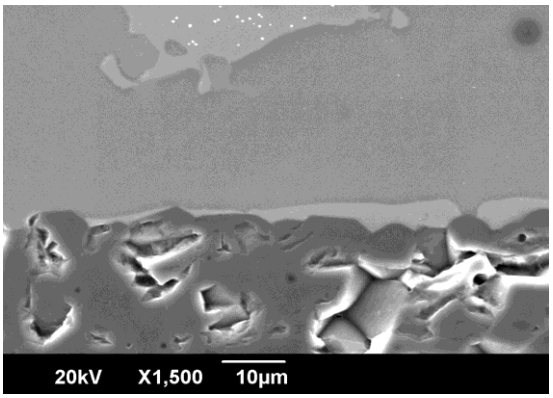

Figure 37 SEM of ($Ti_{0.92}Ni_{0.08}$)Al joining Al_2O_3-to-Al_2O_3 bright area at interface rich of Ni element from braze system

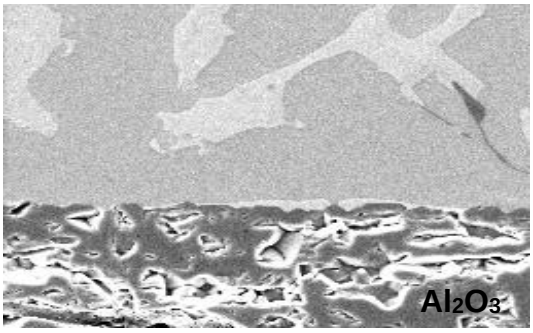

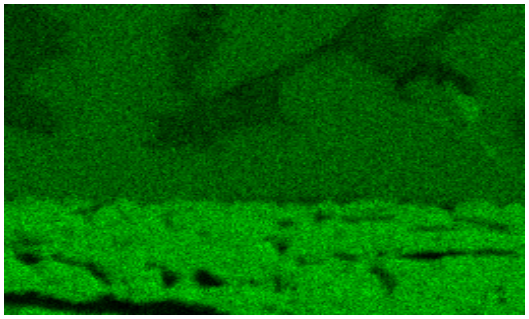

Al

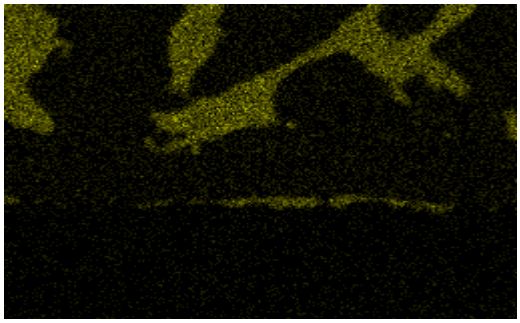

Ni

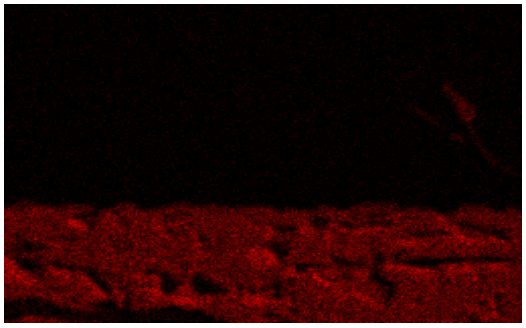

O

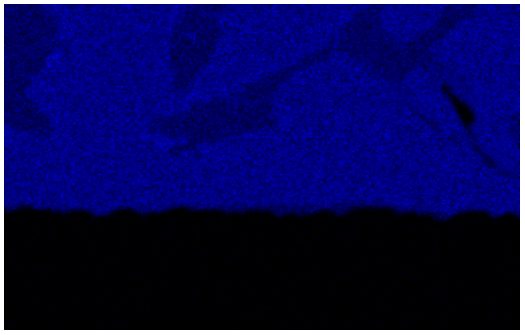

Ti

Figure 38 Mapping area of $(Ti_{0.92}Ni_{0.08})Al$ joining Al_2O_3-to-Al_2O_3

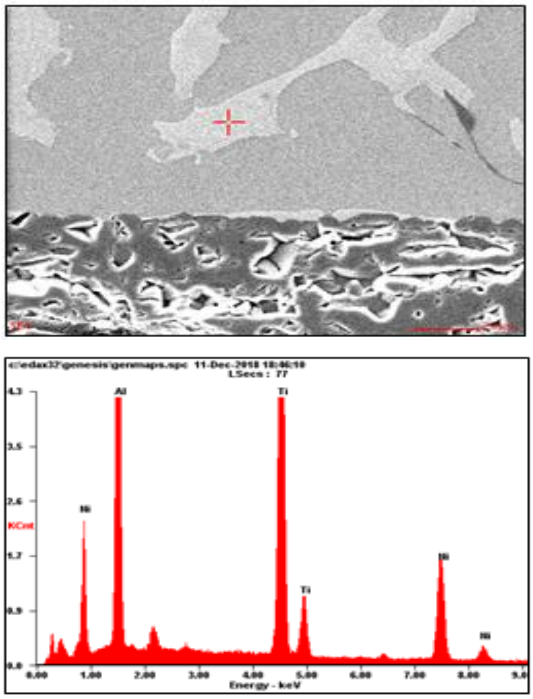

Figure 39 EDAX result showing Al_3NiTi_2 phase

The observation that the Al_3NiTi_2 phase covers the entire interface with Al_2O_3 suggested that the two phases may be chemically more compatible in relation to the TiAl-Al_2O_3 couple.

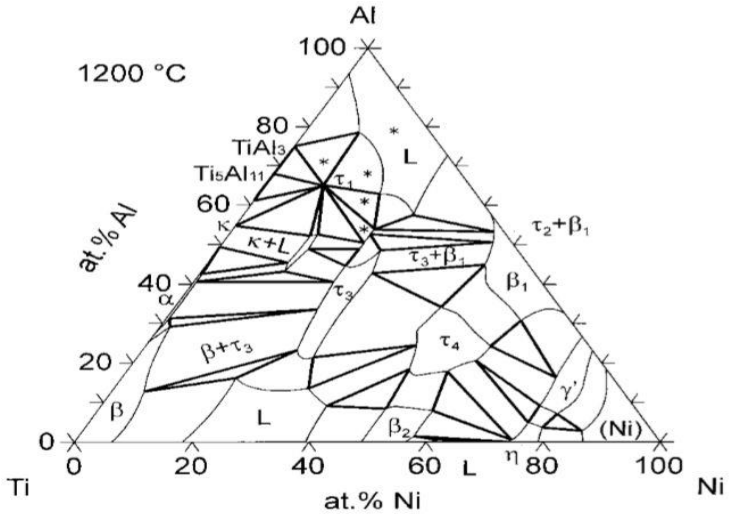

Figure 40 Al-Ni-Ti ternary phase diagram [34]

4.2.1.2 Brazing using (Ti, Fe)Al

The contact angle measurements showed that the addition of iron to TiAl had led to an improvement in the wettability with Al_2O_3. The best results were achieved with TiAl7.2Fe_Al_2O_3 with a contact angle of 32°. Figure 42 shows an SEM micrograph from brazing using this

composition. It is evident that there is a continuous phase layer forming on the interface with Al_2O_3. EDAX analysis taken from the interfacial layer of the braze with Al_2O_3 shows the presence of a small amount of iron (1.26 at%) in addition to titanium (42.35 at%) and aluminium (56.39 at%). However, EDAX analysis taken from the inner and central parts of the braze shows that iron was absent form these areas. The only region where iron was present was right at the interface with Al_2O_3. These observations suggested that the entire iron that was in the braze was situated at the interface with Al_2O_3. By referring to the equilibrium ternary phase diagram for the Al-Fe-Ti system shown in figure 41, the observed EDAX composition at the interface consisted of TiAl with iron dissolved in it. As mentioned earlier in the thesis, interaction between Al_2O_3 and aluminium is possible via reaction to form Al_2O, while dissolution of Al_2O_3 in titanium can also take place. However, further improved wetting was observed in the present study when iron was added to the Ti-Al-based braze. The effect of the improved wettability with additions of iron is evident in the micrograph in figure 42 that shows bonding between the braze and Al_2O_3. This improvement in the wetting has been attributed to the ability of iron to dissolve Al_2O_3. Iron has a lower affinity for oxygen than titanium does, and this allows the former to achieve greater dissolution of Al_2O_3 and hence to lead to improved wetting.

Away from the interface, the braze microstructure appeared to be two-phase showing a lamellar structure between a dark and a bright phase. The composition obtained by EDAX lies very close to the boundary between TiAl and (TiAl + $TiAl_2$). The darker area is likely to represent TiAl, while the brighter lamellar areas are likely to be the $TiAl_2$ phase. It must be noted that the results of the EDAX analysis differ slightly from the original composition which was 41.2 at% Al, 53.8 at% Ti and 5.1 at% Fe. It is not clear why such a difference in composition was observed. Considering that the braze composition dwelled at 1500°C for one hour, the possibility of some loss of the three metals by evaporation is possible given the relatively high partial pressure values at that temperature. However, it would be expected that there would be greater loss of aluminium by vaporisation in comparison the titanium. Clearly that was not happening. It is possible that the higher presence of aluminium at the interface with Al_2O_3 as suggested by EDAX was being picked up from the Al_2O_3; however, this would not be so for the composition within the inner areas of the braze. In addition, the Al-Fe-Ti equilibrium phase

diagram shows that the TiAl single-phase region can extend to contents above 50 at% titanium and therefore even if the aluminium analysis had been wrong, the observed single-phase layer would probably be TiAl anyway. Inspection of the Al-Fe-Ti phase diagram shows that the original composition used lay within the τ_2 + TiAl phase field. According to Palm et al [34] the τ_2 phase is represented by the formula Al_2FeTi by from the EDAX analyses in the present study, no such phase was observed. The discrepancy between the initial and final compositions may therefore be because of evaporation. In any case, whatever the cause, one thing was clear and that was the fact that all the iron was dissolved in the TiAl phase and that it was situated at the interface with Al_2O_3.

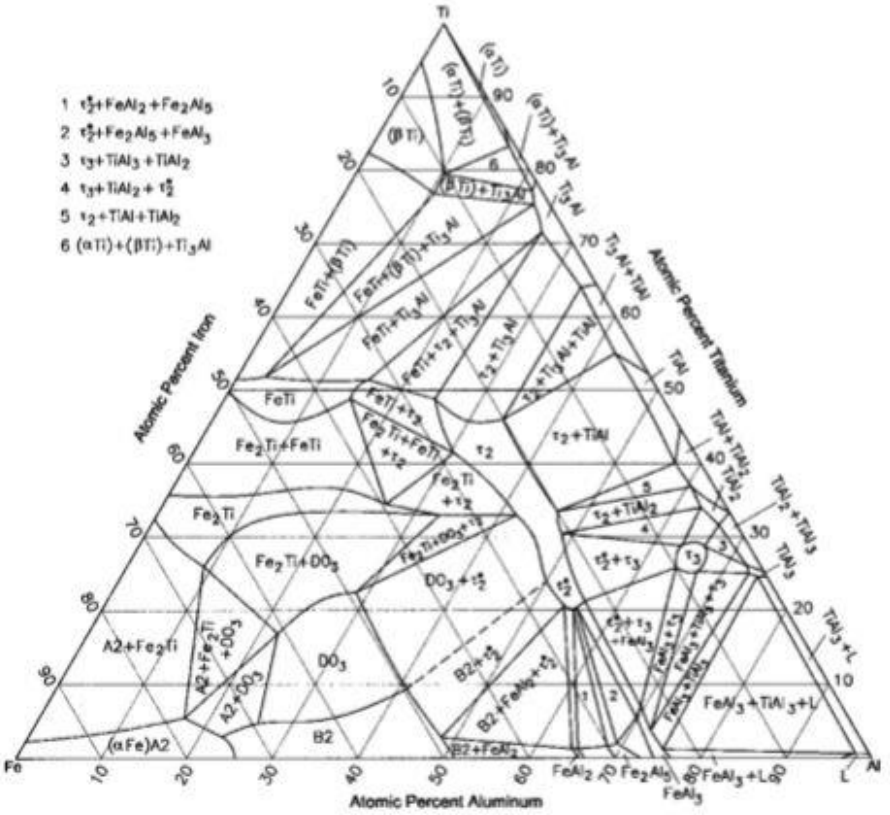

Figure 41 Al-Fe-TI [35]

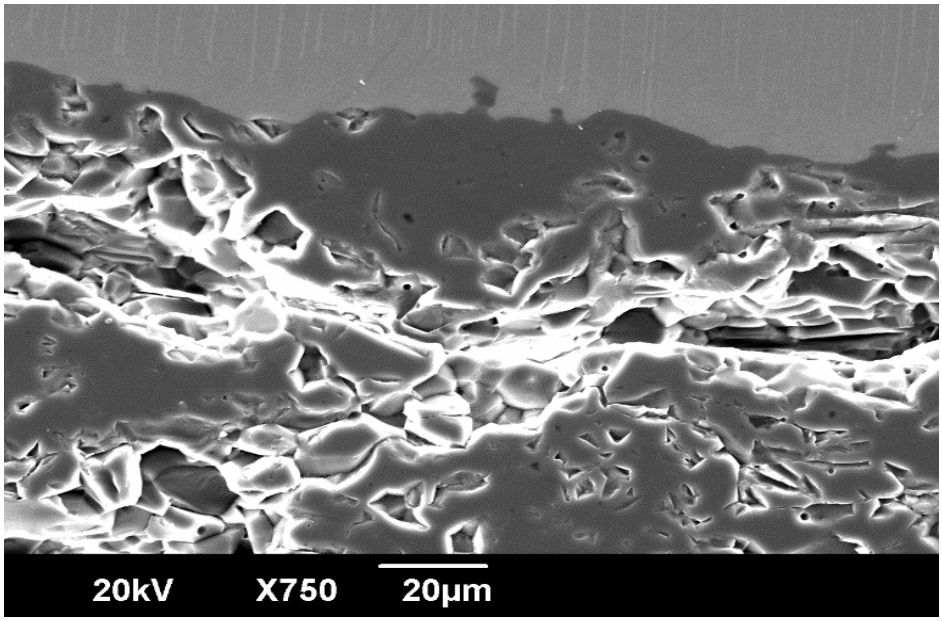

Figure 42 SEM for ($Ti_{0.96}Fe_{0.04}$)Al

Element	Wt%	At%
AlK	42.02	56.39
TiK	56.03	42.35
FeK	01.95	01.26
Matrix	Correction	ZAF

Figure 43 EDAX analysis of the braze at the interface with Al_2O_3.

Element	Wt%	At%
AlK	39.38	53.55
TiK	60.62	46.45
FeK	00.00	00.00
Matrix	Correction	ZAF

Figure 44 EDAX analysis from the central area of the braze.

The brazing experiments that were carried out with additions of iron to Ti-Al compositions have shown that the presence of iron led to improved wetting with Al_2O_3. Similar results were observed when nickel was added to Ti-Al compositions. In both cases, phases the were formed at the interface with Al_2O_3 contained the additive elements (iron or nickel). The improved wettability in comparison to the Ti-Al brazes was therefore attributed to the presence of either iron or nickel which are able to dissolve Al_2O_3. As in the case of nickel, iron has also been

shown to dissolve small amounts of Al_2O_3 [84]. The results of the present study suggest that any choice of third-element addition to Ti-Al brazes must be based on the ability of the third element to dissolve Al_2O_3. As proposed earlier, the third element would be more effective if it has lower affinity for oxygen than both titanium and aluminium. Elements that have high affinity of oxygen are more likely to form stable oxides and less likely to dissolve Al_2O_3.

The wetting between the molten Ti-Al-based braze and Al_2O_3 is achieved and extended by the addition of the third element like iron and nickel. During the subsequent solidification, phases are formed that contain the third element. In the case of nickel, the τ_3-Al_3NiTi_2 phase is formed which is an intermetallic compound. However, in the case of iron, the solid phase that forms are based on TiAl with a small amount of iron dissolved in it. The entire iron within the braze is found dissolved in the TiAl at the interface with Al_2O_3, while in the case of nickel, the intermetallic τ_3-Al_3NiTi_2 solidifies at the interface, but is also found in the adjacent part of the braze. In each case there is preferential solidification at the interface with Al_2O_3 of a phase that contains the third element. The preferential solidification of these phases occurs by heterogeneous nucleation at the ceramic surface.

4.2.2 Brazing of Al_2O_3- Al_2O_3 using Ni_2Al_3

As previously discussed in the literature review, some researchers found that Ni, unlike Fe and Co, would not react with neither Ti nor Al. However, not enough proof was mentioned in their work, such as wettability. When wettability and SEM were checked on other experiments, involving (Ti, Ni)Al, it actually shows that Ni blends in with TiAl as aforementioned. On the other hand, other researchers have found increasing the aluminium in a braze involving nickel can enhance the wettability even more. Hence, it was decided to use Ni_2Al_3 as a braze instead of Ni_2Al due to the high temperature interest. A joint between the braze, Ni_2Al_3, and Al_2O_3 have been achieved. Further experiments are due to understand the quality and reliability of using this braze to bond alumina, effectively at high temperature. Ni_3Al has been examined for contact angle, it shows improvement with respect to pure Ni, yet the angle did not drop below 70°. As mentioned in the literature review, Al can improve wettability. Therefore, choosing a phase

which contains more Ni than pure as well as more Al, Ni_2Al_3, to achieve better wettability and higher melting temperature; serving the purpose of this project.

4.2.3 Pre-treatment of $(Ti_{0.83}Ni_{0.17})Al$

Another interesting joining process was trying to pre-treat the following composition, $(Ti_{0.83}Ni_{0.17})Al$, with 25% of the total weight of aluminium foil. This treatment was mainly due to enable a layer of aluminium to spread the surface of the substrate before trying the process of joining the braze. Therefore, allowing more diffusion into the substrate. However, in theory Al might form an alumina layer which can disallow diffusion into the substrate; failing to bond, or it might result in a weak bond. Nonetheless, after undergoing the experiment, it seems to bond, this treatment has not yet been examined. Initially, a joint was observed. Further work to be conducted to investigate this joint.

4.3 *Joining of Al_2O_3 -to- Ti6Al4V*

After adding Ni to TiAl as a third element addition. The distinct behaviour of Ni migrating to the alumina interface, has influenced the choice of trying brazes where Ni is either the base or part of a braze. Hence the selection of two commercial brazes: Palni (Pd60wt%-Ni40wt%) and TiCuNi (Ti-Ni15wt%-Cu15wt% and Ti-Ni20wt%-Cu20wt%). In addition to two novel brazes that have been developed in this project: Ti68.4wt%-Ni3.6wt%-Al28wt% and Ni-Zr14wt%. Even though Ni is a very interesting element when introduced in brazes. It was never thought of developing a Ni braze on it is own, the reason behind that, is simply the fact that metals on their own are much weaker than alloys. In each of these four brazes, Ni is always found at the interface with Alumina. The braze forms a phase that contains Ni and it then bonds onto the alumina substrate. Another reason than the free Gibbs energy, is the D shape electrons in Ni are incomplete and therefore are able to participate in bonding. Certainly, if this braze was used to bond tungsten carbide, understanding this complex behaviour of Ni would become easier. Seeing as tungsten carbide have metallic behaviour and there is interaction between Tungsten electrons and Nickel electrons. However, it is not the case with Alumina since all the free electrons are bound to the oxygen. The nickel in this situation will become free.

It has been well established that a typical TLP bonded joint may consist of three distinct zones: (1) an athermal solidification zone (ASZ), (2) an isothermal solidification zone (ISZ), and (3) a diffusion-affected zone (DAZ) [86]. These zones have been identified using SEM. Relevant phase tables have conducted via EDAx to show elements in scanned areas, spots or mapping.

4.3.1 Brazing of Al_2O_3-Ti6Al4V using a novel Ti-3.6Ni-28Al braze

The Ti-3.6Ni-28Al braze composition was specially proposed for use in this project to examine the effect of adding nickel as a third-element addition to a potential Ti-Al braze system. Prior to attempting to braze Al_2O_3 toTi6Al4V, a successful joint was produced by bonding Al_2O_3-Al_2O_3. The Ni-containing braze system as mentioned previously was selected following chosen mainly due to the observation that it exhibited better wetting behaviour with alumina than the TiAl braze. After wettability measurements at the surface of the alumina, the results were extremely favourable for brazing using this braze composition based on the Ti-Al-Ni system. However, the shear test results recorded for alumina-to-alumina brazing were not favourable due to damage caused at the alumina surface during interaction of alumina with nickel (melting in nickel).

Following brazing, some samples broke apart while handling. These samples were investigated further using SEM and EDAX accordingly. Specifically, the investigation was concerned with detecting any chemical reactions between the braze and the Ti6Al4V substrate leading to changes in the chemical composition of the braze. In addition, the joints were aged for 500 hours at 450°C to also examine for any chemical reactions and possible changes when used at higher temperatures. Unfortunately, the joints fractured while handling following brazing; prior to this the samples had a visually weak bond.

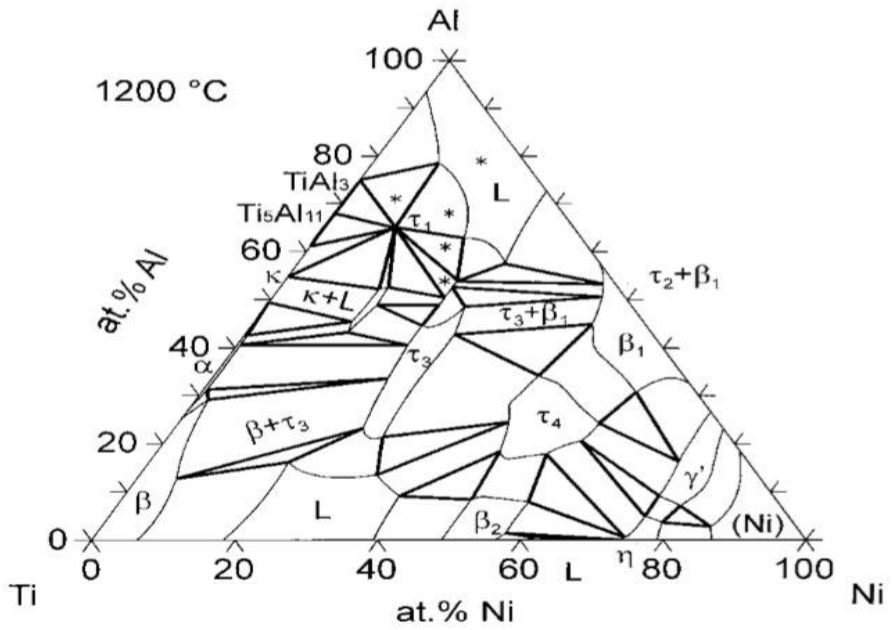

Figure 45 ternary phase diagram of Ti-Ni-Al

4.3.1.1 SEM and EDAX analysis of Al_2O_3-Ti6Al4V joints using the Ti-3.6Ni-28Al braze

The interfacial behaviour between the Ti-3.6Ni-28Al braze and the alumina substrate when joining alumina to Ti6Al4V is shown in Figure 46 with evidence of formation of a thin white layer of about 4-10 μm at the interface. The results of EDAX analysis differ from those that were obtained for the Al_2O_3-Al_2O_3 joints. It is apparent that the braze composition at the interface with alumina for the Ti6Al4V-Al_2O_3 joints contained a higher level of titanium in comparison to the Al_2O_3-Al_2O_3 joints. The reason for this observation is the fact that there was interaction between the braze and the substrate Ti6Al4V alloy with, primarily, more titanium dissolving into the braze. While the original braze composition lay within the α + τ_3 phase field (with the τ3-Al_3NiTi_2 phase forming in contact with alumina), the interaction with the titanium alloy substrate altered the behaviour. Based on the EDAX results of figures 46 & 47, the phase that formed at the interface with alumina was TiAl with Ni dissolved in it (11.44at%), while the main body of the braze had also changed and was based on Ti_3Al with much lower levels of Ni dissolved (1.19at%) in it. As this interaction takes place, the behaviour becomes difficult to predict because the interaction between the braze and the Ti6Al4V alloy is likely to continue at high

temperatures and at extended brazing times. However, it is clear from these observations that the nickel preferentially migrated to the interface with alumina to enhance the wetting between the alumina and the braze as discussed earlier in the thesis. This interaction is responsible for the improved wettability between the braze and the alumina.

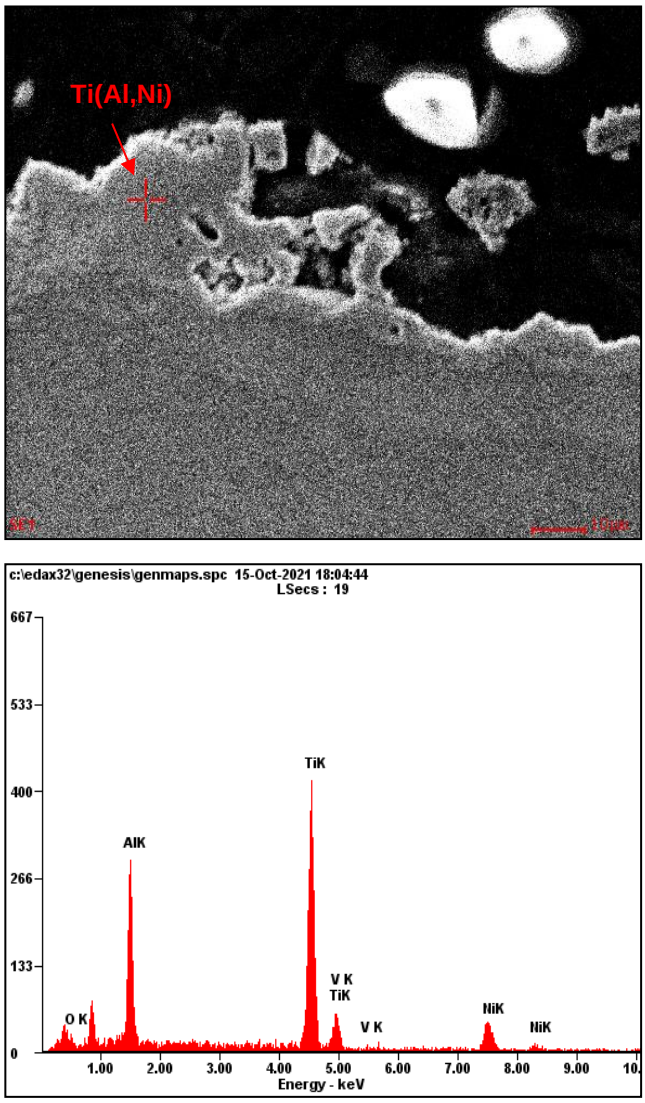

Element	Wt%	At%
OK	06.05	14.32
AlK	22.94	32.17
TiK	53.26	42.08
VK	00.00	00.00
NiK	17.75	11.44
Matrix	Correction	ZAF

Figure 46 SEM microstructure and EDAX analysis of the interfacial layer between the Ti-3.6Ni-28Al braze and Al_2O_3 for the Ti6Al4V-Al_2O_3 joint

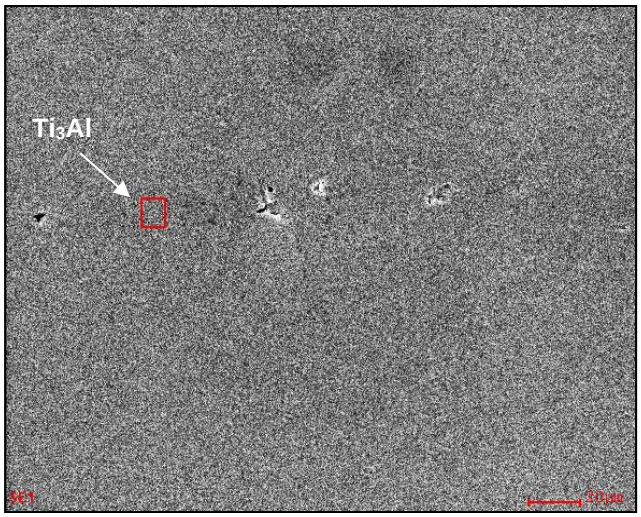

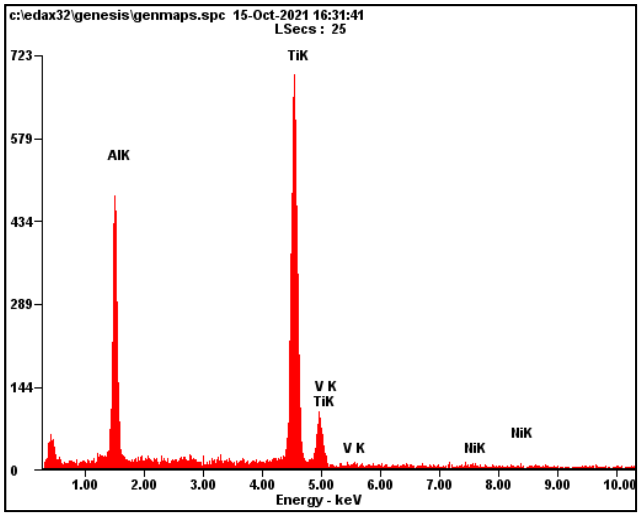

Element	Wt%	At%
AlK	26.66	39.33
TiK	71.58	59.48
VK	00.00	00.00
NiK	01.76	01.19
Matrix	Correction	ZAF

Figure 47 EDAX analysis of the main part of the Ti-3.6Ni-28Al braze for an Al_2O_3-Ti6Al4V joint

4.3.1.2 Ageing at 450°C of Al_2O_3-Ti6Al4V joints brazed using Ti-3.6Ni-28Al

The aim of this research project was to develop brazes for joining ceramics to ceramics and ceramics to metals. It addressed joining of Al_2O_3 to Al_2O_3 as well as Al_2O_3 to Ti6Al4V alloy. These systems were specifically chosen because they are usually used and / or have the potential to be used in extreme conditions, for example, in engine applications where they can

be exposed for various lengths of time at high temperatures. This part of the thesis is concerned with the operational behaviour of the Ti-3.6-28Al braze joint for joining Al_2O_3 to Ti6Al4V alloy. The joints were exposed to ageing at 450°C in air 500 hrs. Operational temperatures for titanium alloys can extend up to about 600°C so a temperature of 450°C was considered to be a typical operational temperature.

4.3.1.2.1 SEM and EDAX analysis of aged samples of Al_2O_3-Ti6Al4V joints brazed with Ti-3.6Ni-28Al

Figure 48 is showing a micrograph of the interface between the braze and Al_2O_3 following ageing at 450°C in air for 500 hrs. The EDAX analysis in Figure 49 shows that the interfacial phase is based on TiAl with some Ni dissolved in it. Based on the EDAX analysis, the darker regions represent alumina and there is evidence of the braze having climbed over or having penetrated into the alumina at areas close to the interface. This observation illustrates the ability of the braze to effectively wet the alumina surface. It is also apparent that some of this TiAl phase with dissolved Ni has formed at the interface with some of the exposed alumina areas that have been penetrated by the braze. These findings are also evident in the elemental mapping results in Figure 50. From the EDAX results, the composition of the phase that had formed at the interface with Al_2O_3 following ageing at 450°C for 500 hrs was 47.83at% Ti, 27.27at% Al and 7.81at% Ni in comparison to 42.08at% Ti, 32.17at% Al and 11.44at% Ni after brazing and prior to ageing. In both cases, the interfacial braze phase is based on TiAl with Ni dissolved in it, that is, Ti(Al,Ni). During the ageing process, the amount of titanium increased slightly, while there was a decrease in both Ni and Al. It appears that during ageing, there was diffusion of titanium from the substrate into the braze producing an interfacial phase Ti(Al,Ni) phase that was richer in Ti. While there was a slight change in the chemical composition, there is clear evidence of most of the nickel had migrated to the interface with alumina to form and slightly Ti-richer Ti(Al,Ni). As mentioned earlier in the thesis, during the brazing of Al_2O_3 to Al_2O_3 there was evidence of small amounts of the alumina substrate dissolving in the braze due to the presence of nickel (and titanium). Upon cooling from the brazing temperature, the τ3-Al_3NiTi_2 phase was observed to form in contact with Al_2O_3. When brazing Al_2O_3 to Al_2O_3, the only interaction involving the braze was with Al_2O_3 and therefore the composition of the braze remained constant. However, when brazing Al_2O_3 to the Ti6Al4V alloy, there was reaction

between the braze and the Ti6Al4V alloy and the braze composition changed and became richer in titanium. After cooling from the brazing temperature, there was no evidence of the τ3-Al_3NiTi_2 phase as some titanium from the alloy had melted and dissolved in the braze thus changing the composition of the latter. From EDAX analysis, the composition in contact with alumina was based on TiAl with nickel dissolved in it, Ti(Al,Ni), while the main body of the braze appeared to be based on Ti_3Al. The EDAX analysis also established that most of the nickel was present in the Ti(Al,Ni) phase that was in contact with the alumina. In both cases (brazing Al_2O_3 to Al_2O_3 or Al_2O_3 to Ti6Al4V), there was preferential presence of nickel in the interfacial phase with Al_2O_3.

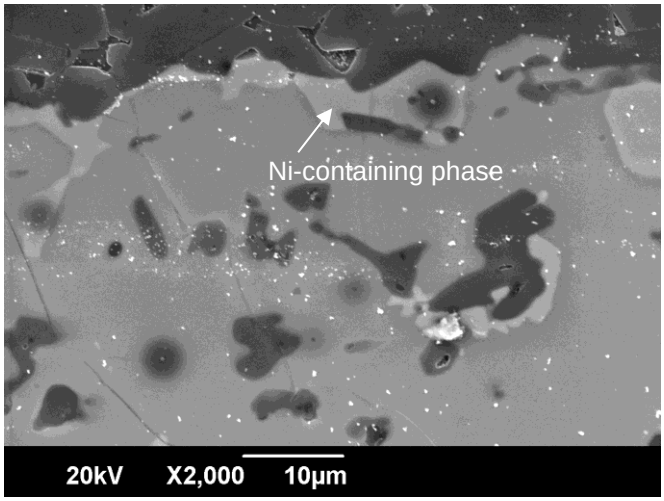

Figure 48 overview of interface with alumina after ageing treatment for Al_2O_3-to-Ti6Al4V

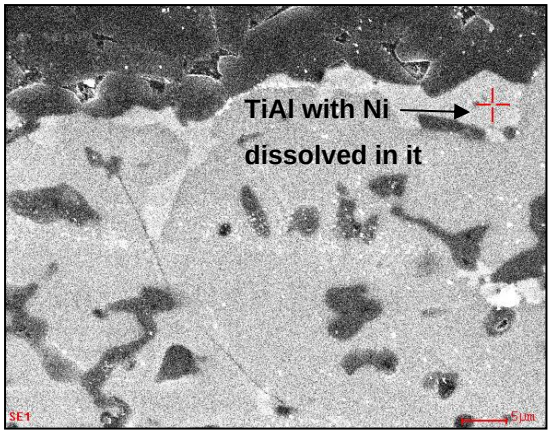

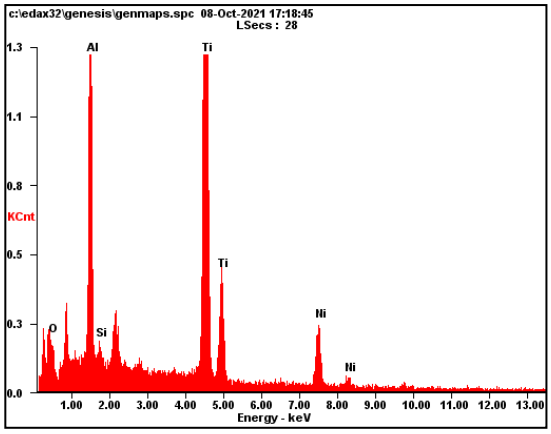

Element	*Wt%*	*At%*
OK	06.97	16.42
AlK	19.53	27.27
SiK	00.50	00.67
TiK	60.83	47.83
NiK	12.17	07.81
Matrix	Correction	ZAF

Figure 49 spot analysis at bright area showing Ni element dissolving in Ti from Ti6Al4V substrate

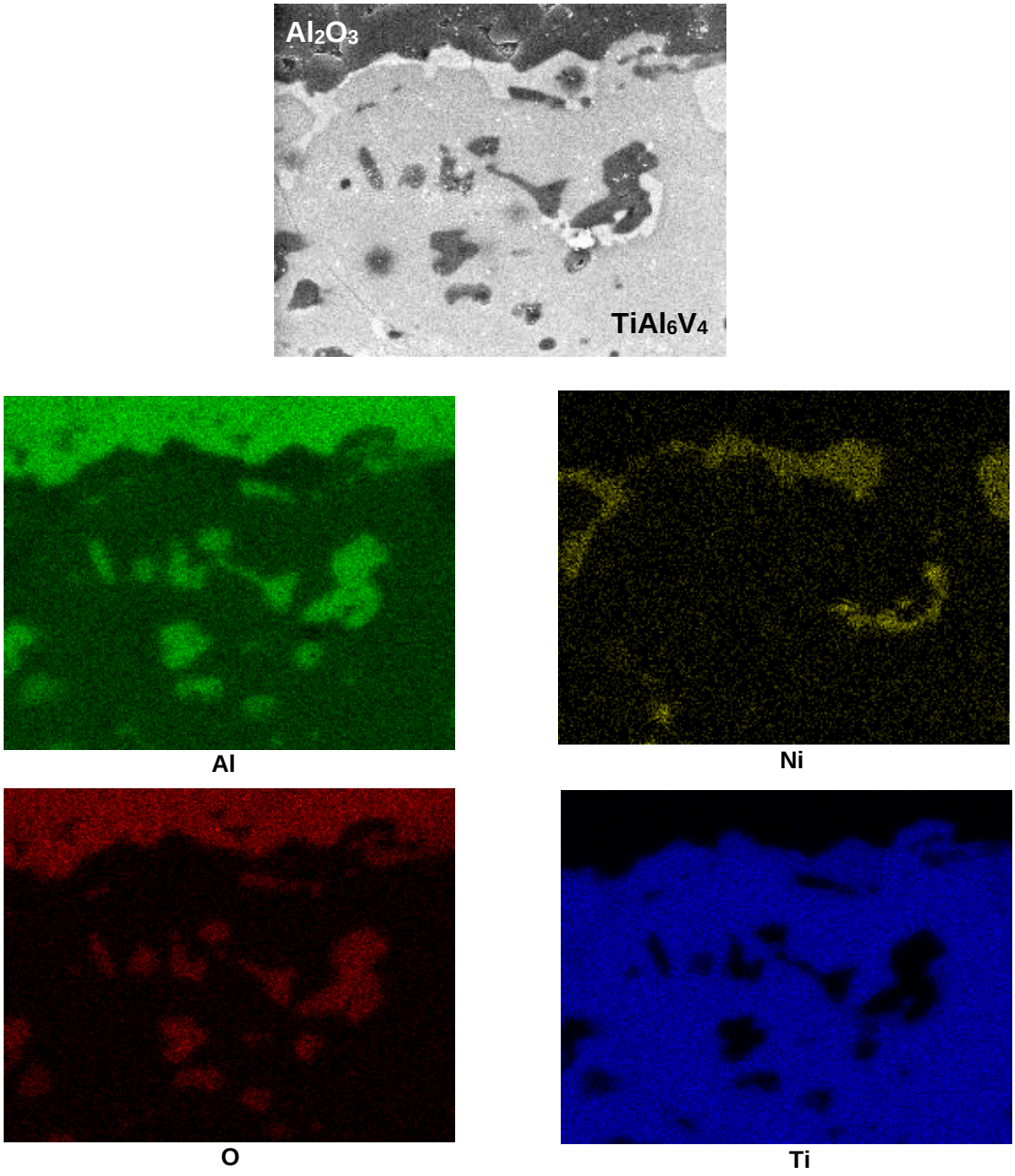

Figure 50 Elemental mapping analysis from an area close to the interface between Al_2O_3 and the braze for an aged Al_2O_3-Ti6Al4V joint brazed with Ti-3.6Ni-28Al

4.3.2 Brazing of Al_2O_3-Ti6Al4V using a commercial Ti-15Ni-15Cu braze

The Ti-15Ni-15Cu brazing system is actually a commercial braze which is used to join Ti6Al4V titanium alloy in aircraft engine applications [87]. To the knowledge of the author of the thesis, this braze has not been used to join ceramics in the past. In this investigation, it was used to join Ti6Al4V alloy to Al_2O_3. It was specifically selected because of its ability to join titanium

alloys and because of the earlier observations of the current study that showed interaction between nickel-containing brazes and Al_2O_3 leading to good wettability.

The melting point of this commercial braze is 960°C, however, this braze has been examined using different brazing parameters and the optimum brazing temperature that was used in the study was 1200°C with a dwell time of one hour. Inspection of cross-sectioned joints by SEM as presented in figure 51 revealed the presence of a good bond between the braze and Al_2O_3. The presence of a continuous bright layer of thickness of about 1-2 µm was observed at the interface between the braze and Al_2O_3. The EDAX analysis includes aluminium and oxygen from Al_2O_3, but if these are excluded the composition of the metallic phase corresponds to 68.7 wt% Ti, 9.2% Ni and 22.1 wt% Cu (34.7at% Ti, 8.43at% Cu and 3.79at% Ni).

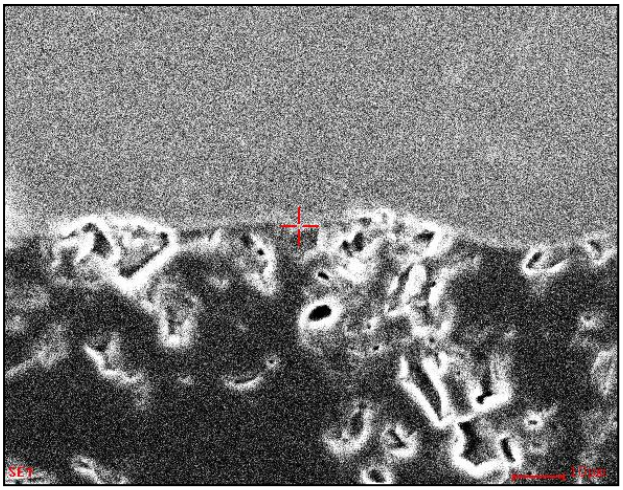

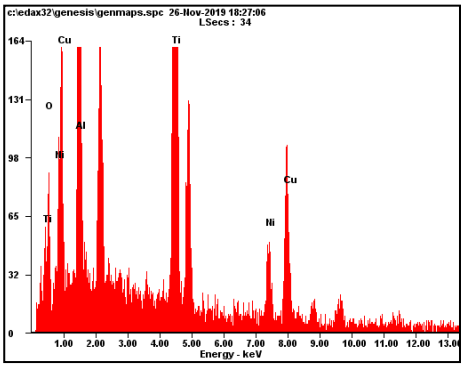

Element	Wt%	At%
OK	09.60	21.68
AlK	23.45	31.41
TiK	45.99	34.70
NiK	06.15	03.79
CuK	14.82	08.43
Matrix	Correction	ZAF

Figure 51 showing an SEM micrograph and EDAX analysis at the interface between the Ti-15Ni-15Cu braze and Al2O3.

This composition can be identified as the η phase that was reported by Ho et al [88]. In addition to the continuous η phase layer, the braze microstructure contained two other phases. An SEM micrograph from showing the microstructure at the middle part of the braze is shown in figure

52. According to EDAX analysis, the dark phase was rich in titanium with presence of 3.08 wt% aluminium. This phase represented α titanium.

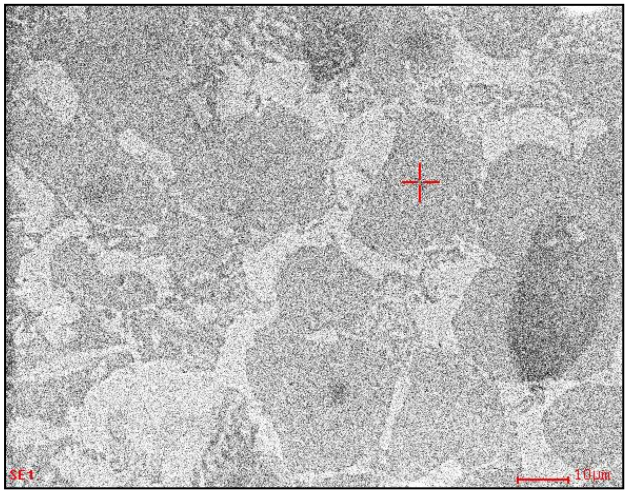

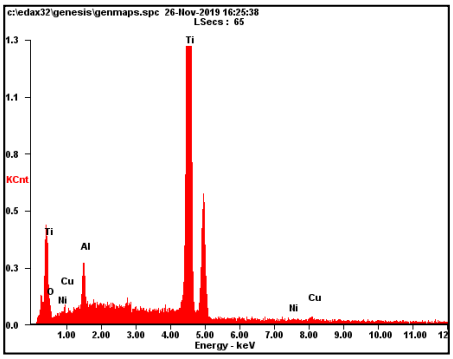

Element	Wt%	At%
OK	04.03	10.99
AlK	03.08	04.97
TiK	90.50	82.36
NiK	00.64	00.48
CuK	01.75	01.20
Matrix	Correction	ZAF

Figure 52 showing the microstructure and EDAX analysis for the central parts of the braze. The EDAX results are from the darker particles.

The presence of aluminium suggested that the braze was active with respect to the base metal (Ti6Al4V) with diffusion of this element being evident almost throughout the braze. EDAX analysis of the large bright regions is shown in figure 53; based on analysis presented by Ho et al [88] this phase is the ε phase and differs from the η phase in that it contains more nickel and less copper. It must be noted that there is a slight contrast between the ε and the η phases; the ε phase is the slightly darker of the two and is richer in nickel than in copper. The EDAX analysis of the smaller bright precipitates is shown in figure 54 and represents presence of the η phase. The microstructure in the central areas typically consisted of α-titanium along with ε and η. This observation is in agreement with the isopleth of the Ti-Ti15Ni15Cu section that was constructed by Ho et al [88]. Lower down and close to the interface with Ti6Al4V, the microstructure consisted of α, ε and η, but had a different morphology as shown in figure 51. Again, there was evidence of the presence of aluminium that was associated with the α phase. No vanadium was detected within the braze and therefore It was concluded that the bond between the braze and the titanium alloy was achieved by diffusion of titanium and aluminium from the substrate

alloy into the braze. The microstructure of the braze just below the Al_2O_3 and the interfacial η phase consisted primarily of α-titanium.

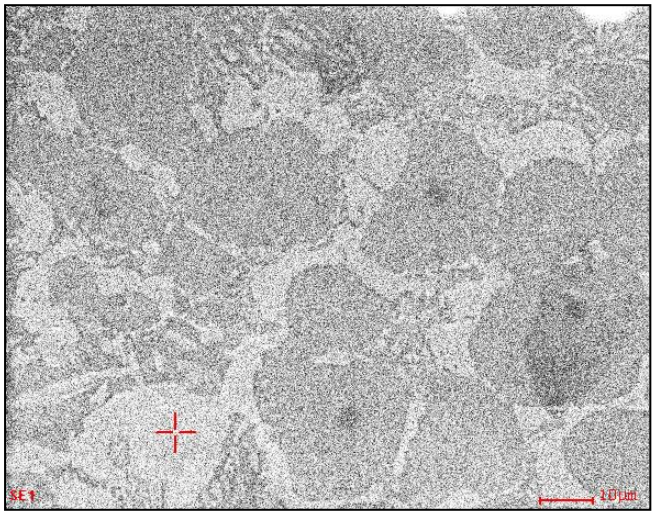

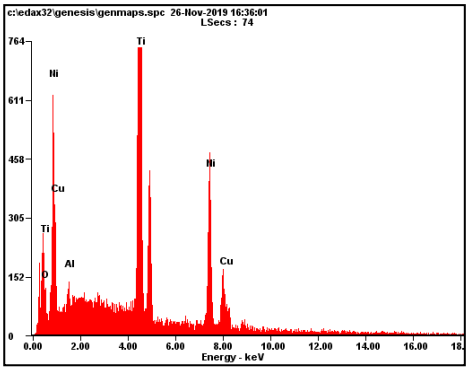

Element	Wt%	At%
OK	04.65	13.51
AlK	01.02	01.75
TiK	59.65	57.91
NiK	23.76	18.82
CuK	10.93	08.00
Matrix	Correction	ZAF

Figure 53 An SEM micrograph from the central regions of the braze and EDAX analysis of large bright area.

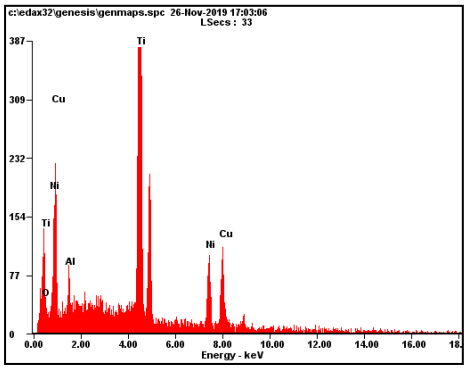

Element	Wt%	At%
OK	03.11	09.21
AlK	01.68	02.94
TiK	66.59	65.81
NiK	11.60	09.35
CuK	17.02	12.68
Matrix	Correction	ZAF

Figure 54 showing EDAX analysis of the smaller bright particles that represent the η phase.

The results that were obtained from this part of the investigation yielded two main conclusions. Firstly, the bond between the braze and the A_2O_3 was achieved by the molten braze through dissolution Al_2O_3 in titanium, nickel and copper. Equilibrium studies have shown dissolution of Al_2O_3 in titanium and nickel as mentioned in the earlier chapter. The dissolution of Al_2O_3 in

molten copper was previously studied by Hamuyuni and Taskinen [89]. As in the previous chapter for the case of titanium and nickel, the affinity of oxygen by copper is relatively low as demonstrated by the Gibbs Free energy of formation of CuO which is (-36,390 + 20.40 T) x 4.18 J /mol. Therefore, copper is more likely to dissolve Al_2O_3 than react with it. Upon cooling, the three elements that are capable of dissolving Al_2O_3 combine to form the η phase. The second conclusion is that the bond with the titanium alloy was achieved by diffusion of titanium and aluminium into the braze to form α-titanium.

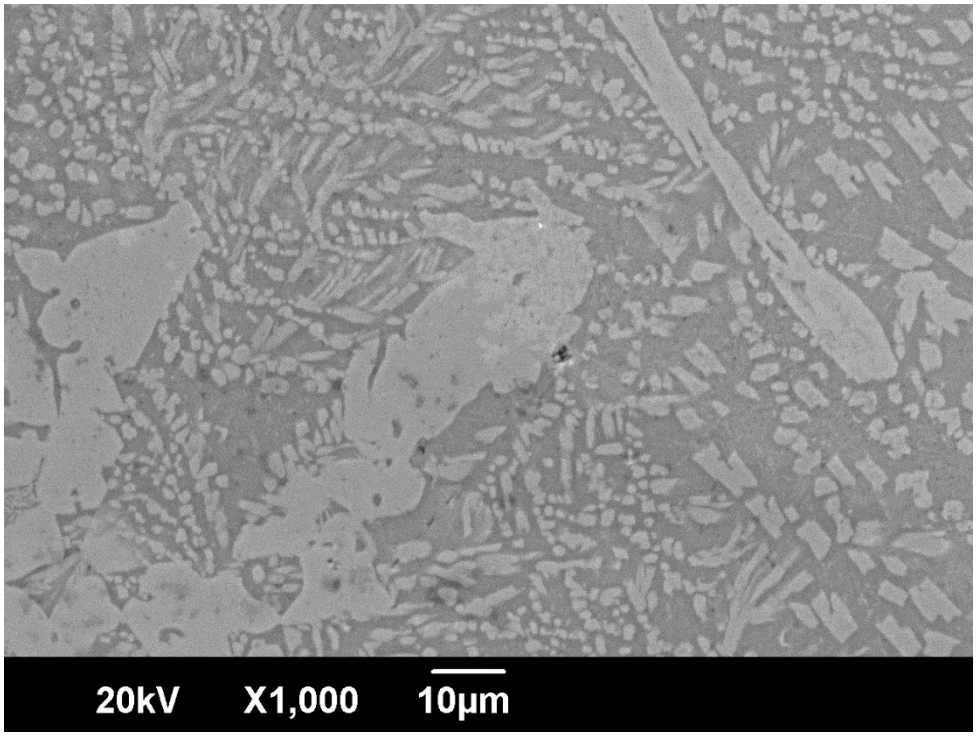

Figure 55 representing the microstructure of the Ti15Ni15Cu braze just above the interface with the Ti6Al4V alloy.

In spite of these favourable observations that suggest that the Ti-15Ni-15Cu braze can bond alumina to Ti6Al4V alloy, the overall performance of this braze was not satisfactory as it appeared to lack the necessary flowability. The melting point of the braze was 960°C; even by brazing at 1200°C and by using a dwell time of 2 hours, it was not possible to achieve a consistent bond. For reasons of lack of flowability, the quality of the brazed joints was not good. One other problem was the lack of consistency between various studies of phase relationships in the Ti-Ni-Cu system. The results of the present study seem to agree well with the observations of Ho et al [88] and confirm the existence of the ε and η phases. Their composition

almost matches that of the $Ti_2(Ni,Cu)$ phase which has been described by other researchers [88], [90], [91] as brittle.

4.3.3 Brazing of Al_2O_3-Ti6Al4V using a commercial Pd-40Ni braze

The brazing temperature that was used for the Pd-40Ni braze system was 1350°C and the dwelling time was one hour. SEM inspection of cross-sections of joints produced using the Pd-40Ni braze showed a non-uniform distribution of the composition with three zones of different microstructures in evidence as shown in figure 56. According to the equilibrium phase diagram in figure 57 there are no intermetallic phases between palladium and nickel. The two metals form a solid solution of face-centred cubic crystal structure over the entire range of the phase diagram. The Pd-40Ni braze may therefore be expected to form a single-phase solid solution, however, based on the SEM observations this was not the case as three distinct microstructural zones and various phases were present. EDAX analysis was therefore undertaken to examine these phases and to understand why the resulting braze was not in the form of the Pd-Ni solid solution.

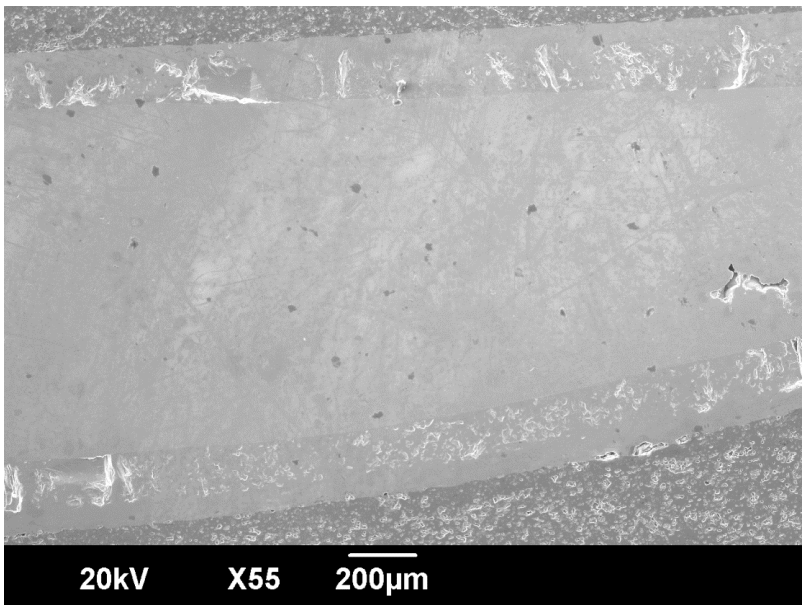

Figure 56 showing a brazed cross-section between the alumina block and the alumina crucible (occurred by overflow of the molten braze)

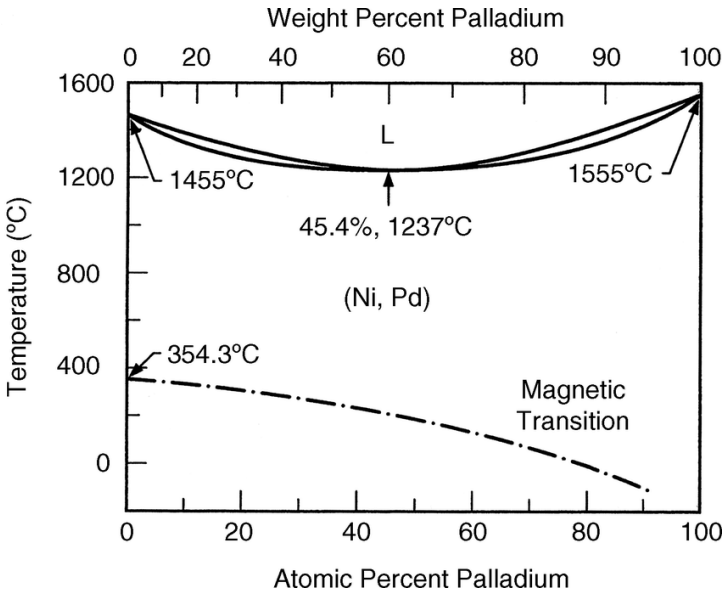

Figure 57 Pd-Ni binary phase diagram

4.3.3.1 SEM and EDAX analysis of brazing Ti6Al4V to Al_2O_3 using a commercial Pd-40Ni braze

SEM examination at high magnification revealed the presence of a distinct continuous layer of about 3μm thickness at the interface between the braze and Al_2O_3 as presented in figures 58 and 59. Based on the results of EDAX analysis, this phase was deduced to be Ti_3(Pd,Ni) or Ti_3(Pd,Ni,Al). The EDAX analysis shows substantial presence of aluminium, but most of this seems to come from Al_2O_3. As in the case of the earlier work using the braze from the Ti-Al-Ni and Ti-Ni-Cu systems, there is again evidence of both titanium and nickel being active in providing adhesion with Al_2O_3. This is based on the ability of both nickel and titanium to dissolve small amounts of Al_2O_3. In addition to the melting of the braze constituents (Pd and Ni), there was also melting of some of the titanium alloy. The final braze composition therefore contained aluminium and slightly more titanium in addition to the original braze components and amounts. Nickel (from the braze) and titanium (from the alloy) migrated to the surface of Al_2O_3 with which they interacted to dissolve part of the ceramic phase. Therefore, the ability of nickel and titanium to dissolve Al_2O_3 acted as the thermodynamic driving force for the two metals to migrate to the surface of the ceramic. It is of interest to note that previous work [92] has demonstrated that palladium particles can adhere onto the surface of Al_2O_3, but the mechanism for achieving this has not been explored. This suggests that there is some additional influence from the presence

of palladium to promote the adhesion and wetting for Al_3O_3 and this is demonstrated by the fact that all three metals (Ti, Ni and Pd) were found at the interface with the ceramic. Some aluminium has probably migrated to the same area as well since that has also been observed to interact with Al_2O_3. However, there is another crucial reason as to why there is intermetallic formation of Ti_3(Pd,Ni,Al) and this is due to the fact that the Pd-Ni system forms only a solid solution between the two metals and does not show any formation of intermetallic phases. During the brazing operation, there is interaction between the titanium alloy (the substrate) and palladium and nickel to form a phase like Ti_3(Pd,Ni,Al) which is thermodynamically more stable than the Pd-Ni solid solution. In figures 58 and 59, it is also apparent that the interfacial Ti_3(Pd,Ni,Al) phase has “climbed” over the ceramic and this provides further evidence for the enhanced wetting/adhesion at the interface.

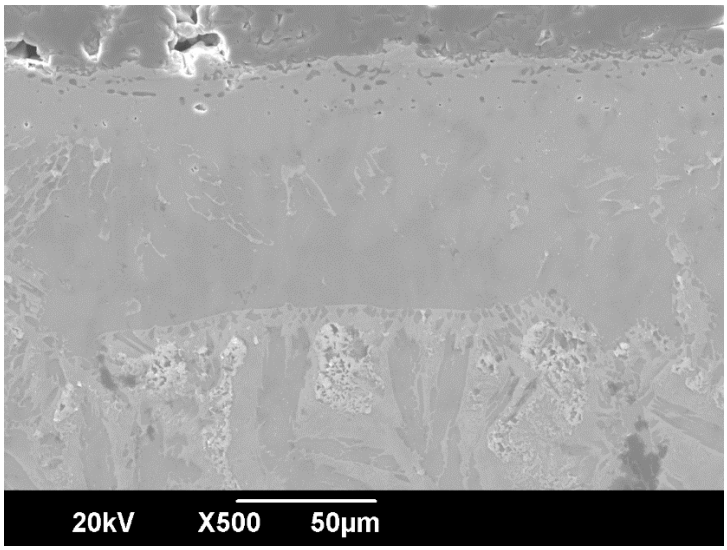

Figure 58 overview of interfacial Ti_3(Pd,Ni,Al) phase with alumina from joining Al_2O_3-to-Ti6Al4V using commercial Pd-40Ni braze

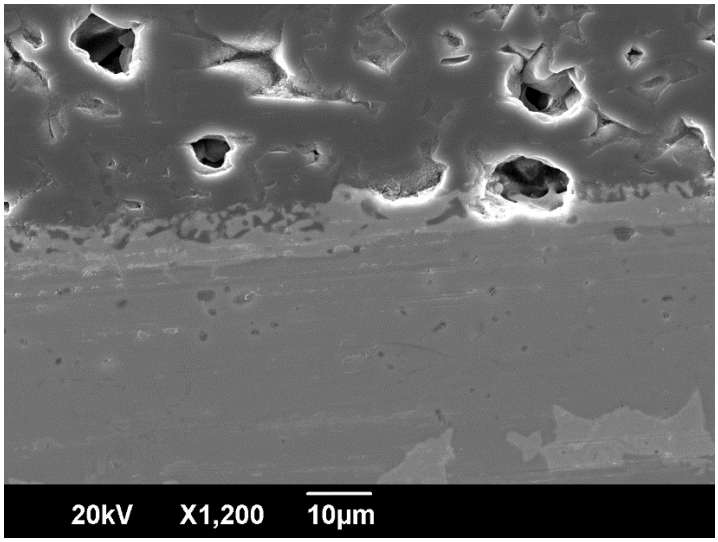

Figure 59 interface of Pd-40Ni braze system with alumina substrate.

EDAX analysis of the zone just below the Ti_3(Pd,Ni,Al) layer is shown in figure 60. The results show a region which is very rich in titanium. The analysis is suggestive of the presence of α-titanium with aluminium dissolved in it along with small amounts of palladium and nickel. are suggestive of just below. The observed contrast within this microstructural region is likely to be due to non-homogeneous solution of palladium and nickel in the α-titanium. The EDAX analysis that was obtained from next layer that developed at the interface with the Ti6Al4V alloy, suggested the presence of two phases. The results of the darker areas in figure 61 represent the α-titanium phase, while the brighter phase that was analysed in figures 62 and 63 were identified as Ti_2(Ni,Pd). It is clear that the Pd-40Ni braze reacts with the Ti6Al4V alloy. The observed reactions were beneficial in terms of achieving a good bond between the braze and the titanium alloy. Further support for this is provided by the fact that the reactions did not cause any porosity within the braze. In some of the experiments with the Pd-40Ni braze, there was evidence of overflow of the braze leading to a bond between the alumina boat and the alumina that was used to bond to Ti6Al4V alloy. A typical example is presented in figure 58.

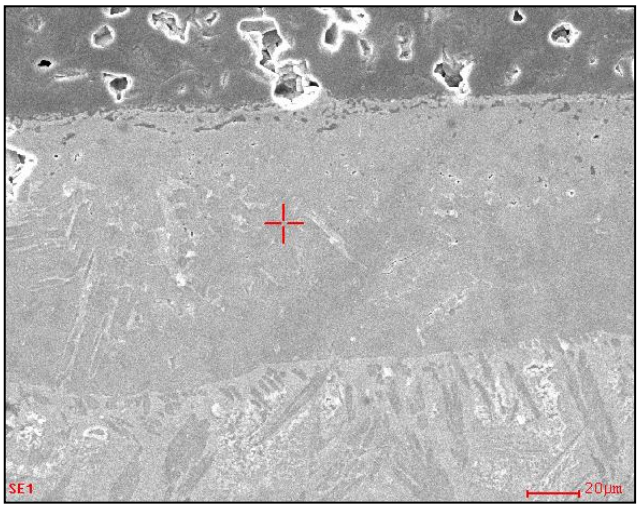

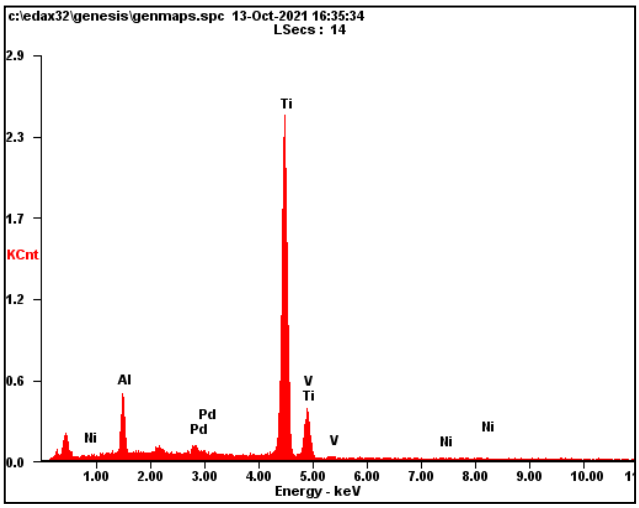

Element	Wt%	At%
AlK	09.10	15.34
PdL	03.15	01.35
TiK	87.62	83.21
VK	00.00	00.00
NiK	00.13	00.10
Matrix	Correction	ZAF

Figure 60 EDAX analysis of the region adjacent to the interfacial layer below the Ti_3(Pd,Ni,Al) layer and rich of Ti in Pd-40Ni braze system of joining Al_2O_3-to-Ti6Al4V.

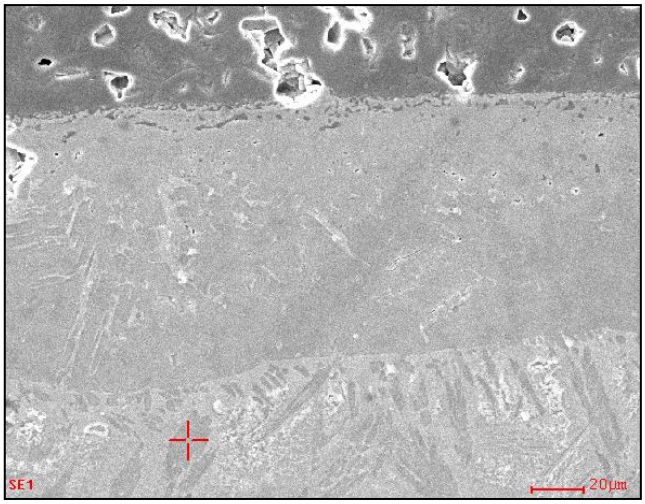

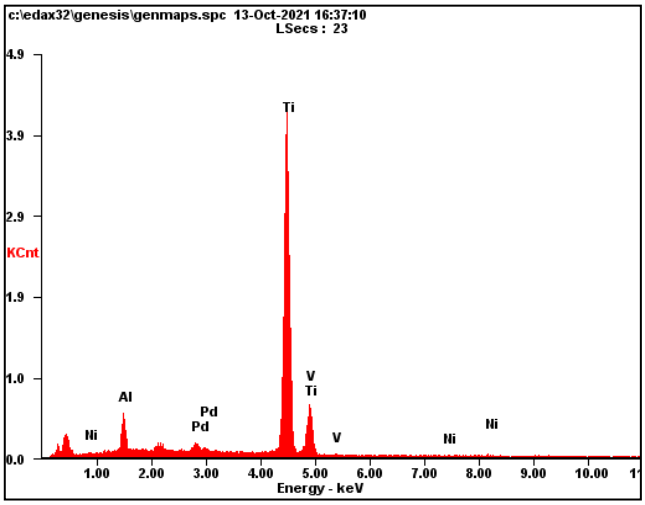

Element	Wt%	At%
AlK	06.18	10.67
PdL	03.24	01.42
TiK	90.12	87.55
VK	00.00	00.00
NiK	00.46	00.37
Matrix	Correction	ZAF

Figure 61 Ti alloy composition at different layer from Pd-40Ni braze system joining Al_2O_3-to-Ti6Al4V.

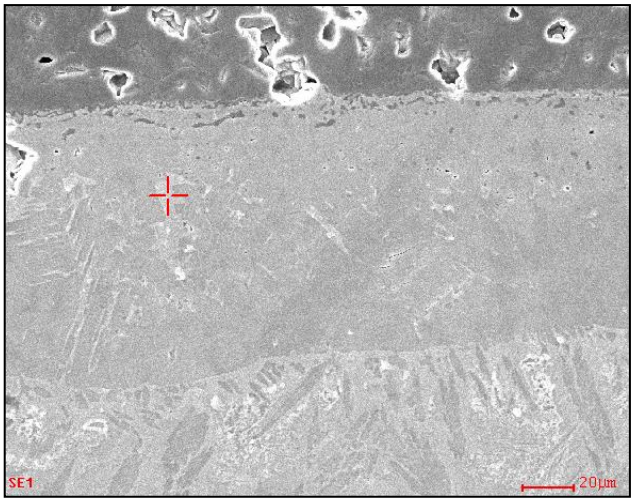

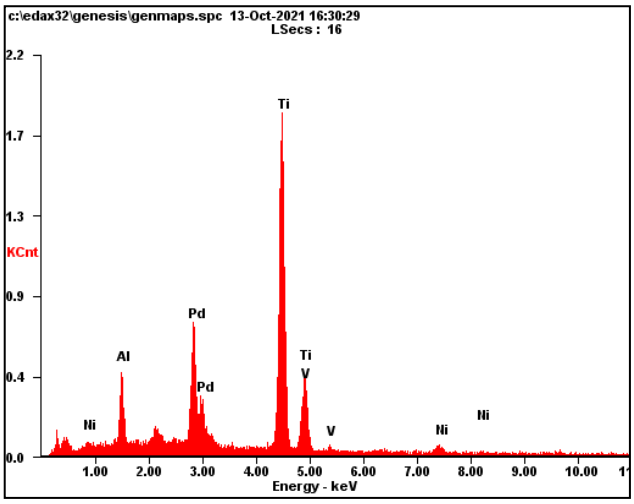

Element	Wt%	At%
AlK	06.97	13.74
PdL	26.08	13.04
TiK	57.98	64.40
VK	05.05	05.28
NiK	03.91	03.55
Matrix	Correction	ZAF

Figure 62 White phase below interface showing Pd & Ni elements from Pd-40Ni commercial braze system used to join Al_2O_3-to-Ti6Al4V.

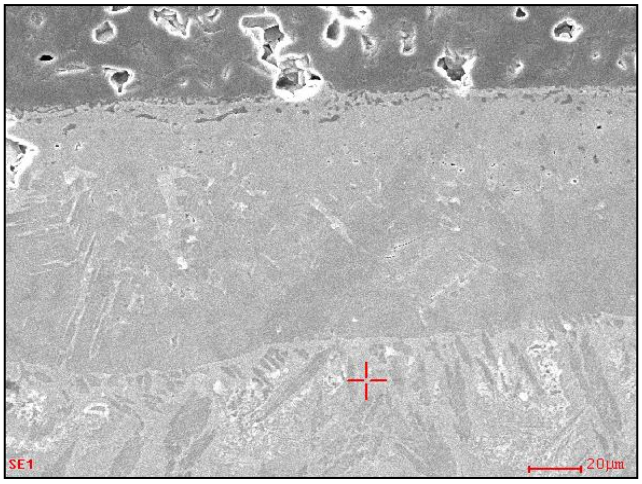

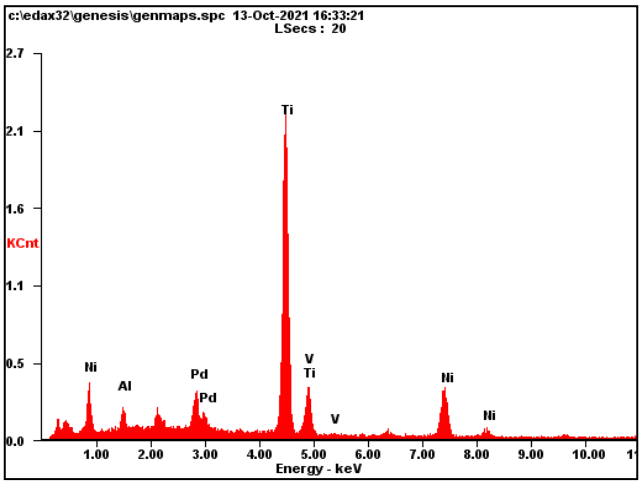

Element	Wt%	At%
AlK	03.13	06.03
PdL	09.93	04.85
TiK	59.95	65.12
VK	00.60	00.62
NiK	26.39	23.39
Matrix	Correction	ZAF

Figure 63 White phase deeper showing more Ni and Pd from Pd-40Ni commercial braze used to join Al_2O_3-to-Ti6Al4V.

The interaction between titanium with Pd-40Ni appeared to have formed a melt that had enhanced flowability. The melt that contained titanium and aluminium from the Ti6Al4V alloy and palladium along with nickel (from the braze) seemed to have enhanced flowability and in one brazing experiment it even overflowed out of the gap between the Pd-40Ni and Ti6Al4V. The overflown melt that contained titanium, palladium, nickel and aluminium was drawn by capillary action into the gap between the alumina crucible and the alumina block that was used

to join to the Ti6Al4V alloy. Thus, in addition to bonding the Ti6Al4V alloy to alumina, the overflown molten material also achieved bonding with the alumina crucible. The microstructure of a cross-section showing bonding with the alumina crucible is shown in figure 63 and revealed a thin layer of $Ti_3(Pd,Ni,Al)$ at the interface with Al_2O_3 (at both ends). The α-titanium phase was observed adjacent to this (on both sides) with α-titanium and flakes of $Ti_2(Ni,Pd)_2$ being sandwiched in the middle.

Bonding between the Ti6Al4V alloy and Al_2O_3 was achieved by interactions that took place at both ends of the braze. Part of the Ti6Al4V alloy melted and some of the titanium and aluminium dissolved into the molten braze. The resulting melt appeared to possess enhanced flowability to such an extent that it was drawn into the gap between the sample and the holding crucible. Thus, the interaction between the braze and the titanium alloy was beneficial in not only achieving the bond between the ceramic and the metal, but also in enhancing the flowability of the molten material. The bond between the Al_2O_3 and the braze was achieved by the ability of titanium and nickel to dissolve part of the ceramic leading to formation of $Ti_3(Pd,Ni,Al)$ at the interface, see figure 64 below.

On one occasion, while brazing treatment, the braze flew above the titanium button and joined the sample with the boat producing a three-layer joint. On the top and bottom there was alumina, while in the middle was the Ti-substrate (see figure 56). This was an accidental joint; however, it can confirm that the braze has favourable wettability and flowability characteristics.

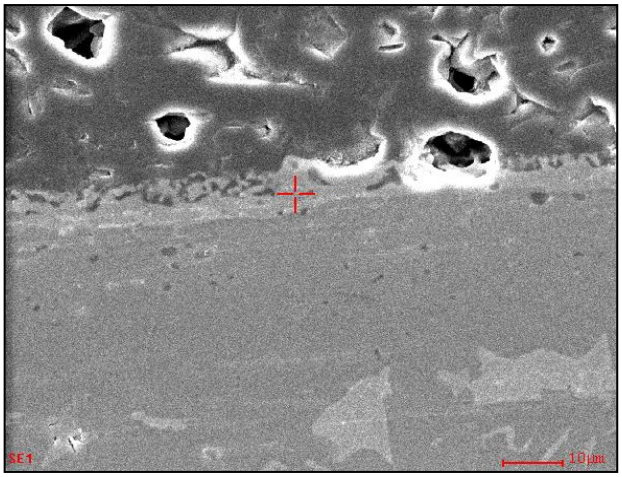

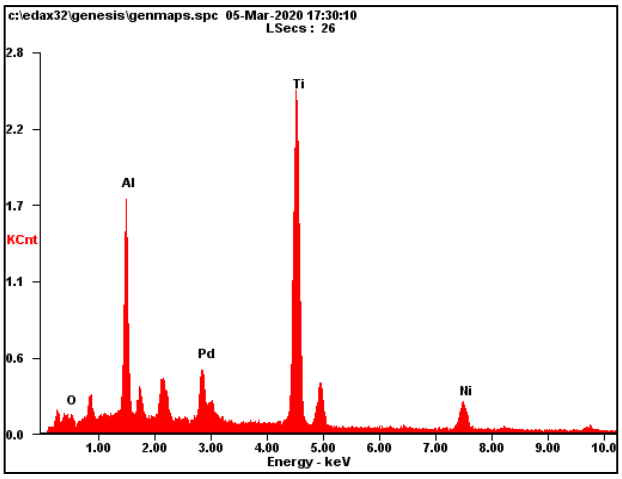

Element	Wt%	At%
OK	04.52	11.74
AlK	19.20	29.56
PdL	11.53	04.50
TiK	52.37	45.43
NiK	12.39	08.77
Matrix	Correction	ZAF

Figure 64 interfacial analysis confirming Ni & Pd elements appearance at interface between Al_2O_3 and Ti6Al4V substrates.

4.3.3.2 Ageing at 450°C of Al_2O_3-Ti6Al4V joints brazed using Pd-40Ni

In this section, brazed samples were heated in a conventional furnace at 450°C for 500 hours. As discussed earlier, these parameters are set to ensure that no oxidation takes place for Ti. This part of the work was undertaken to examine and explore any further reactions at this

temperature. After examination of the joints using SEM and EDAX analysis, it was apparent that no further reactions had taken place at that temperature.

4.3.3.2.1 SEM analysis of aged samples of Al2O3-Ti6Al4V joints brazed with Pd-40Ni

The micrograph in figure 65 shows three distinct sectons with different microstructure as observed in samples prior to heating at 450°C. The braze maintains good wetting with the alumina substrate. Figures 66 and 67 show a close up at the interface confirming the integrity of the bond between the braze and the alumina substrate.

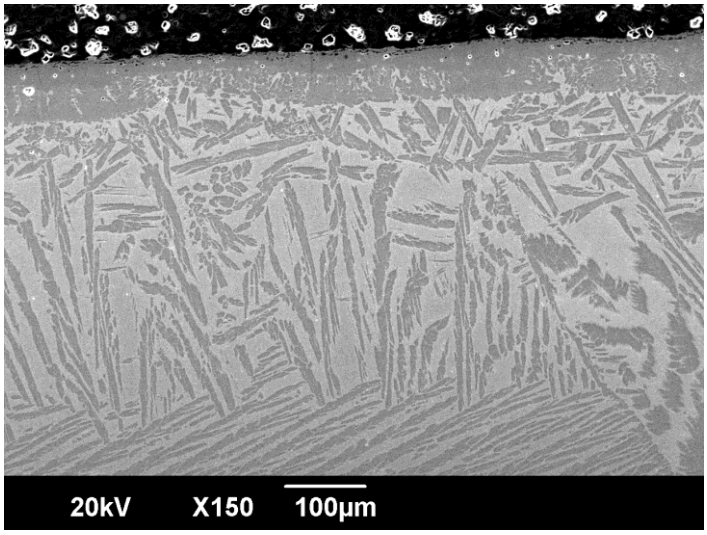

Figure 65 joint overview between Ti6Al4V substrate and Pd-40Ni commercial braze for aged samples

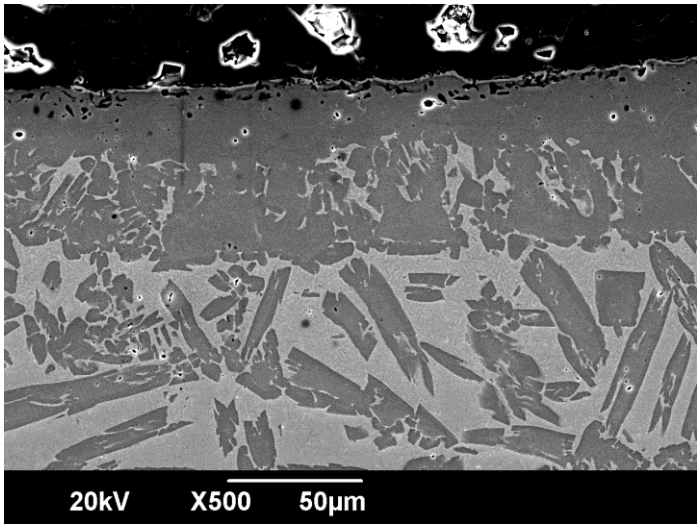

Figure 66 overview of interface between Pd-40Ni commercial braze and alumina substrate for aged Al_2O_3-to-Ti6Al4V joints

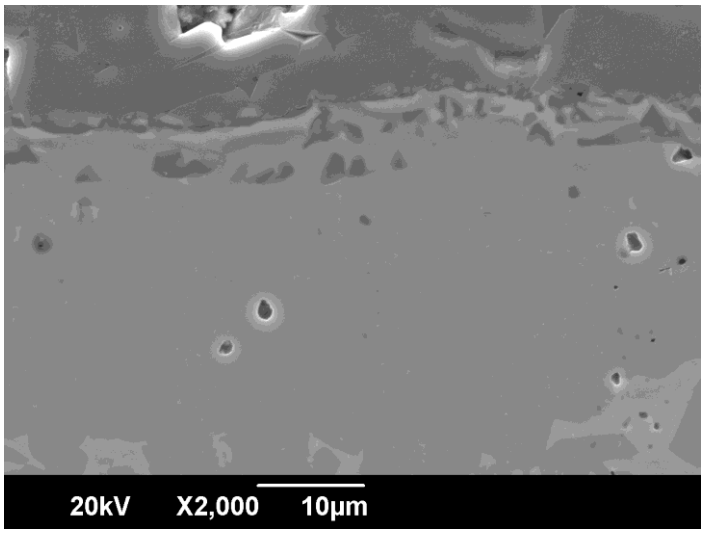

Figure 67 closeup micrograph of interface between Pd-40Ni commercial braze and Al_2O_3 substrate for aged Al_2O_3-to-Ti6Al4V joints

4.3.3.2.2 EDAX analysis of aged samples of Al2O3-Ti6Al4V joints brazed with Pd-40Ni

Figure 68 shows elemental spot analysis of an area where the presence of alumina is apparent. The spot of analysis is situated on a dark area underneath a bright area; this observation indicates that the dark area is Al_2O_3 and the braze has flown over the alumina.

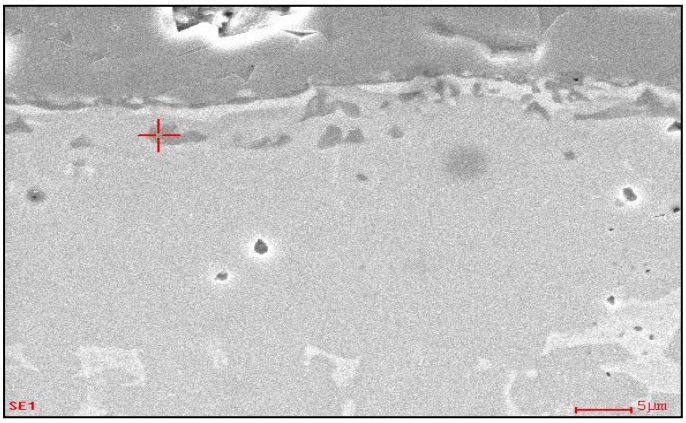

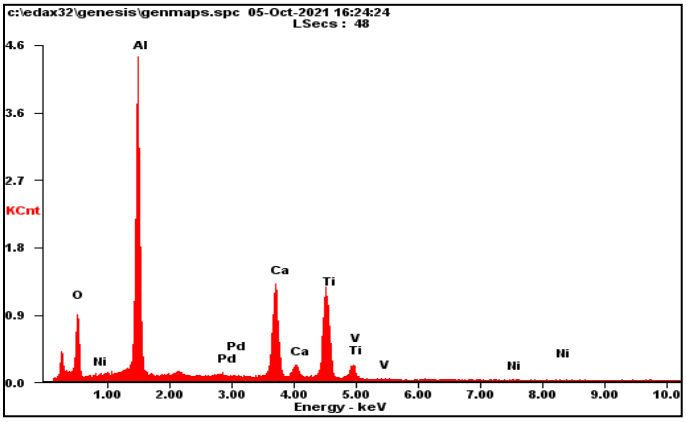

Element	Wt%	At%
OK	30.03	48.19
AlK	31.35	29.82
PdL	00.89	00.22
CaK	15.37	09.85
TiK	21.71	11.63
VK	00.24	00.12
NiK	00.40	00.18
Matrix	Correction	ZAF

Figure 68 Analysis of exposed alumina, with sintering additive Ca, covered by elements from Pd-40Ni braze and Ti6Al4V substrate.

Figure 69 shows the results of EDAX analysis of the intermetallic phase in contact with alumina. The analysis for aluminium was exaggerated due to the nearby presence of alumina. From the results, the interfacial phase was deduced to be $Ti_3(Pd,Ni,Al)$ as previously observed for the as-brazed samples.

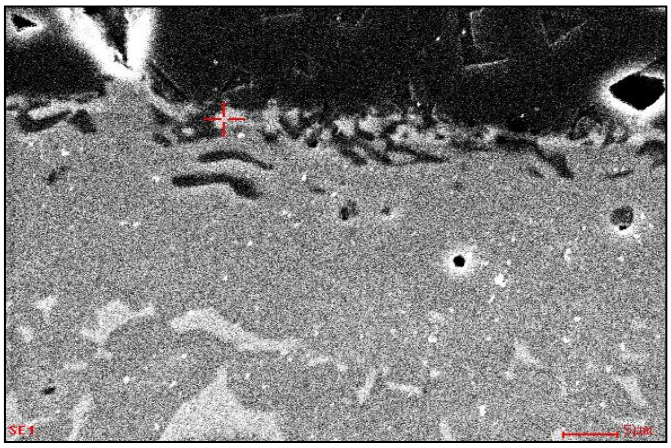

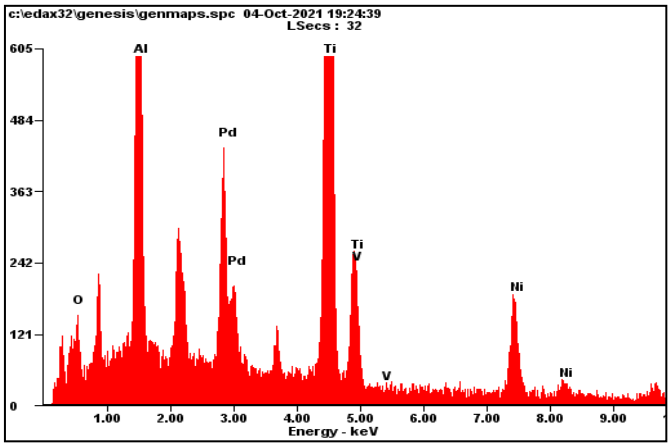

Element	Wt%	At%
OK	06.89	16.91
AlK	22.10	32.16
PdL	12.29	04.54
TiK	47.19	38.68
VK	00.00	00.00
NiK	11.52	07.71
Matrix	Correction	ZAF

Figure 69 EDAX analysis of the interfacial layer between the braze (initial composition Pd-40wt%Ni) and Al_2O_3 after ageing at 450°C for 500 hrs

In figure 70, similar microstructure to the original brazing process was observed. The elemental mapping analysis shows that the main area of the braze contained α-titanium and flakes of $Ti_2(Ni,Pd)$.

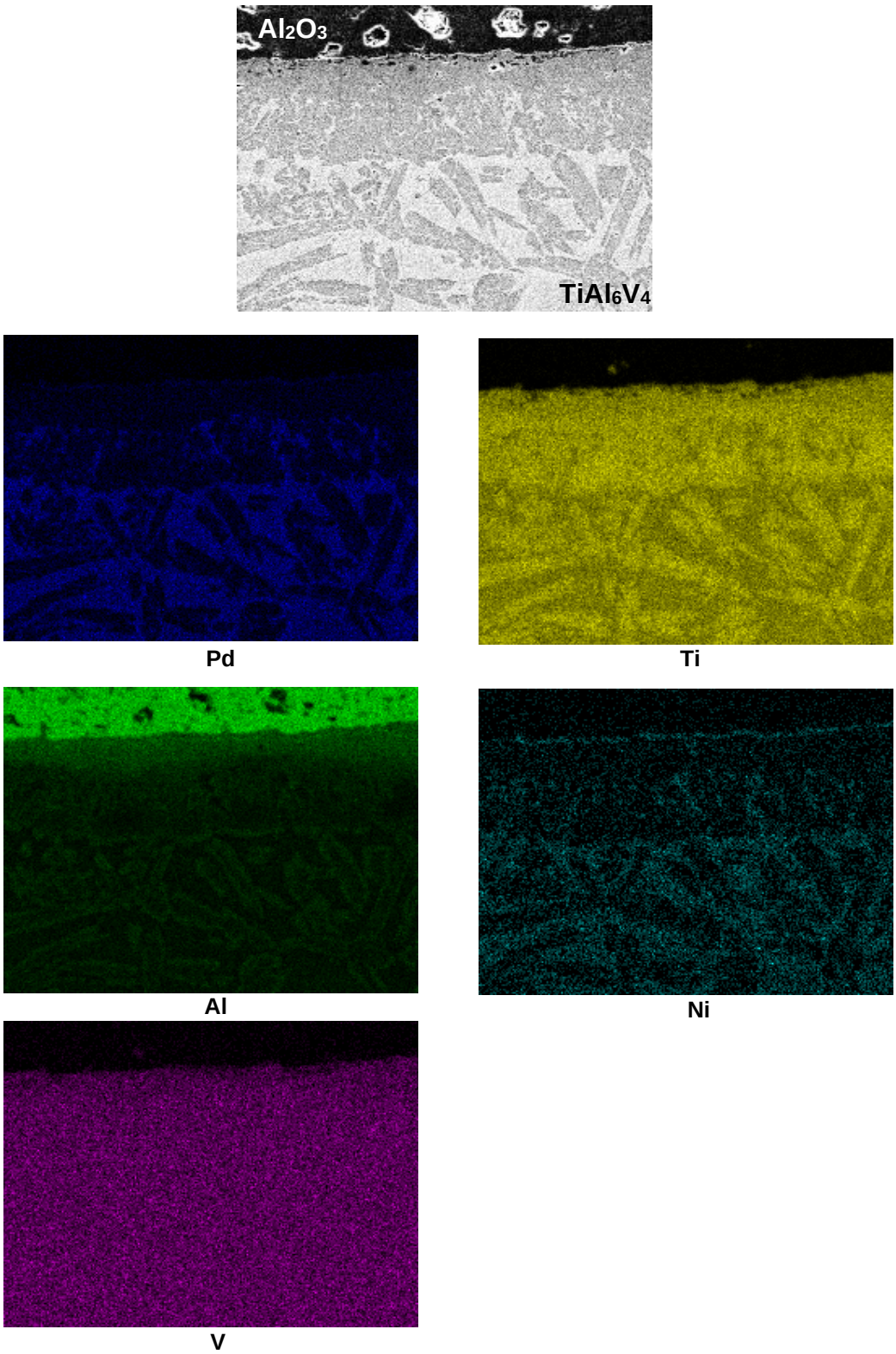

Figure 70 Elemental mapping analysis of Pd-40Ni commercial braze system used to join Al_2O_3-to-Ti6Al4V after ageing at 450°C for 500 hrs

Some porosity was observed at the alumina substrate, this potentially can affect the results. It is inherent that sintering methods do not fully eliminate porosity. However, the failure is observed at the interface where Ni and alumina interaction had taken place.

4.3.4 Brazing of Al_2O_3-Ti6Al4V using a novel Ni-14wt%Zr braze

A novel braze of composition Ni-14wt%Zr was proposed for use in the present study. The reason for the selection of this composition was based on several reasons including the earlier observations of this study that nickel can dissolve Al_2O_3 and thus achieve a strong bond with it. Inspection of the Ni-Zr equilibrium phase diagram [93] shows that the Ni-14wt%Zr composition forms a eutectic microstructure and therefore it would be expected to melt easily and probably flow well when in the molten state. In addition, the melting temperature of the eutectic is 1170°C and fits the requirement to use the joint at elevated temperatures.

4.3.4.1 SEM and EDAX analysis of brazing of Ti6Al4V to Al_2O_3 using a novel Ni-14Zr braze.

Following a number of trials, the brazing temperature that was chosen was 350°C with a dwelling time of one hour. SEM examination of a cross-section at the interface between the braze and Al_2O_3 is presented in figure 72. The micrograph revealed the presence of a continuous interfacial layer that ranged between about 5 μm to 8 μm thickness. There was evidence of a bond having been formed between the braze and Al_2O_3. The braze had climbed over the alumina (black spots in figure 72) indicating good wetting and flowability. The EDAX analysis presented in figure 73 shows the presence of both titanium and nickel within the interfacial layer. Some aluminium is also present but most of this comes from the alumina. The atomic ratio between titanium and nickel from the EDAX analysis is about 3. However, inspection of the Ni-Ti equilibrium phase diagram in figure 71 [94] shows that no Ti_3Ni phase exists. The observed interfacial layer was most likely based on Ti_2Ni with probably some aluminium dissolved in it, i.e., $Ti_2(Ni,Al)$. The formation of Ti_2Ni or $Ti_2(Ni,Al)$ at the interface with alumina bears strong similarity with the observations for the other titanium and nickel-containing brazes; the bond between the braze and alumina was established as a result of the dissolution of the ceramic into both titanium and nickel. In addition, there was reaction between the

intended Ni-14wt%Zr braze with the Ti6Al4V alloy. The Ni-Zr equilibrium phase diagram shows that the Ni-14wt%Zr eutectic composition would yield a microstructure of nickel and Ni_5Zr. However, there was no evidence of these phases in the final braze because of reaction with the Ti6Al4V alloy. Effectively the Ni-14wt%Zr composition has been used as a reactive braze. Melting had taken place at the dwelling temperature to yield a melt that contained titanium, aluminium and vanadium in addition to nickel and zirconium. Titanium and nickel have both been shown to be able to dissolve small amounts of alumina [73], [77], [79] and therefore these two elements migrated to the interface to interact with the ceramic. Consideration of the Gibbs Free energy of formation of ZrO_2 shows $\Delta G°_{ZrO2}$ = (-261,000 + 43.9T) x 4.18 J/mol which is a very negative value (more negative than that for the formation of NiO and TiO_2) suggesting that zirconium has a great affinity for oxygen and would not dissolve any of the alumina. For this reason, zirconium is virtually absent from the interface with Al_2O_3 and does not partake in the formation of the bond with the ceramic.

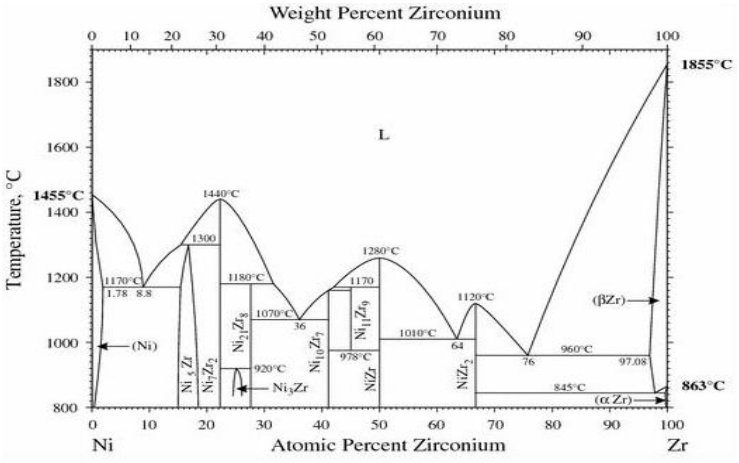

Figure 71 Ni-Zr binary phase diagram [90]

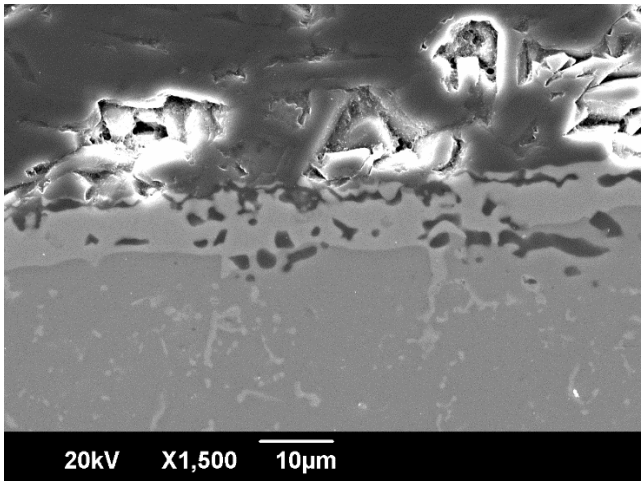

Figure 72 cross-section micrograph at the interface between the Ni-14Zr novel braze and Al_2O_3 substrate for Al_2O_3-to-Ti6Al4V joints

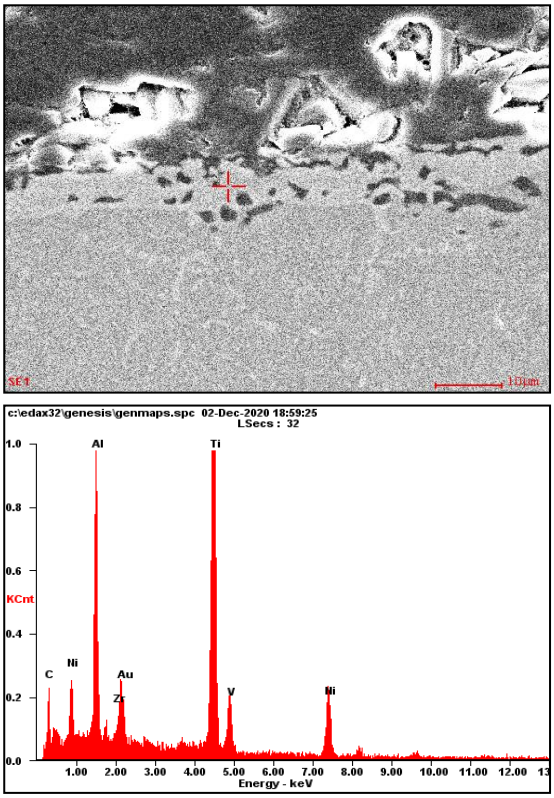

Element	Wt%	At%
CK	20.83	50.82
AlK	14.53	15.78
ZrL	02.06	00.66
AuM	08.18	01.22
TiK	38.90	23.79
VK	00.00	00.00
NiK	15.49	07.73
Matrix	Correction	ZAF

Figure 73 Spot analysis showing the presence of both titanium and nickel within the interfacial layer for Al_2O_3-to-Ti6Al4V joints

EDAX analysis of the area just below the interfacial layer is presented in figure 74. These results are suggestive of the presence of α-titanium. It is interesting to note the presence of 11.05 wt% of zirconium in this region. According to the Ti-Zr equilibrium phase diagram [95], no intermetallic compounds exist between titanium and zirconium. The entire composition at room temperature consists of an α solid solution with the two elements intermixing into each other. The third area is shown in figures 75 and 76 and consists of a mixture of α-titanium and Ti_2Ni sandwiched between two layers of Ti_2Ni. The EDAX analysis of the Ti_2Ni is shown in the two figures. The Ti6Al4V substrate lies below having bonded to the Ti_2Ni layer. As mentioned above, the Ni-14wt%Zr braze is reactive with regard to the Ti6Al4V alloy. In an unreacted state, the Ni-14wt%Zr braze is expected to have a eutectic microstructure consisting of nickel and Ni_5Zr. Since this was a reactive braze both of these phases participated in reactions and therefore, they were not present in the solidified braze microstructure. Nickel was present in the final solidified braze microstructure in the form of Ti_2Ni. By using Gibbs Free energy data for Ni_5Zr [93] and for Ti_2Ni [96], the relative stability of these intermetallic phases can be compared.

$$Ni_5Zr + 11Ti \rightarrow 5Ti_2Ni + Ti(Zr)$$

$$\Delta G^\circ = 5\,(-80{,}800 + 9.8T) - (-33{,}205 - 10.371T)$$

$$= -370{,}795 + 59.37T$$

In the calculation, the ΔG° for Ti(Zr) was assumed to be zero (it is expected to have a small negative value). The calculation confirmed the greater stability of the Ti_2Ni phase in comparison to Ni_5Zr. For this reason, there was no formation of Ni_5Zr and therefore virtually all of the zirconium that was present in the original composition had dissolved in the titanium.

The observations for the brazing process to bond Al_2O_3 to Ti6Al4V have shown that the braze was reactive. The bonding of the titanium alloy involved two parts; the first was the reaction between titanium and nickel to form a layer of Ti_2Ni and the second was the dissolution of zirconium in titanium. The bond with Al_2O_3 involved dissolution of the ceramic in titanium and nickel. Upon cooling down, a Ti_2Ni layer was formed at the interface with Al_2O_3. The reactivity of the original braze composition (Ni-14wt%Zr) with Ti6Al4V was crucial in achieving the bond

on either side of the joint. This interaction between the Ni-14wt%Zr and Ti6Al4V involved some melting of the titanium alloy and this enabled the titanium to migrate to the ceramic surface where some dissolution of Al_2O_3 took place.

The braze is interacting with the alumina, but also some of that braze is reacting with the titanium substrate. This interaction is caused by the Ni in the braze system; there is melting of Al2O3 into the nickel (and in the titanium that dissolved into and reacted with the braze) resulting in a good interfacial bond. However, there is also an indication that the interaction between Ni and alumina is causing some damage to the surface, which is also confirmed by poor outcome of the shear test results reported in Section 4.4.

The layer just below the interfacial Ti2Ni phase underwent EDAX analysis the results of which are shown in Figure 74. The analysis shows a very small presence of Ni and suggests that it is composed of Ti3Al; 5.01at% zirconium was observed to be present in this region and this is probably dissolved in Ti3Al since the Ti-Zr equilibrium phase diagram forms solid solutions over the entire composition range [97].The next layer that forms below this has the characteristic microstructure of α and β titanium which are sandwiched by two bright layers that are shown in Figure 75 and Figure 76. The EDAX analysis results that are shown in these two figures suggest that the bright phase is Ti2Ni.

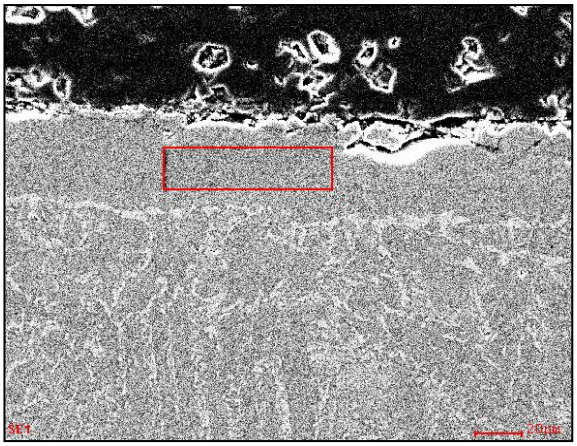

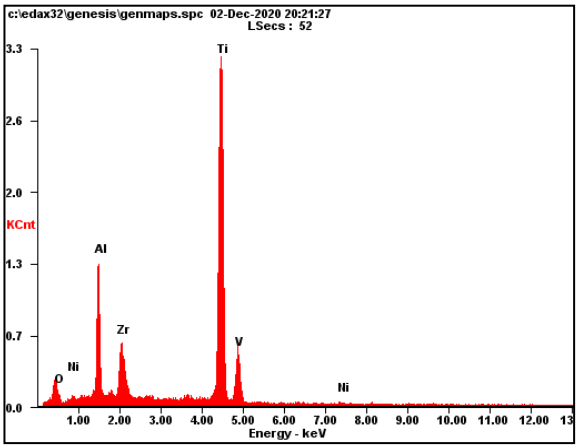

Element	Wt%	At%
OK	05.84	15.11
AlK	12.36	18.95
ZrL	11.05	05.01
TiK	69.48	60.03
VK	00.00	00.00
NiK	01.27	00.90
Matrix	Correction	ZAF

Figure 74 area analysis of layer below the interfacial Ti_2Ni phase for brazed Al_2O_3-to-Ti6Al4V joints using novel Ni-14Zr braze.

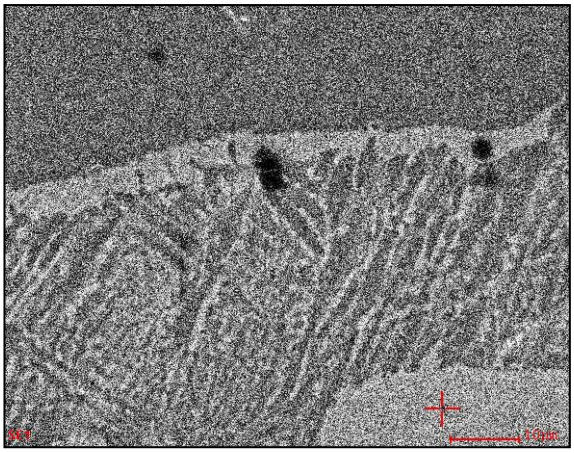

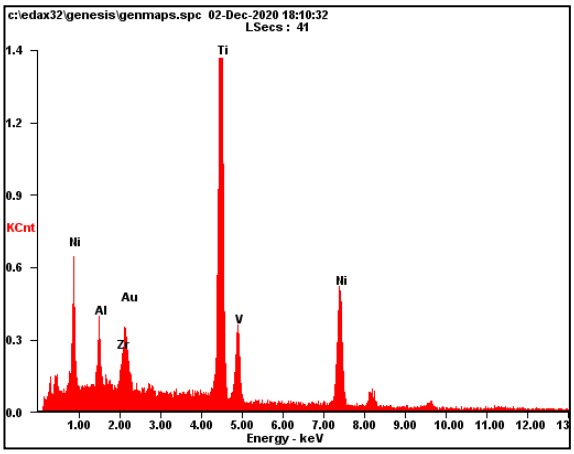

Element	Wt%	At%
AlK	04.27	08.56
ZrL	03.18	01.88
AuM	09.66	02.65
TiK	50.74	57.27
VK	00.18	00.19
NiK	31.98	29.45
Matrix	Correction	ZAF

Figure 75 analysis of a layer consisting of a mixture of α-titanium and Ti_2Ni

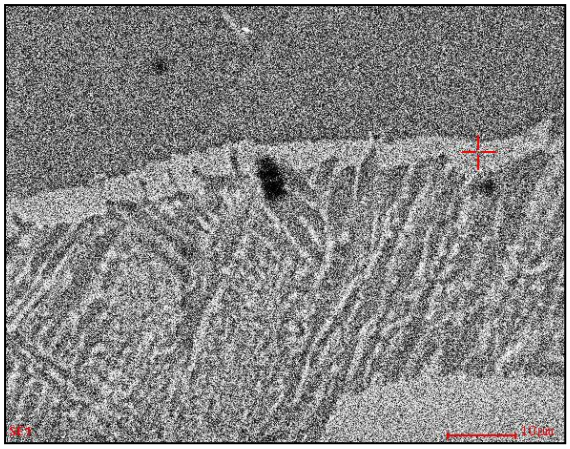

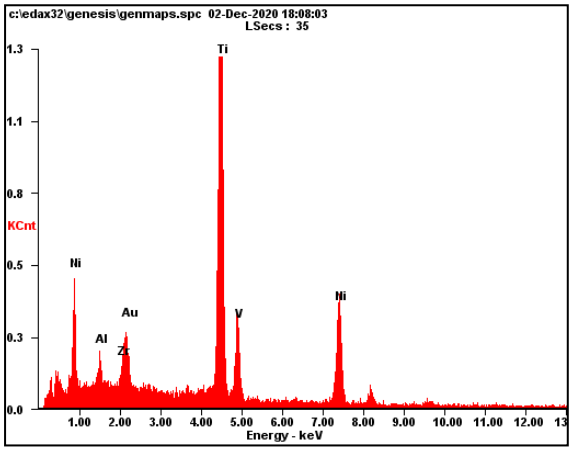

Element	Wt%	At%
AlK	02.26	04.56
ZrL	02.72	01.63
AuM	09.35	02.59
TiK	54.77	62.40
VK	00.63	00.68
NiK	30.27	28.14
Matrix	Correction	ZAF

Figure 76 analysis of another layer consisting of a mixture of α-titanium and Ti_2Ni

Overall, the microstructural and EDAX analyses show evidence of melting and this indicates that the interaction between the braze and the Ti6Al4V alloy did not take place by solid-state diffusion, but rather the interaction involved a transient liquid phase. Titanium and aluminium from the Ti-Al6-4V substrate diffused into and reacted with the braze to form Ni_2Ti along with alpha and beta titanium.

4.3.4.2 Ageing at 450°C of Ti6Al4V-Al_2O_3 joints brazed with Ni-14wt%Zr

This braze is novel and has been specially proposed in the course of this study. It is important to carry out further examination to understand any additional chemical reactions assuming operation at high temperatures of around 450°C. Similar to the observations of the previous braze system, no further chemical reactions were observed at 450°C. SEM and EDAX analyses were conducted to examine the behaviour at 450°C.

4.3.4.2.1 SEM of Ti6Al4V-Al_2O_3 joints brazed with Ni-14wt%Zr following ageing at 450°C

Figure 77 shows three different microstructural regions that were observed following ageing of the joints at 450°C. Figure 78 shows the interfacial region between the braze and the alumina substrate and shows evidence of the presence of a white phase that is bonded onto the alumina. EDAX analysis was subsequently undertaken to identify the phases that had formed within the braze.

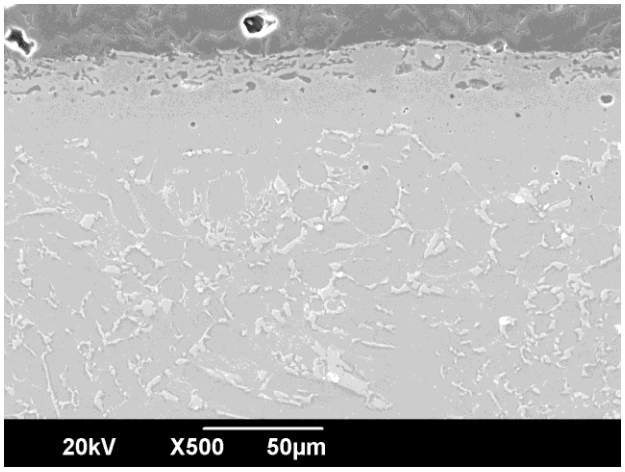

Figure 77 overview of three different microstructural layers at Ti6Al4V substrate for aged Al_2O_3-to-Ti6Al4V joints using novel Ni-14Zr braze.

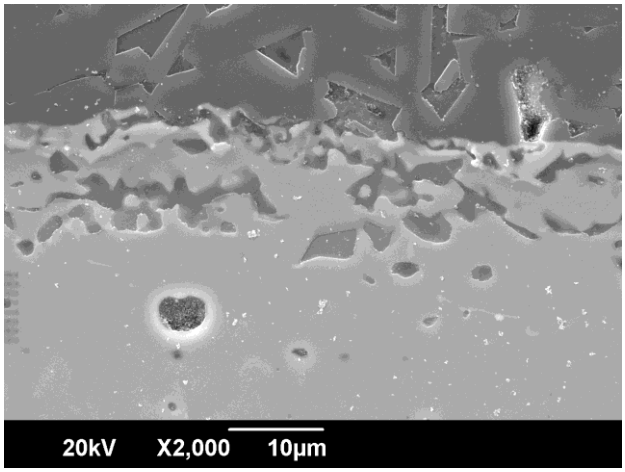

Figure 78 closeup micrograph of interfacial layer at Al_2O_3 braze for Al_2O_3-to-Ti6Al4V joints using novel Ni-14Zr braze.

4.3.4.2.2 EDAX analysis of Ti6Al4V-Al_2O_3 joints brazed with Ni-14wt%Zr following ageing at 450°C

EDAX analysis was conducted to examine the two layers within the braze below the interface with alumina and the phase that had formed in contact with the interface with alumina. Figure 79 shows EDAX analysis of the layer just below the interfacial phase with alumina. The elemental composition of this region was similar to that for the as-brazed samples and comprises of Ti_3Al (the EDAX analysis for aluminium includes some of the aluminium in the alumina substrate). Below this in Figure 80, there appears to be a layer composed of α and β titanium. Futher down the white phase that was identified to be Ti_2Ni is present (as identified in Figure 76); the only microstructural difference with the as-brazed sample was that the top Ti_2Ni layer (above the α and β region) was no longer continuous.

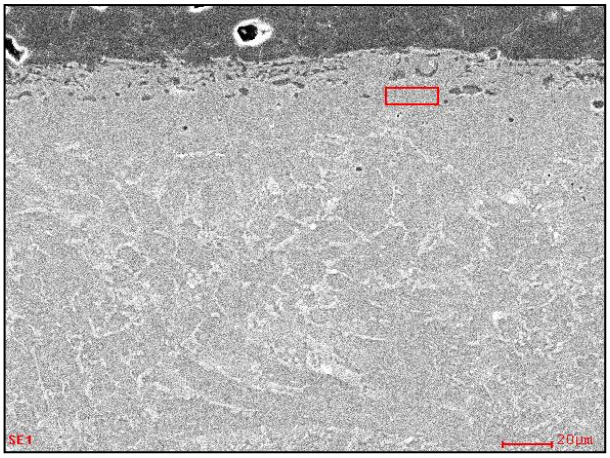

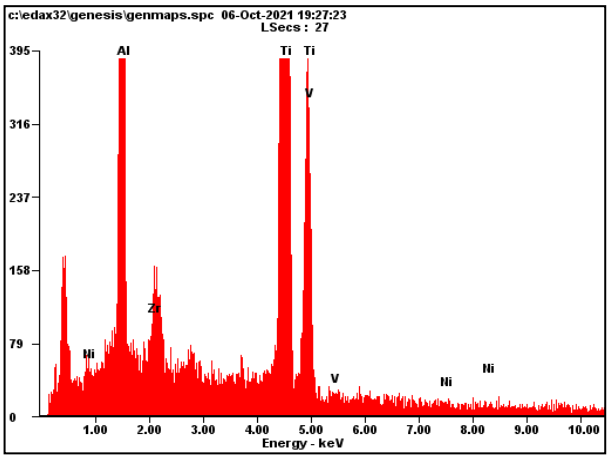

Element	Wt%	At%
AlK	21.91	33.65
ZrL	02.46	01.11
TiK	74.17	64.14
VK	00.59	00.48
NiK	00.87	00.62
Matrix	Correction	ZAF

Figure 79 top layer below braze interface with alumina showing Ti_3Al for aged Al_2O_3-to-Ti6Al4V joints using Ni-14Zr novel braze.

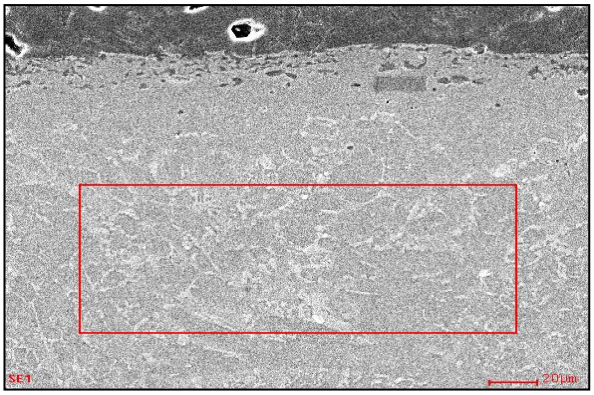

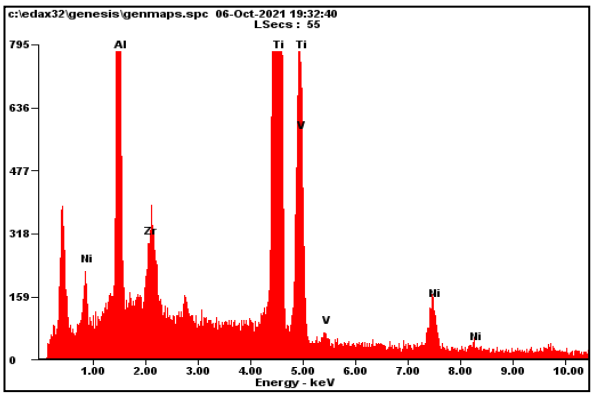

Element	Wt%	At%
AlK	12.13	20.18
ZrL	03.14	01.54
TiK	76.47	71.68
VK	02.23	01.97
NiK	06.04	04.62
Matrix	Correction	ZAF

Figure 80 lower layer composed of α and β titanium for aged Al_2O_3-to-Ti6Al4V joints using Ni-14Zr novel braze.

Figure 81 presents EDAX analysis of the metallic phase that was present at the interface of the braze with alumina. This phase was identified as Ti_2Ni or $Ti_2(Ni,Al)$ the latter being the former phase with some aluminium dissolved in it. This is the same phase that was observed for the as-brazed sample. Overall, there was no significant change between the as-brazed samples and the samples that were aged at 450°C.

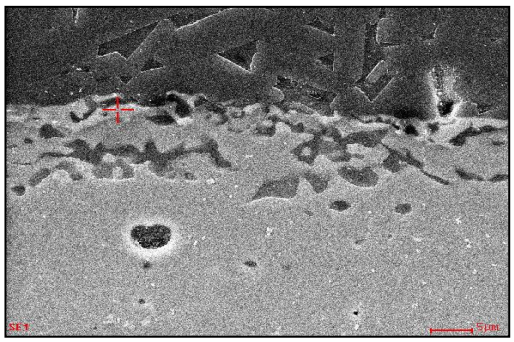

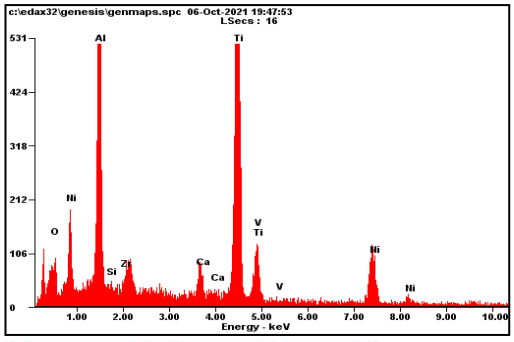

Element	Wt%	At%
OK	11.22	24.41
AlK	24.36	31.41
SiK	00.15	00.19
ZrL	02.54	00.97
CaK	02.27	01.97
TiK	43.35	31.50
VK	00.00	00.00
NiK	16.10	09.54
Matrix	Correction	ZAF

Figure 81 Analysis of the metallic phase identified as Ti2Ni or Ti2(Ni,Al) for aged Al_2O_3-to-Ti6Al4V joints using Ni-14Zr novel braze, bright area at the interface with alumina (including sintering additive elements).

The pore in the alumina section in figure 81 is understood to be an influence of the process of manufacturing. These pores might have been covered in some areas by the dissolution in Ni element.

4.4 *Mechanical Testing (Single-lap offset shear test)*

4.4.1 Al_2O_3-Al_2O_3 joints using (Ti,X)Al Braze

Following the contact angle measurements and the SEM investigation to examine the effect of the addition of Ni or Fe to Ti-Al based brazes, the mechanical strength of the joints was tested. The mechanical strength (apparent shear strength) of the joined samples was determined using a single lap offset (SLO) test in compression according to a method adapted from the ASTM D1002-05 standard (universal testing machine SINTEC D/10). The following braze compositions were used for single lap offset testing: TiAl7.2Ni_Al_2O_3, TiAl7.2Fe_Al_2O_3, TiAl3.6Ni_Al_2O_3 and Ti50Al50.

All the samples used for the SLO tests were cut into 25mm x 25mm and the braze was applied to cover an area of 12.5mm x 25mm as shown previously in figure 31. Macrographs of sheared samples are shown in Figure 82, and it is apparent that in the case of the TiAl7.2Ni_Al_2O_3, TiAl7.2Fe_Al_2O_3, and TiAl3.6Ni_Al_2O_3 samples, the braze did not spread sufficiently enough to cover the entire interfacial area. The flow for the Ti50Al50_Al_2O_3.braze appeared to be better and covered a greater area. Figures 83-86 represent the load response from the single lap offset experiments. The results are summarised in Table 9.

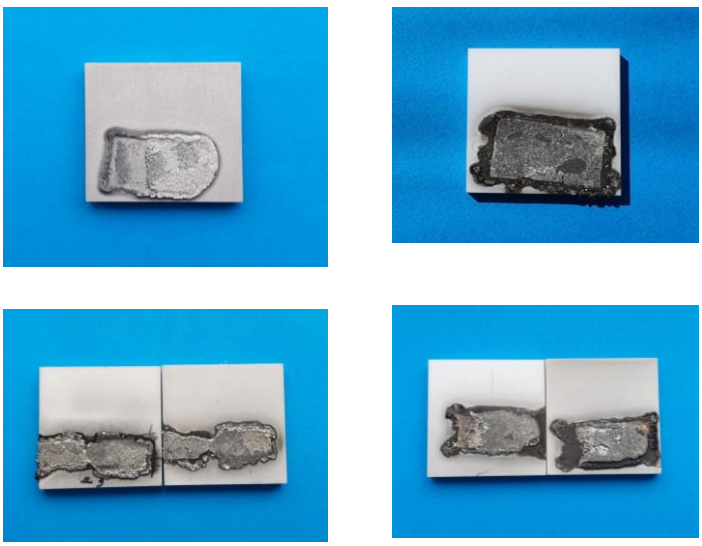

Figure 82 Samples after conducting SLO

Table 9 Single lap offset results

Composition (wt%)	Apparent Shear Strength (MPa)
TiAl7.2Ni_Al_2O_3	20.9
TiAl7.2Fe_Al_2O_3	32.3
TiAl3.6Ni_Al_2O_3	21.8
Ti50Al50_Al_2O_3	27.6

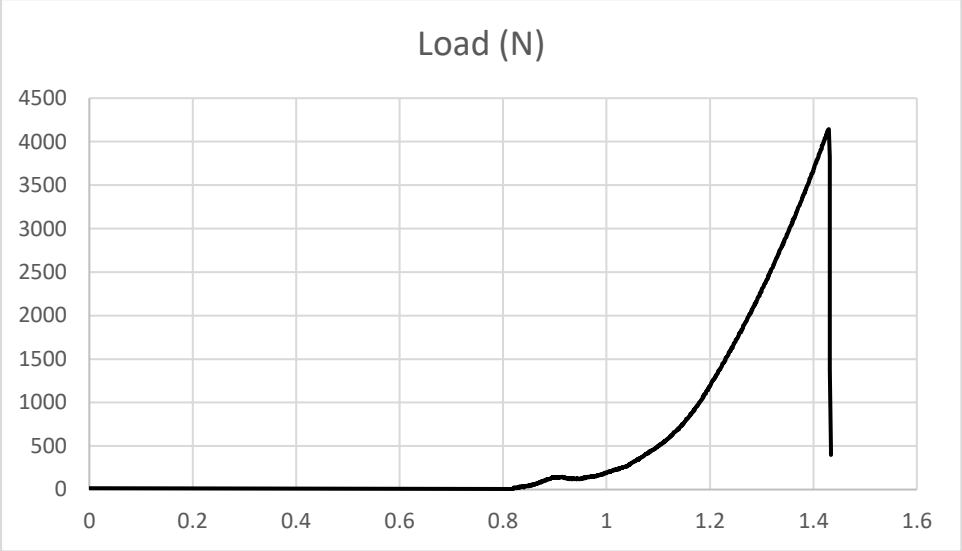

Figure 83 Load graph of TiAl7.2Ni_Al_2O_3

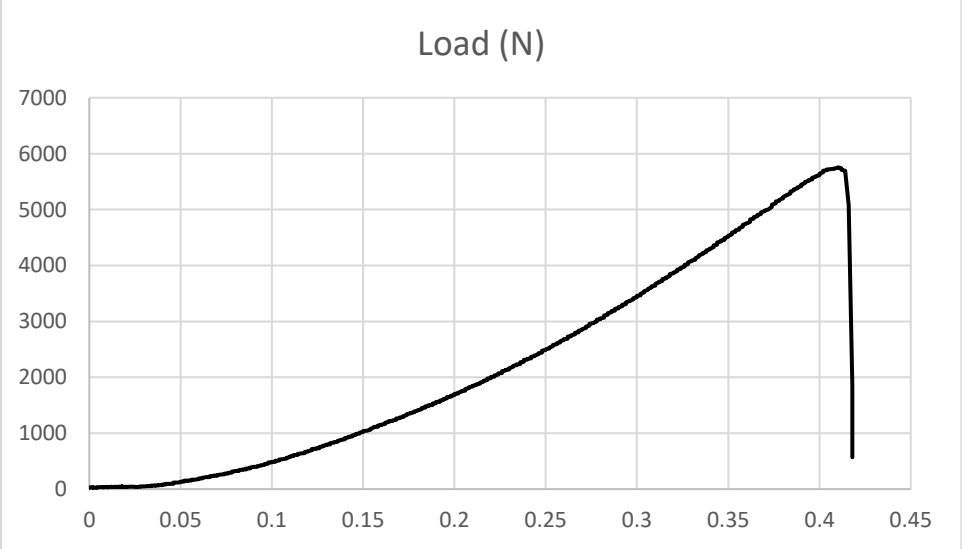

Figure 84 Load graph of TiAl7.2Fe_Al_2O_3

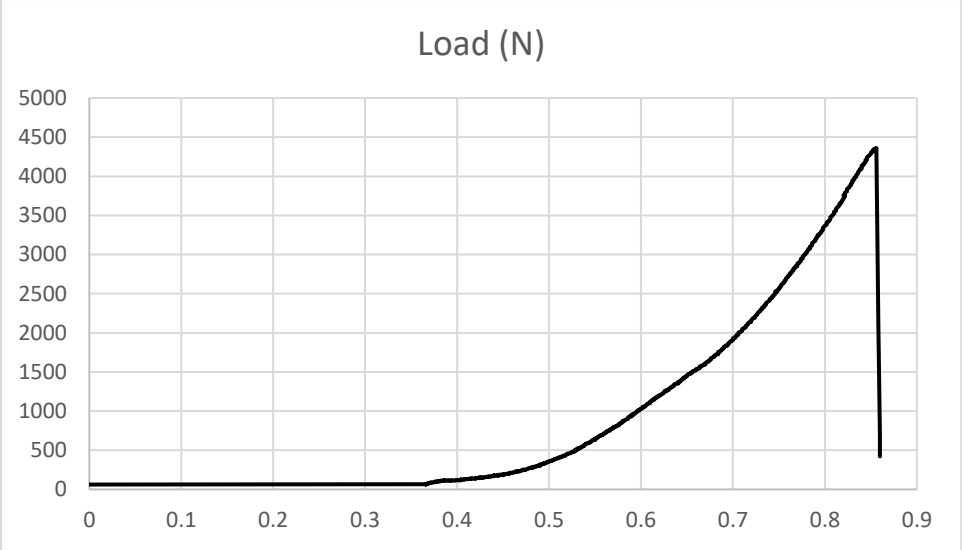

Figure 85 Load graph of TiAl3.6Ni_Al_2O_3

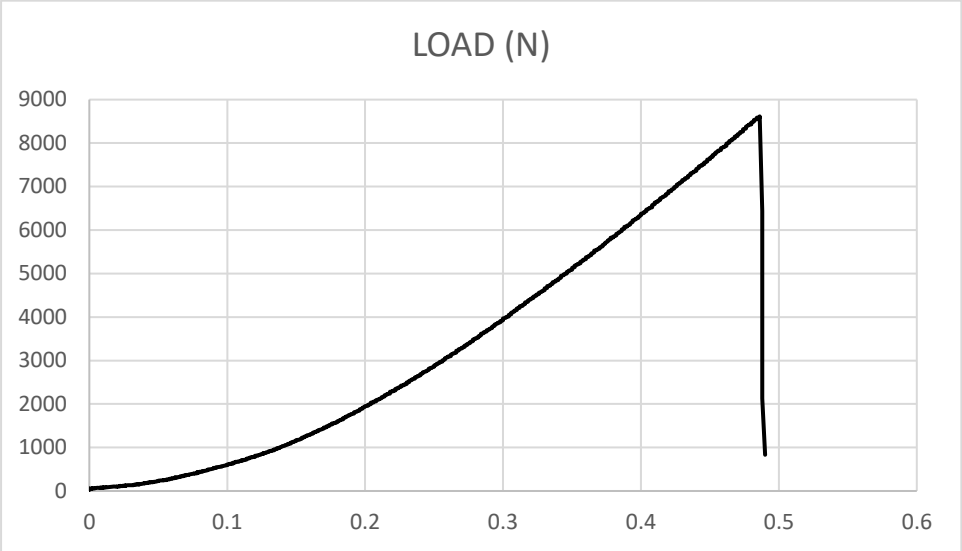

Figure 86 Load graph of Ti50Al50_Al2O3

In the case of the nickel addition, it is evident that the lap shear strength had dropped from 27.6 MPa for the Ti50Al50_Al_2O_3 sample to 21.8 MPa and 20.9 MPa for the TiAl3.6Ni_Al_2O_3 and TiAl7.2Ni_Al_2O_3 samples respectively. Considering that the contact angle measurements had shown that the addition of nickel to the Ti-Al braze had led to improvement in the wettability with Al_2O_3, there was an expectation that the shear strength would also increase. Therefore, the shear strength results were rather surprising and contrary to expectations when considering the contact angle measurements. SEM examination and EDAX analysis were undertaken over a wide sheared area. Figure 87 shows the sheared surface from near the edge of the shear fracture. It is apparent that this area presents mainly the sheared surface of Al_2O_3 with only little

evidence of the presence of the braze. EDAX analysis from the sheared surface from within the central regions of the brazed joint are presented in Figure 88 and show only partial presence of the braze. A wider overview of the fractured area is presented in Figure 89 and shows evidence of small, localised areas of the braze material; however, most of the fractured surface consisted of alumina. Inspection of the plots of shear load against extension suggests that there was no plastic deformation. This observation is typical of brittle fracture implying that sample failure had taken place within the alumina. Previously in Figure 24 there was evidence of dissolution of Al_2O_3 by both titanium and nickel leading to decrease in the contact angle between Al_2O_3 and the Ti-Al-Ni-based braze. Similar evidence of the surface of the alumina receding due to dissolution in the braze is also shown in an SEM micrograph in Figure 87 which was taken from a sideview at the edge of the fractured surface. On the right-hand side of the micrograph, there is evidence of a portion of about 80 μm of alumina receding away due to dissolution in the melt (in titanium and nickel). The top layer consists of part of the braze that has penetrated part of the alumina. As a result of dissolution, the surface of alumina became uneven and damaged at the interface with the braze. The SEM micrograph also shows evidence of cracks running into the alumina. During the lap shear tests, stress concentration is likely to form at the uneven and damaged alumina surface leading to crack formation. From this evidence, it was concluded that fracture had taken place within the alumina at a damaged region that coincided with the area of maximum braze penetration.

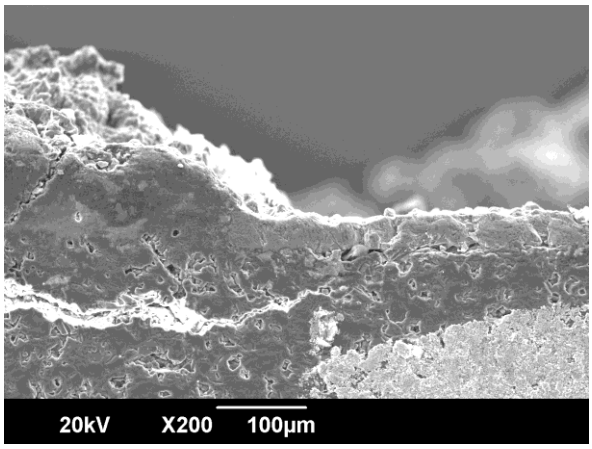

Figure 87 Sideview of fractured surface showing alumina receding away for Al_2O_3-to-Al_2O_3 joints using (Ti, X)Al novel braze system.

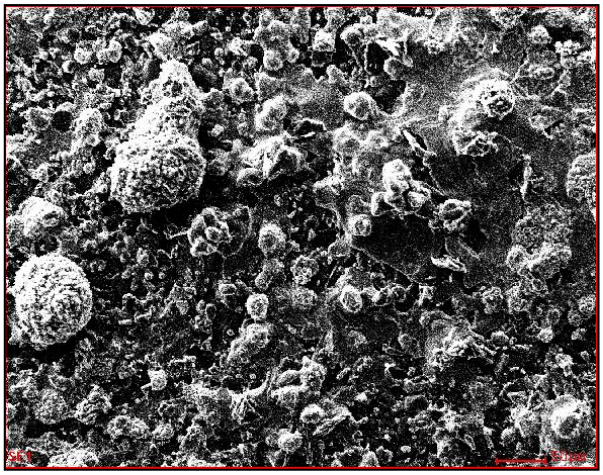

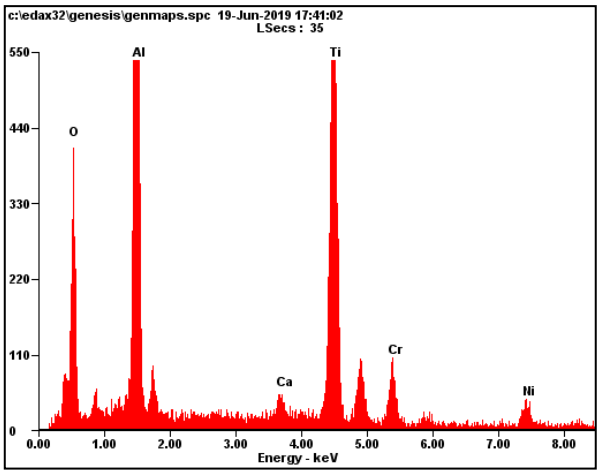

Element	*Wt%*	*At%*
OK	30.28	50.23
AlK	27.28	26.83
CaK	01.40	00.93
TiK	30.88	17.11
CrK	05.28	02.69
NiK	04.88	02.20
Matrix	Correction	ZAF

Figure 88 Middle sheared area analysis showing nickel for Al_2O_3-to- Al_2O_3 joints using (Ti, X)Al novel braze system.

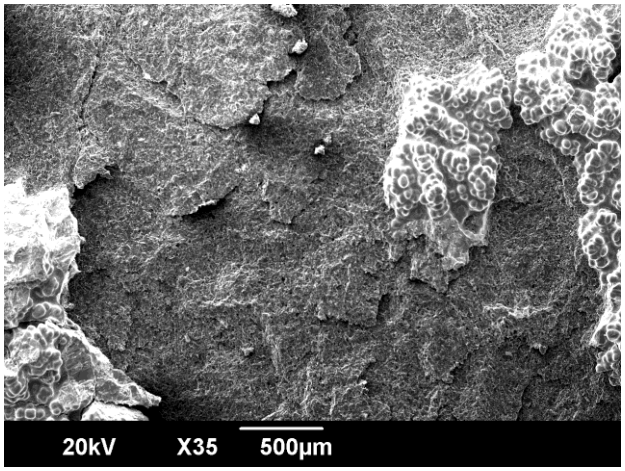

Figure 89 overview of fracture for Al_2O_3-to-Al_2O_3 joints using (Ti, X)Al novel braze system.

4.4.2 Single lap shear test results for Al_2O_3-Ti6Al4V joints

The joint strength between Alumina and Titanium using four different braze systems were tested with reference to the ASTM D905-08 standard.

4.4.2.1 Single lap shear test results for Al_20_3-to-Ti6Al4V joints using Ti-3.6Ni-28Al braze.

The surface fracture of the Al_2O_3-Ti6Al4V sample that was joined by the Ti-3.6-28Al braze following the lap shear test was examined using SEM and EDAX analysis. An SEM micrograph of the fractured surface is shown in figure 90. The micrograph shows evidence of fracture of alumina at an area where there was maximum penetration by the braze.

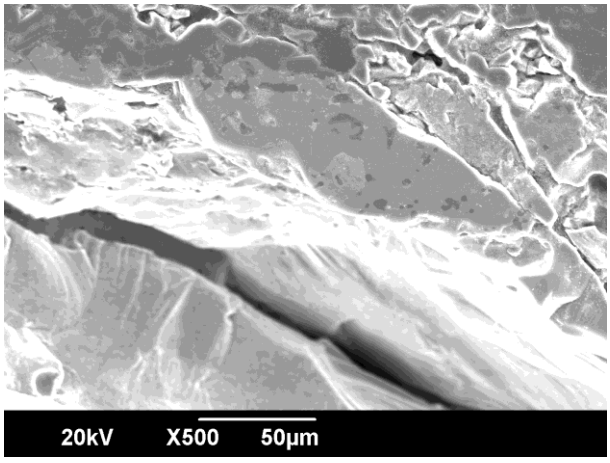

Figure 90 SEM micrograph showing evidence of cracks at interface with alumina for Al2O3-Ti6Al4V joints using Ti-3.6-28Al novel braze.

EDAX analysis in figure 91 shows the presence of the braze constituents. There is also clear evidence of the presence of Ni near the fractured zone. This confirms the earlier observations of a nickel-containing phase forming at the interface with alumina and supports the fact that wettability was enhanced by dissolution of alumina into nickel. However, such dissolution can cause interfacial damage leading to initiation of cracks and fracture at the alumina surface. The micrographs show fracture occurring within the alumina with evidence of penetration of the braze into the alumina. Again, the fractured surface coincided with the area of maximum braze penetration. These observations are suggestive of fracture occurring within the alumina at a point where there was damage due to dissolution of the alumina into the molten braze.

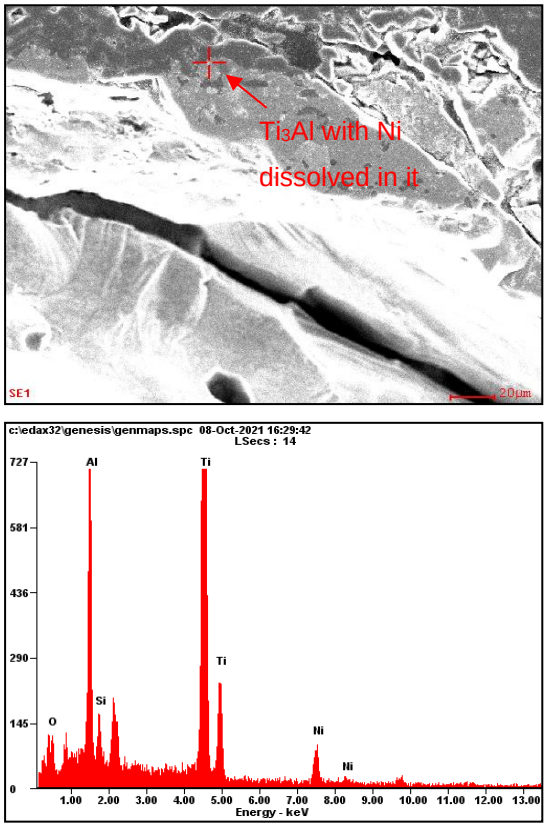

Element	Wt%	At%
OK	11.05	24.29
AlK	17.99	23.46
SiK	02.29	02.87
TiK	60.96	44.77
NiK	07.71	04.62
Matrix	Correction	ZAF

Figure 91 spot analysis above crack showing braze constituents for Al2O3-Ti6Al4V joints using Ti-3.6-28Al novel braze.

Uday et al [4] outlined the factors that can affect the reliability of metal-to-ceramic joints. The coefficient of thermal expansion (CTE) of various materials in figure 92 [4] show that the data for Al_2O_3 and titanium are not too dissimilar. The CTE values for the Ti-based braze are probably not very different.

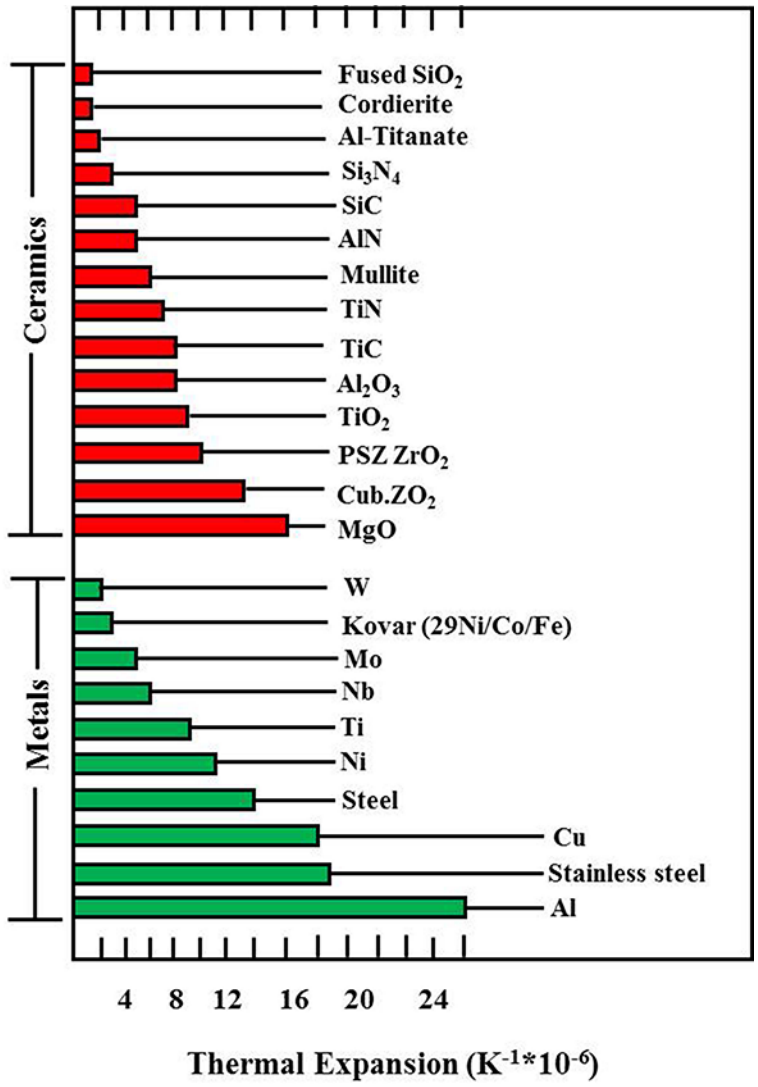

Figure 92 CTE of metal and ceramic comparison [4]

Despite this some element of residual stress is likely to be present at the interface between Al_2O_3 and the braze. Figure 93 presents development of residual stresses as well as the potential cause of damage within the ceramic. While a major concern is the achievement of good wetting, chemical or physical changes that occur at the interface may lead to damage. Cracks that are initiated at the interfacial layer generally weaken the joint strength.

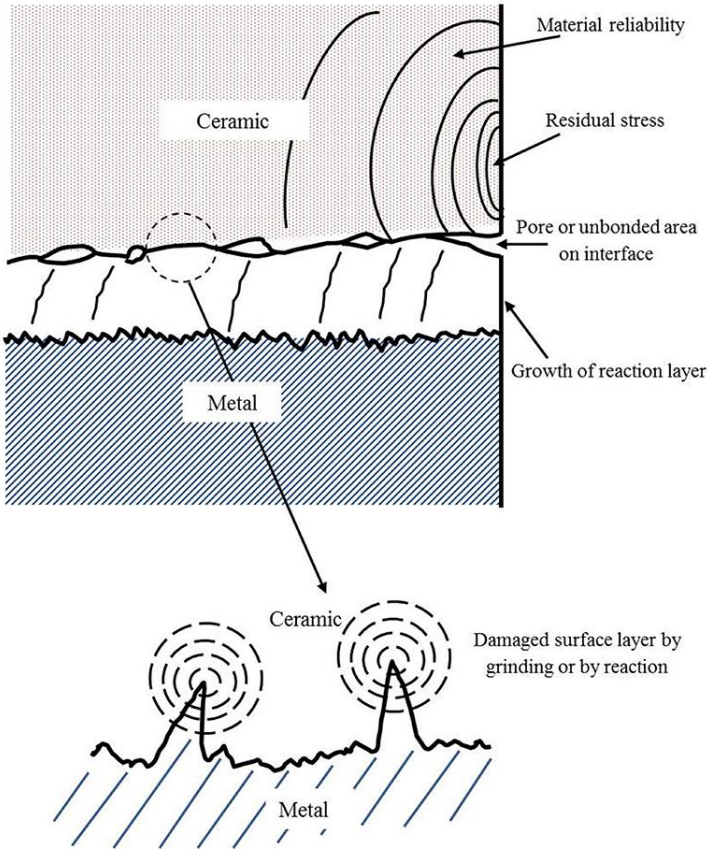

Figure 93 schematic diagram of influential factors determining the reliability of metal-ceramic joints [4]

Thermal stress, or residual stress in a joint, is another vital factor. High thermal stresses during joining processes cause defects in joints. The joint strength is substantially reduced when a large number of unbonded or weakly bonded defects are present on the interface. Hence, another interpretation of the weak joint or failure to join is the fact that titanium is very reactive, unlike ceramics which are much more stable.

Uday et al. [4] have also explained that equilibrium thermodynamics also can be used to predict possible reactions at an interface by considering the possible reaction potentials, which can produce a net negative free energy. Having a net free energy can be assumed to have favourable thermodynamic properties. Nonetheless, having more than three elements in a metal-ceramic system, makes the process of predicting all the phases occurring from such reaction difficult. Chemical thermodynamics calculations that were presented in Section 4.2.1 suggest that low-level interaction between alumina and aluminium is possible thus contributing to damage at the surface of the alumina. In addition, evidence has been presented showing

dissolution of alumina in the molten braze (in nickel and titanium) and this is also likely to create interfacial defects from which cracks may initiate and propagate during lap shear testing.

4.4.2.2 Single lap shear test results for Al_20_3-to-Ti6Al4V joints using Ti-15Ni-15Cu Braze

As described in Section 4.3.2, brazing of Ti6Al4V to Al_2O_3 was achieved using a Ti-15Ni-15 Cu braze at 1200°C. In that part of the investigation, small samples of Al_2O_3 were joined to titanium. For the preparation of samples for lap shear testing, the geometry of the Ti6Al4V and Al_2O_3 was larger (25 mm x 25 mm and 4 mm thickness) and the intended lap shear area was 25 mm x 12.5 mm. Following brazing at 1200°C, the samples were cooled down in the furnace. All the lap shear samples that were prepared for this system failed while handling. Figure 94 shows macrographs of the Al_2O_3 section of the joint; it is evident that the braze did not flow sufficiently to cover the entire alumina section. This was rather surprising because in the earlier part of the work brazed samples had been obtained achieving good wetting between the braze and alumina. More careful examination of the surface of the part of the braze attached to the alumina shows the presence of a “ridge” near the centre of the braze. In the earlier section, evidence was shown of reactions occurring between the braze and the Ti6Al4V alloy and in particular with titanium. Most of this reaction seems to be taking place near the centre of the braze with utilisation of the braze components that were situated around the central regions. The aluminium and copper components (in the form of foil) have melting points (660°C and 1083°C respectively) below the brazing temperature of 1200°C and they are expected to melt first. Reaction with the titanium foil and with the titanium in the substrate is likely to commence below the brazing temperature. It appears that in this sample, the reaction was localised within that narrow region and prevented the spreading of the braze to cover the entire interface. It is apparent from Figure 94 that there was fracture only within the central regions at the position of the “ridge” and that the surrounding areas had not bonded together (there is no evidence of bonding or debonding from the Ti6Al4V substrate). The resulting bonded area was very small and was very fragile and broke off during handling. The EDAX mapping that follows from the fractured central area in Figure 95 shows evidence of fractured spots that had been brazed (the areas containing Ti, Ni and Cu). Even in these areas the bond area is limited.

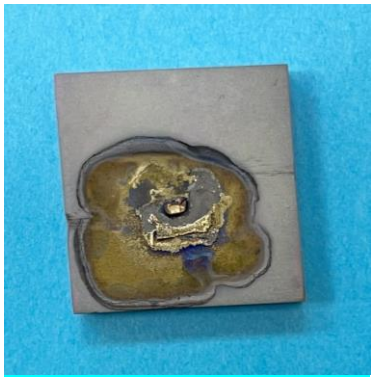

Figure 94 Attempt to join Al203-to-Ti6Al4V using Ti-Cu-Ni commercial braze.

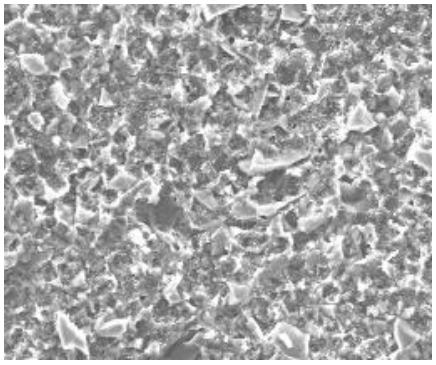

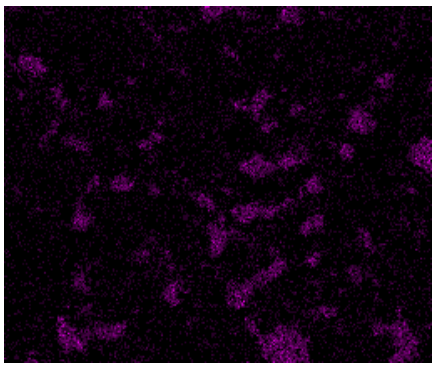

Cu

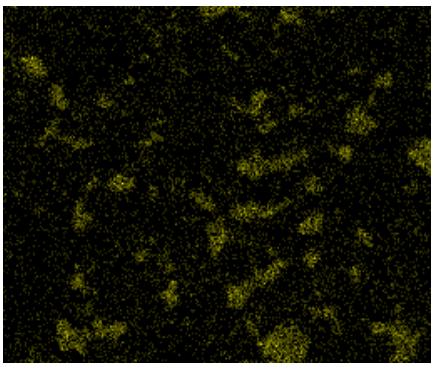

Ni

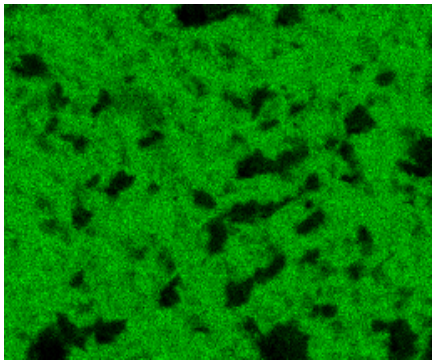

Al

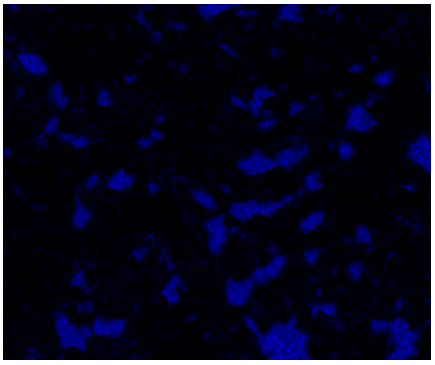

Ti

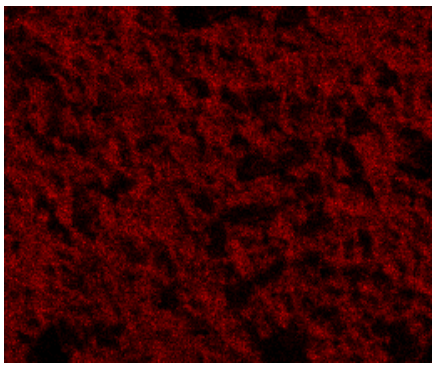

O

Figure 95 mapping for fractured braze at alumina surface

4.4.2.3 Single lap shear test results for Al_20_3-to-Ti6Al4V joints using Pd-40Ni Braze

Figures 96 and 97 show views of brazed joints between Ti6Al4V and Al_2O_3, while figure 98 presents a macrograph of the fractured surface following the shear test. The latter macrograph shows that the braze had covered the entire interface between the two materials very well indicating excellent braze flowability. However, the recorded shear strength for the samples joined by the Pd-40Ni braze was remarkably low. Figure 99 is a representation of the shear test results for this system and shows fracture at a force of 622 N which corresponds to a shear strength of only about 1 MPa. The results show that there was no plastic deformation as fracture occurred within the alumina. As with the observations for the earlier nickel-containing brazes, the reason for the low shear strength was attributed to the interaction of Ni in the braze with the alumina substrate.

Figure 96 side view of Al_20_3-to-Ti6Al4V joints using Pd-40Ni commercial braze before shear test.

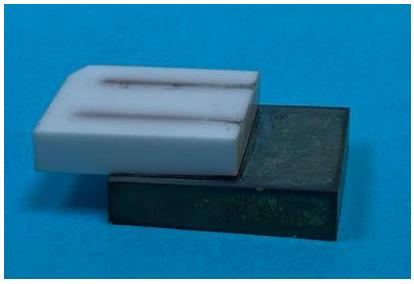

Figure 97 top-side view of Al_20_3-to-Ti6Al4V joints using Pd-40Ni commercial braze before shear test.

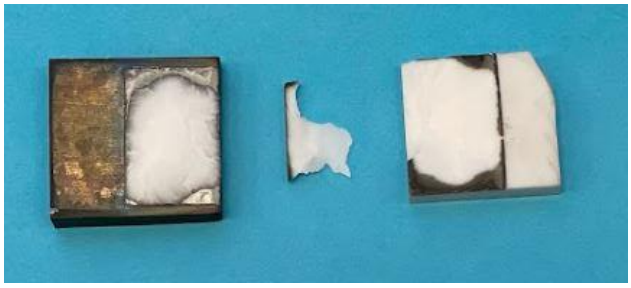

Figure 98 fractured joint of Al_20_3-to-Ti6Al4V joints using Pd-40Ni commercial braze after shear test.

The graph in figure 99 is a representation of the shear test conducted on the Pd-Ni braze system which fractured at a force of 622 N or ~1 MPa. These values are relatively low compared to data from the joining of Al_2O_3 to Al_2O_3.As explained earlier, the dissolution of alumina in Ni is likely to lead to interfacial damage.

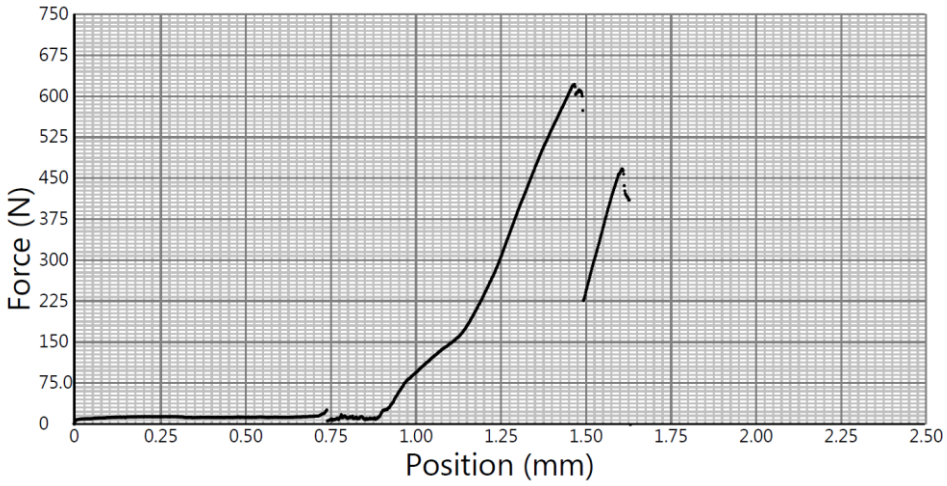

Figure 99 Load graph of Pd-40Ni braze system

The cross-section of the fractured surface appears to be flat at the edges (perpendicular to the load) of the samples showing metallic presence of the braze. Away from the edges there is evidence of fractured alumina; this area appears to be flat as well. Farther away, the presence of a “ridge” of alumina was observed. The edges of this “ridge” of alumina show dark colouration which represents part of the braze that had penetrated the alumina. At the edge of the alumina ridge (parallel to the load) there is evidence of the presence of the braze. It is quite likely that the dark areas around the alumina ridge represent the regions where fracture initiated, and these coincide with the points of damage at the alumina surface due to its dissolution in nickel.

4.4.2.4 Single lap shear test results for Al_20_3-to-Ti6Al4V joints using Ni-14Zr Braze

Figures 100 and 101 are images for joints before shear test procedure. Fractured joints after shear test can be seen in figure 102.

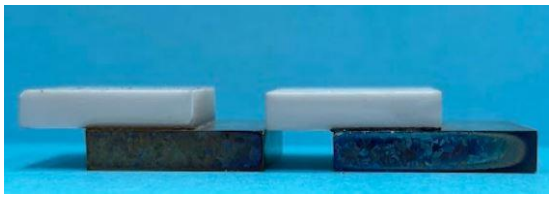

Figure 100 side view of Al_20_3-to-Ti6Al4V joints using Ni-14Zr novel braze.

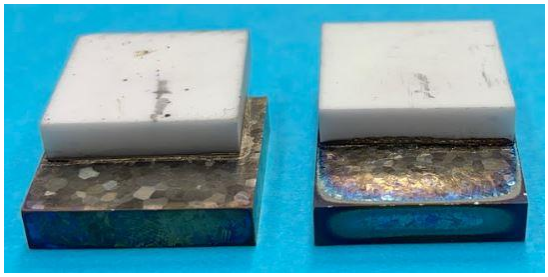

Figure 101 top-side view of Al_20_3-to-Ti6Al4V joints using Ni-14Zr novel braze.

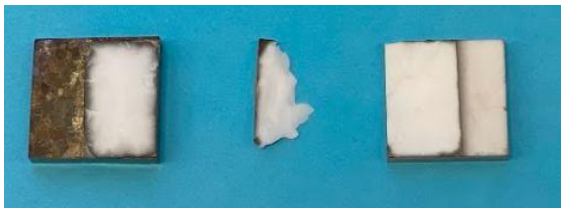

Figure 102 fractured joint of Al_20_3-to-Ti6Al4V joints using Ni-14Zr novel braze after shear test.

The graph in figure 103 is a representation of the shear test conducted on the Ni-14Zr braze system which fractured at a maximum force of 1220 N representing a value of about 1.95 MPa for the shear stress. These results were similar to those for the Pd-Ni braze system. In addition, the mechanism of fracture seems to be very similar and can be attributed to the aforementioned dissolution behaviour of the Al_2O_3 substrate in nickel from the braze.

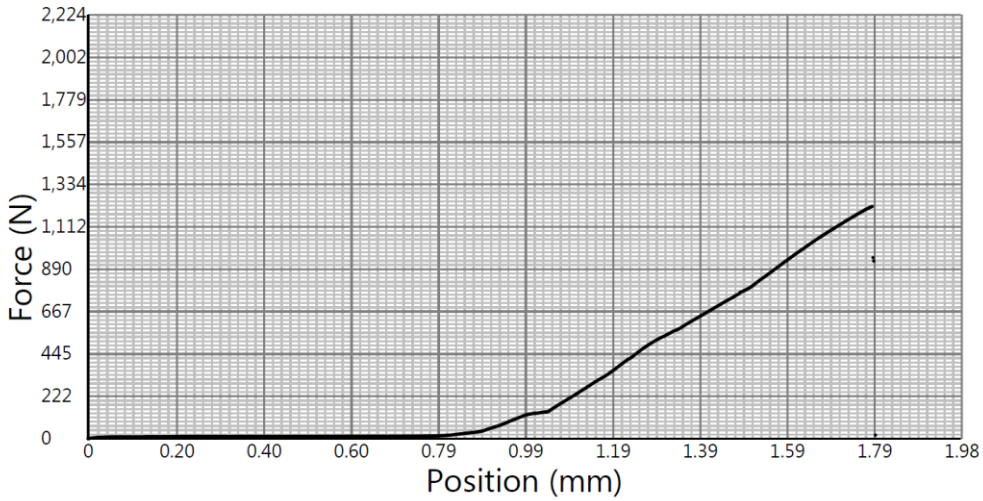

Figure 103 Load graph of Ni-14Zr braze system

4.5 *Nano-indentation Testing*

In this section nano-indentation testing was carried out to examine hardness, hardness, and elastic modulus. Both brazed samples, and those sample that were treated after brazing procedure were compared to see if there will be any further reaction at that stage. The long heat treatment procedure was to expose brazed samples to industrial standards. In general, it seems that, there was minimal change in hardness, but no signs of further chemical reaction. These results are an indication, that at 450°C and for 500 hrs, it will be performing in a stable manner.

4.5.1 Brazing Ti6Al4V-Al_2O_3 using Pd-40Ni braze

Carrying out this test was extremely important to understand the effect of this normal operating parameters at industrial setting. Favourably, the behaviour of the three layers observed during the original brazing treatment and heat treatment are majorly similar. The data presented in graphs 104 and 105 depicting examination results reveal a consistent pattern in the layers' hardness results following the initial brazing treatment, post heat treatment. This similarity indicates the potential for a durable brazing joint at operational temperatures, suggesting its feasibility for industrial production and application. It is believed that those three layers observed, in figure 106, did not have a major impact on the strength or integrity of joint. What is understood to be affecting the joint strength could be the dissolution behavior of Al_2O_3 and what has been mentioned previously in section 4.4.2.4, where the fracture of the joint can be

seen at the interface with the alumina. Noticeably, it appears that the middle layer has the highest value of Hardness 9.6 and 8.8 (GPa), for original brazing and heat treatment respectively.

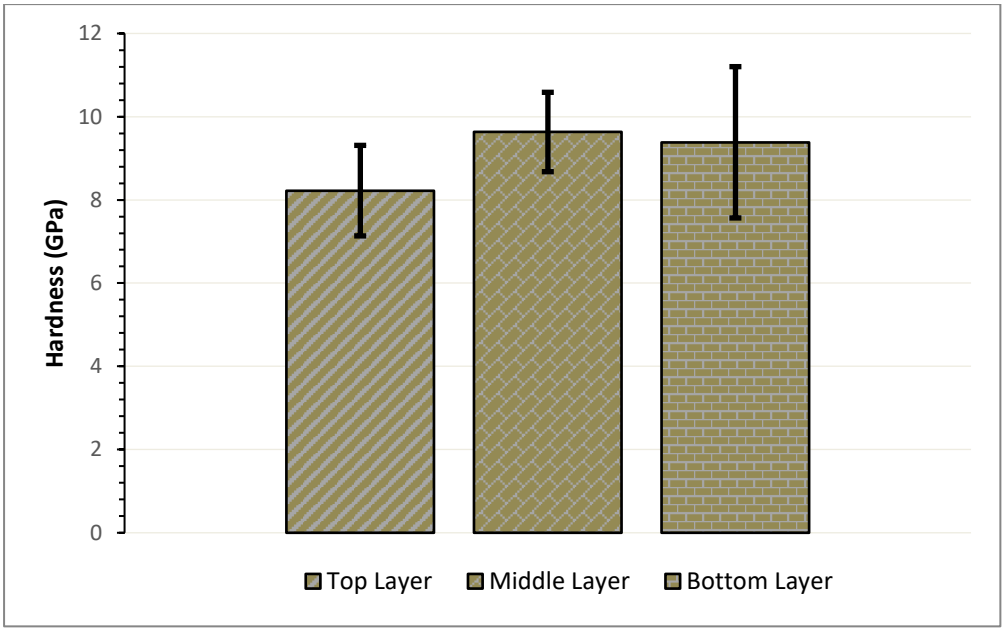

Figure 104 Hardness (GPa) before ageing treatment for Al_20_3-to-Ti6Al4V joints using Pd-40Ni commercial braze.

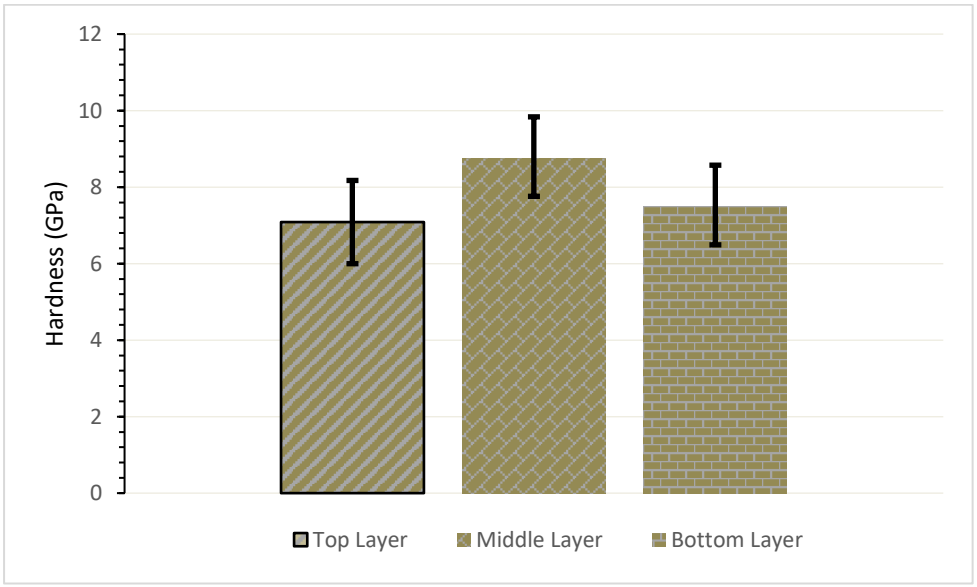

Figure 105 Hardness (GPa) after ageing treatment for Al_20_3-to-Ti6Al4V joints using Pd-40Ni commercial braze.

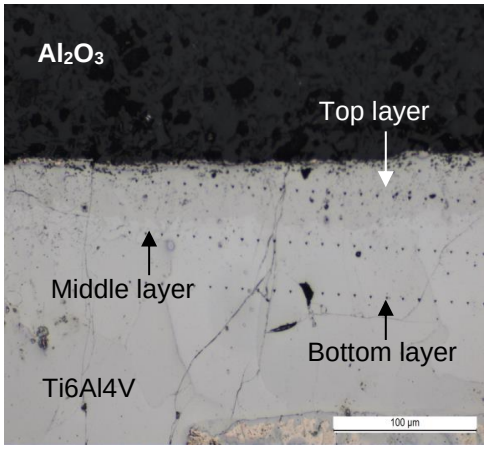

Figure 106 Micrograph of layers from Pd-40Ni after ageing

Table 10 shows all the other parameters that were observed using the nano-indentation technique. In general, and as mentioned, the results remain in-range with before and after heat-treatment. However, the Youngs Modulus seems to have increased, from 175 to 183 (GPa) after heat treatment indicating that the joint can withstand more load/force when applied to. From these findings, it can be assured that the heat treatment can improve some of the mechanical properties.

Table 10 Nano-indentation results comparison for Pd-40Ni commercial braze.

	Before treatment			After treatment		
	Top Layer	Middle Layer	Bottom Layer	Top Layer	Middle Layer	Bottom Layer
Hardness (GPa)	8.2	9.6	9.4	7.1	8.8	7.49
Reduced Modulus (GPa)	157.8	164.9	163.0	169.7	171.8	155.9
Young's Modulus (GPa)	166.5	175.2	172.9	181.2	183.8	164.3
Elastic Recovery Parameter	0.17	0.20	0.19	0.14	0.17	0.16
Plastic Work (nJ)	7.31	6.7	6.9	8.2	7.2	8.00
Elastic Work (nJ)	3.32	3.4	3.5	2.9	3.1	3.2
Plasticity Index	0.688	0.663	0.662	0.740	0.698	0.716
H/E_r	0.0521	0.0584	0.0576	0.0417	0.051	0.048
H^3/E_r^2 (GPa)	0.022	0.033	0.031	0.012	0.023	0.017

4.5.2 Brazing Ti6Al4V-Al_2O_3 using Ni-14Zr braze

Since this is a novel braze, it was vital to carry out similar behaviour examinations to observe any further chemical reactions that might take place at such a low operating temperature. From the graph of the examination results, figures 107 and 108, it is clear that the trend of the layers remain similar to the heat treatment after the original brazing treatment. Hence, this can be an indication of having a stable braze at an operating temperature, making it viable to be produced and utilised in industrial settings.

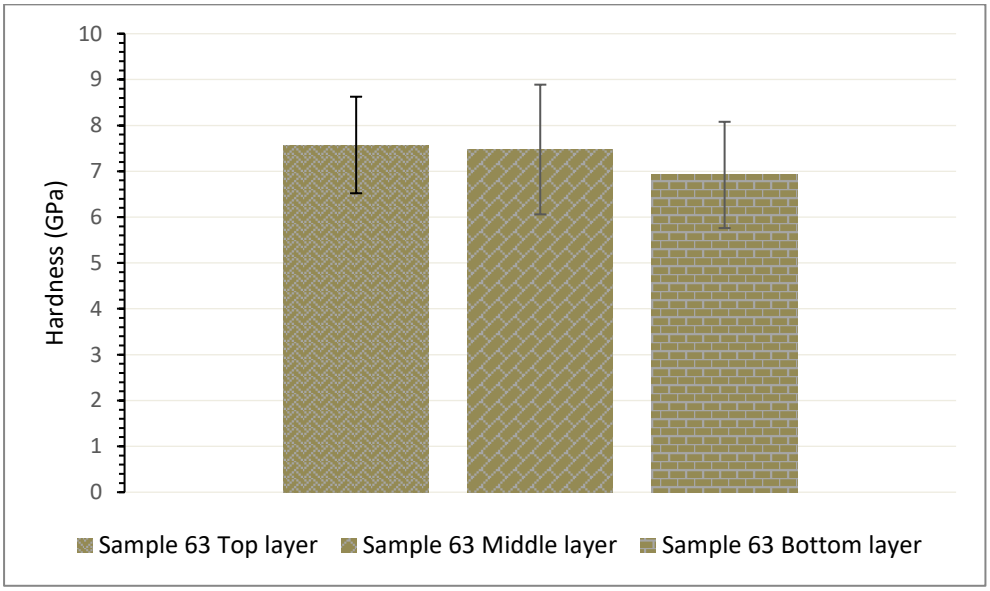

Figure 107 Hardness (GPa) before ageing treatment for Al_20_3-to-Ti6Al4V joints using Ni-14Zr novel braze.

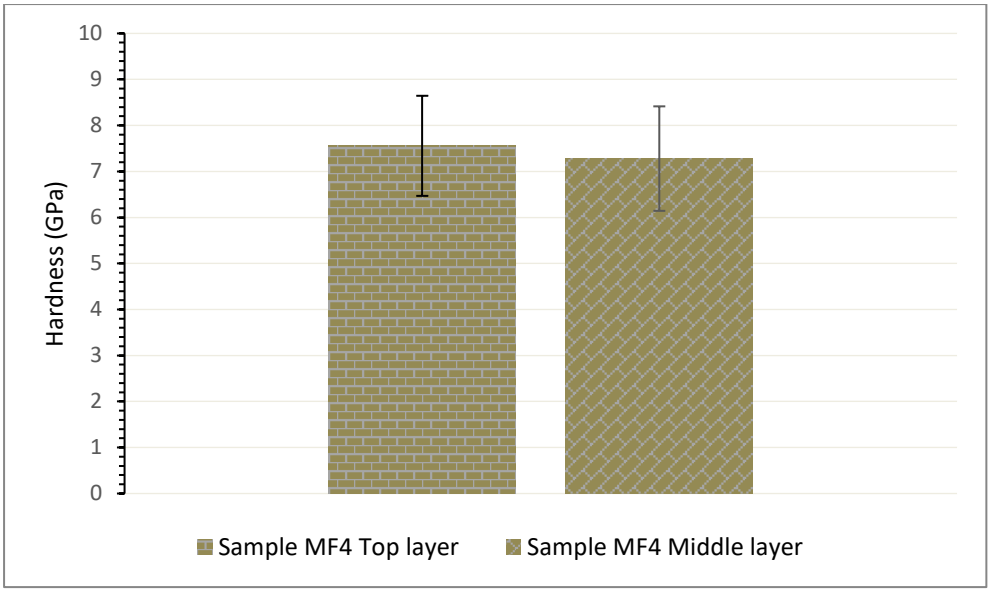

Figure 108 Hardness (GPa) after ageing treatment for Al_20_3-to-Ti6Al4V joints using Ni-14Zr novel braze.

Only two layers were clear enough under the optical microscope, hence two layers were carried out for this braze after long heat treatment. From table 11 it is clear that the Hardness has remained 7.6 GPa on both occasions, before and after heat treatments. Similar to the previous braze, the Young's Modulus has increased in the case of after heat treatment, from 172 to 182.5 GPa. The joint integrity was not affected by the existence of two layers, see figure 109. However, what has affected the joint is the dissolution of Al_2O_3 which can be determined from the previous analysis of adding Ni to TiAl braze as a third element, but also can observed by the mechanism of fracture.

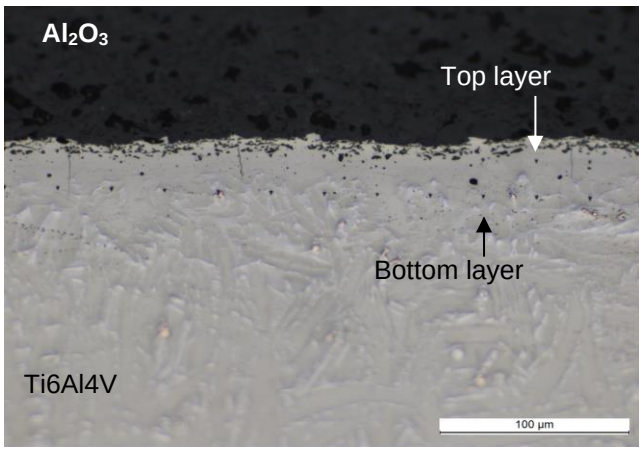

Figure 109 Micrograph of layers from Ni-14Zr after ageing

Table 11 shows all the other parameters that were observed using the nano-indentation technique. Overall, as previously stated, the outcomes stay within the expected range both prior to and following heat treatment. Nevertheless, there's a noticeable rise in the Young's Modulus, from 162 to 170.7 (GPa) post-heat treatment. This increase implies that the joint's capacity to endure higher loads or forces has improved. Based on these observations, it can be concluded that heat treatment has the potential to enhance certain mechanical properties.

Table 11 Nano-indentation results comparison for Ni-14Zr novel braze.

	Before treatment			After treatment		
	Top Layer	Middle Layer	Bottom Layer	Top Layer	Middle Layer	Bottom Layer
Hardness (GPa)	7.6	7.5	6.9	7.6	-	7.3
Reduced Modulus (GPa)	162.3	152.9	149.7	170.7	-	168.5
Young's Modulus (GPa)	172.0	160.5	156.6	182.5	-	179.8
Elastic Recovery Parameter	0.17	0.16	0.15	0.15	-	0.14
Plastic Work (nJ)	7.5	7.7	8.0	8.0	-	8.1
Elastic Work (nJ)	3.1	3.2	3.1	3.0	-	3.0
Plasticity Index	0.71	0.71	0.72	0.72	-	0.73
H/E_r	0.047	0.049	0.046	0.044	-	0.043
H^3/E_r^2 (GPa)	0.016	0.018	0.015	0.015	-	0.014

4.6 *Summary of Results*

Upon a very successful attempt to join Al_2O_3-to-Ti using a Ni-based braze, LM braze, this braze is used commercially, the elements are mentioned in 4.2.2. It was then decided to produce two novel braze systems, Ni-14Zr and Ti-3.6Ni-28Al. In addition to two commercial brazes: Ti-15Ni-15Cu and Pd-40Ni. The metal-to-ceramic joints were attempted after the third element addition was introduce for a ceramic-to-ceramic joining attempt. Which obtained successful joints. A different Ti substrate was used, Ti6Al4V, for later joining attempts with alumina using the four aforementioned braze systems.

Unlike joining ceramic-to-ceramic, Ti-Al-Ni system has not produced a joint for metal-to-ceramic joining attempt. This has a couple of explanations and expectations. One of these predominant assumptions is the lack of pressure during heating and/or cooling down. Another clarification could be the fact that, during cooling down there are almost five components with their relevant CTE's that need to be considered. When this system was developed to join alumina-to-alumina, the results obtained were proven theoretically using EDAX. However, after the Ti6Al4V introduction, the system seems to be refusing any kind of bonding, with cracks seem to be initiating at the interface between the braze and the ceramic substrate, and in some cases, foil was observed to not completely melt.

Obtaining strong joints is dependent on the melting of the filler metal, its wettability and flowability. In almost all cases there has been a noticable good wetting characteristics. However, what remains to be questionable is the flowability of the braze. Lack of sufficient information on high temperature brazing examinations, makes it obsecure. Nonetheless, assumptions can be made understanding similar procedures and correalting it to the findings in this project.

Hence, it can be summed that the formation of intermetallic compounds such as $NiTi_2$ in the case of both Ti-Ni-Al and Ti-Ni-Cu, in addition to $CuTi_2$ in the case of Ti-Ni-Cu has made the joining procedure unachievable. It has been reported in different cases to high temperature applications, that increasing the treatment time can demolish these brittle phases. However, other cases has proven that these intermetallic compounds can not be removed by simply increasing time. In matter of fact, the foundings that were observed during the course of this project, proves the latter case. Not only dwelling time was increased, samples were placed in a furnace for a long heat treatment, 500 hours at 450°C.

The results were very simliar to the original brazing treatment. The intermetallic compounds remained in the titanium substrate. With proven reaction to be occuring at the titanium substrate from EDAX. This can explain the failure of producing joints. This doesn't neglect the fact these

brazes can be probably used at a lower temperature. Those brazes, Ti-Ni-Al and Ti-Ni-Cu, can also be used to join similar materials, Alumina-to-Alumina or Ti6Al4V-to-Ti6Al4V.

On the other hand, results from Pd-Ni and Ni-14Zr are very promising considering they are serving the purpose of joining. However, another lack in the area of identifying the strength of brazed joints. In the case of joining alumina-to-Ti6Al4V, when the shear test was carried out the ceramic substrate was broken. This indicates a strong bond. Furhter data collected from the Nano-indentation shows a comparison between samples that were brazed originally and samples that have been heat treated for 500 hours. Generally, no major difference can be noted.

Similar results that were noted in relation to samples that were treated using conventional brazing procedure and those who have been heat treated for long duration, is an indication for having a sound joint. It is primarily due to the fact that the heat treatment parameters are similar if not harsher conditions to the industrial usage of these joints. Hence, explaining that even at these difficult conditions no major or significant alteration chemically. On the mechanical point of view, it remains unknown whether any alteration will happen. To determine this factor, the testing has to be done during high temperature conditions.

5 Conclusions

During the project, Al_2O_3 was successfully joined to Al_2O_3 by means of brazing using novel brazes based on the Ti-Al, Ti-Al-Ni and Ti-Al-Fe systems. The braze based on the Ti-Al-Ni system was subsequently applied to join Al_2O_3 to Ti6Al4V alloy. The study also showed that a commercial braze of Pd-40wt%Ni composition and a novel braze of Ni-14wt%Zr composition could be used to successfully join Al_2O_3 to Ti6Al4V alloy. A commercial Ti-15wt%Ni-15wt%Cu successfully joined small components of Al_2O_3 and Ti6Al4V alloy, but it was not successful when the sample dimensions were scaled to 25 mm x 25 mm and 4mm thickness. The following conclusions were drawn from the study:

1. Contact angle measurements at 1500°C showed that the addition of a third element to a Ti-Al-based braze can lead to significantly improved wetting between the braze and Al_2O_3. The addition of 3.6wt% and 7.2wt% of nickel led to a decrease in the contact angle to 48° and 29° respectively in comparison to 60° for Ti-36wt%Al. The addition of 3.6wt%Fe and 7.2wt% resulted in contact angles of 50° and 32° respectively.
2. By using chemical thermodynamics analysis, it was shown that the presence of aluminium enables wetting with Al_2O_3 by the reverse reaction,

   $$Al_2O_{3(s)} + 4Al_{(l)} \rightarrow 3Al2O_{(g)}$$

   The presence of titanium also encourages the wettability by dissolution of Al_2O_3 in the metal. The presence of nickel further enhances the wettability dissolution of Al_2O_3 in nickel. The role of nickel in enhancing the wettability was further demonstrated by means of SEM and EDAX that showed that upon cooling down, a layer of the τ_3 (Al_3NiTi_2) phase was formed at the interface between the braze and Al_2O_3. The nickel content of the braze was predominantly situated within the τ_3 (Al_3NiTi_2) phase at the interface with Al_2O_3 and within small τ_3 particles dispersed in the α phase. The nickel was observed to preferentially migrate to the interface to wet the alumina. Similar behaviour was observed with additions of Fe to the TiAl-based braze; in this case the interfacial phase in contact with the Al_2O_3 was the τ_2 (Al_2FeTi) phase.

3. When joining Al_2O_3 to Ti6Al4V using the Ti3.6wt%Ni28wt%Al braze, similar behaviour was observed as above in that most of the nickel had preferentially moved to the

interface with Al_2O_3; however, in this case, there was reaction between the braze and the Ti6Al4V substrate to form Ti(Al,Ni) at the interface with alumina.

4. When brazing Al_2O_3 to Ti6Al4V alloy, the Pd-40wt%Ni braze was observed to participate in chemical reactions with the Ti6Al4V substrate. After brazing, the braze was not in the form of a Pd-40wt%Ni solid solution, but had reacted with the substrate alloy to form a continuous intermetallic layer of Ti_3(Pd,Ni) and/or Ti_3(Al,Pd,Ni) at the interface with Al_2O_3. Below this layer, there was evidence of formation of Ti_2(Ni,Pd). In addition, α-titanium was observed within the brazed area due to diffusion of titanium and aluminium from the substrate.

5. The new Ni-14wt%Zr braze was observed to react with the titanium from the Ti6Al4V alloy. An interfacial bond was achieved with the ceramic by dissolution of alumina in the melt that contained nickel and titanium. Upon cooling, a layer of Ti_2(Ni) was observed to form at the interface with alumina. The initial braze composition of Ni-14wt%Zr lay within the Ni + Ni_5Zr phase field. In the presence of Ti6Al4V alloy, the braze was reactive and formed a Ti_2(Ni) layer at the interface with Al_2O_3. The zirconium was observed to dissolve in α-titanium.

6. The Ti-15wt%Ni-15wt%Cu braze achieved a bond with the ceramic by dissolution of alumina in nickel, titanium and copper. Upon cooling, an interfacial product of the η-Ti_2(Ni,Cu) was observed to form in contact with Al_2O_3. The main part of the braze was observed to consist of α-titanium and ε-Ti_2(Ni,Cu); the latter is richer in nickel than copper compared to the η phase. Scaling up the brazing process with this braze was unsuccessful due to localised reaction of the constituent metals (in foil form) preventing the spreading of the molten phases over a wider area.

7. The brazing process relied primarily on dissolution of the Al_2O_3 substrate in nickel and titanium. When producing joints using the brazes based on the Ti-Al-Ni, Ti-Cu-Ni, Pd-Ni and Ni-Zr systems, thin interfacial phases in contact with alumina were formed. In

each case the interfacial phase contained both titanium and nickel. There appeared to be preferential migration of both titanium and nickel to the alumina substrate.

8. The apparent lap shear strength of the brazed Al_2O_3-to-Al_2O_3 joints using the reference Ti-Al system was measured to be 27.6 MPa. The addition of 3.6wt% Ni led to an apparent lap shear strength of 21.8 MPa, while the presence of 7.2wt% exhibited a lap shear strength of 20.9 MPa. The lap shear fracture was observed to mainly occur at the interface between the braze and alumina. The decrease in lap shear strength was attributed to damage that was caused at the surface of by the dissolution of alumina in nickel. The addition of 7.2wt% Fe to the Ti-Al-based braze was more promising as it produced a higher lap shear strength of 32.3 MPa (probably due to lower dissolution effects).

9. When joining Al_2O_3 toTi6Al4V alloy, the brazes based on the Ti-Al-Ni, Pd-Ni, Ni-Zr and Ti-Cu-Ni systems were observed to react with the Ti6Al4V alloy; both titanium and aluminium from the alloy substrate were observed to diffuse into and react with the braze. The apparent lap shear strength of the brazed Al_2O_3-to-Ti6Al4V joints was disappointingly very low at about 1 MPa for all the tested brazes. This behaviour was attributed to the migration and reaction between the braze components and titanium leading to higher alumina dissolution and to greater damage to the ceramic.

After getting irrelevant results, it was decided that the Nickel braze, LM, would be used. The braze was meant to cover the surface of the Titanium to make sure there was contact between Titanium, Alumina and the braze. Nonetheless, this might have been more than enough to bond Titanium with Alumina, ending up with the braze melting on top of the Alumina as well - this can be seen in figure 17. So far it looks like a sound bond covering the maximum area of Alumina. Moreover, light microscopy as well as SEM will be carried out for this bond to understand the strength of the joint and investigate any occurring reactions. The question becomes whether or not fluidity can be extended by adding a third element, if the bond can be strengthened and how the addition of a third element would affect the wettability. In some areas where cracks

appear, it is apparent that it is not bonding very well. Nickel appears to be more fluid and has bonded both samples.

Although these reactions serve the idea of high temperature application, the strength of these joints are doubtful. Images from SEM shows cracks in the part of the SiC that was bonded to Titanium, indicating a poor joint. However, on the interface of the Titanium many voids can be seen - again this can be an indication of weak joint. The other major Aluminides that can be potentially used are Nickel and Iron which might be used as a braze in the future. Nickel and Aluminium will dissolve in the Titanium Aluminide, and then understand what changes would occur, whether it wet better, or if the fluidity changes. Most probably Nickel Aluminides, such as Ni_3Al and/or NiAl, would develop at the interface. It is reported in [36] that Ni_3Al has CTE of 12.5 and a melting point of 1415 °C, while NiAl has a CTE of 13.2 and a melting point of 1682 °C. It is expected when Nickel is added as a braze, Alumina would become stronger due to a potential solid solution strengthening. Solid solution strengthening is best described as dissolving one element into another in a solid state and as a result having the strength increase.

The wetting gets better, having more aluminium. However, the work that has been mentioned in literature had 100 hrs treatment. If it takes 100 hrs, then it is not realistic for industrial use and production. It is considerable that nickel is helping, because nickel is added it migrates to the alumina; doing that because there is compatibility with it. If there is chemical compatibility it means that wetting angle is going to be lower, and if it is lower, the bond is going to be stronger. The microscopy has shown that nickel has dissolved in part of the alumina. That solution into the aluminide is expected to be good, and perhaps reactive systems are better due to the interaction at the interface noticed. What seems to be happening is that aluminium oxide partially dissolving into the system when it is melted, and that’s mainly due to the compatibility between both alumina and nickel as aforementioned. Therefore, when the temperature is going down, it produces a better bond. Iron doesn’t bond, but when samples were sent for wettability test it seemed to have very similar effect to that of Ni, when added to the brazing alloy. Further analysis and EDAX to be conducted on treatments that involve Fe.

Ni_2Al_3 is going to have good wetting, due to better wettability the higher the aluminium (find the paper that proves this). One danger of pre-treating the samples with one layer of aluminium foil is, the aluminium forming an alumina layer; not allowing diffusion into it. $NiAl_3$ has low melting temperature, hence will not survive in the conditions we want to achieve. Ni_2Al_3 will, as mentioned earlier, using this composition was mainly to the proven fact that the higher the aluminium the better it wets. The phase diagram shows that at this temperature there should be partial melting. However not enough melting was noticed.

This process will rely on the alumina being already there and then a layer of nickel, relying on the nickel to diffuse in. There have been concerns as to whether the alumina layer formed from the aluminium foil will disallow nickel to dissolve into it, however the gravity might help for the dissolution process. Also, the fact that the material needs to equilibrate, so with time aluminium might move into the nickel, so effectively the nickel will need to get to the alumina. As well as the good wetting characteristic of nickel can help in the diffusivity.

No information has been mentioned in literature review on wetting of third element addition, not on brazing either but fractural applications. The work on these aluminides has focused on making the material ductile, which was proven in this project that ductility is a problem. As a starting composition Ti50Al50_Al_2O_3 had a wetting angle of 60°, then some of the Titanium was replaced with either Iron or Nickel. So effectively the operation is around 60at% (Ti, (Fe or Ni)). Iron drops the angle to 50° while in the case of Nickel to 49°.

From EDAX and SEM analysis, Ni addition, it is shown that the bright area is (Ni,Ti)Al mixture, while the dark area is mainly TiAl, with some Ni in it. So, it seems to dissolve at the interface. As well as, iron seems to have similar analysis, therefore the bright areas are mainly the mixture (Fe,Ti)Al and the dark area is TiAl, with some Fe in it. The phase appearing at the interface of $(Ti_{0.92}\ Ni_{0.08})Al$, bright area, is not just a random composition. Rather an actual phase that exists from the ternary phase diagram, Al_3NiTi_2. Further work will involve understanding these formation as well as the solution of alumina.

To examine the mechanical strength of the previous mentioned joints, single lap shear tests are being conducted. As recommended from the last set of results, Tungsten Carbide will be used as a weight to keep the arrangement in place.

The results of the single lap shear tests were not observed due to breaking during handling in the case of joining Ti6Al4V-to-Al_2O_3 and that is attributed to the dissolution taking place at the interface with alumina. This dissolution is thought to be initiating an interfacial damage, knowing that the fracture is occurring at the alumina interface.
The results from the wettability examination had very promising results, summarized below:

- Both Fe and Ni improve wetting. Moreover, no difference was observed between the two elements as noticed in joining experiments. So maybe other reasons than wetting hinder the joining in the case of Fe containing alloys.

- During experiments, for the alloys containing 7.2 and 3.6 wt% of Fe and Ni, the interaction started at the interface indicating that some interfacial reactivity occurred rather than simple melting. Micrographs confirmed that a slight dissolution of the Al2O3 occurred without formation of new interfacial compounds. Therefore, it can be said that the enhanced wetting is probably driven by dissolution.

- The binary alloy containing 28wt% of Al did not melt at 1500°C; hence, Fe and Ni seem to lower the melting point, maybe some eutectics form as shown by the microstructures.

- As for the TiAl + 28.8 wt% of Ni alloy, no dissolution was reported but still good wetting, drop sessile illustration can be found in Appendix A..

- Regarding Ni3Al, literature data and tests conducted, say that, compared to pure Ni, the wetting is enhanced but contact angles do not fall below 70°C depending on temperature and oxygen content in the atmosphere.

Due to the reoccurring appearance of Ni at the interface, when Ni was first introduced to join alumina to pure titanium, using LM braze. It was introduced in most braze systems later in the project. The behaviour of how nickel reacts with alumina was interesting enough. In matter of fact this behaviour was observed in all braze systems. In addition to those alumina-to-alumina attempts.

After successful joints were obtained using two Ni-based braze systems joining alumina-to-alumina, a metal substrate was introduced. The metal substrate, Ti6Al4V, was used to produce a butt joint for metal-to-ceramic purposes. The behaviour observed was similar to what has been recorded previously, Ni appearance at the interface with alumina. As well as, good wetting behaviour, as observed from the elemental analysis.

Regarding the viability and strength of the joints, two braze systems has not produced an applicable bond, Ti-15Ni-15Cu and Ti-3.6Ni-28Al. This was mainly due to brittle phases forming in the Ti6Al4V substrate. After SEM and EDAX was conducted to understand the failing behaviour, it was observed that even though it is seemingly wetting really well at the alumina interface. The lack of flowability holds the braze from covering the pores, which were probably during the sintering process of alumina, in the ceramic substrate. Hence, producing either weak joint, having high tendency to be broken easily during handling, in the case of Ti-15Ni-15Cu, or not achieving any joint, in the case of Ti-Ni-Al.

Concerning the two previously mentioned braze systems used to join Ti6Al4V and Al_2O_3, the joints would fail during handling and/or cutting during preparation, on several occasions, prior to shear test examination. Hence, it was not possible to examine their shear strength, nonetheless, SEM and EDAX analyses has been deployed to understand the failing mechanism. Knowing that Ni in the case of (Ti, Ni)Al system have developed cracks at the interfacial layer, owing to the dissolution in the ceramic substrate. While Ti-15Ni-15Cu system had brittle phase formation at the interface zone, therefore, resulting in an unreliable joint.

The bond achieved between the Ti6Al4V alloy and Al_2O_3, using Pd-40Ni commercial braze, was formed through a combination of interactions that took place at both ends of the braze. Some of the Ti6Al4V alloy melted and some of the titanium and aluminum dissolved into the molten braze, which increased its flowability. This allowed the molten material to be drawn into the gap between the sample and the holding crucible. The bond between the Al_2O_3 and the braze was created through the ability of titanium and nickel to dissolve part of the ceramic, leading to the formation of Ti_3(Pd,Ni,Al) at the interface. This process helped to create a strong and durable bond between the two materials.

With regard to the novel braze, Ni-14Zr, the bond between the titanium alloy and the braze was formed through two processes. The first was the reaction between titanium and nickel, which resulted in the formation of a layer of Ti_2Ni at the interface. The second was the dissolution of zirconium in titanium, which helped to strengthen the bond. The reactivity of the original braze composition, which contained Ni and 14% weight percent zirconium (Ni-14wt%Zr), was crucial in achieving the bond on both sides of the joint. During the bonding process, there was some interaction between the Ni-14wt%Zr braze and the Ti6Al4V alloy, which involved some melting of the titanium alloy. This allowed the titanium to migrate to the surface of the ceramic and dissolve some of the Al_2O_3, which helped to create a reliable bond between the two materials.

In the case of the Pd-Ni and Ni-Zr braze systems, even though the results obtained from the shear test showed considerably weaker lap shear strength than expected, two points are to be addressed. Firstly, the lower shear test result assumes that the bond is unreliable and weak, however, the substrate was actually fractured and not the bond. Indicating that the braze has developed a bond which is stronger than the braze. Secondly, the Ni dissolution could actually have affected the zone underneath the fracture area and the substrate, and therefore breaking at that low force.

Moreover, Pd-40Ni and Ni-14Zr, have produced, what seems to be reliable joints. After long heat treatment and other mechanical examination such as shear test and nano-indentation. Nano-indentation was to determine the difference between original brazing procedure and after

long heat treatment for 500 hours at 450°C. There were no major differences in results obtained, metallographically or mechanically. This fact is an important role to prove that these brazes can be utilised industrially. Exposing joints to a more extreme conditions than industry, where the samples are heated for a long period of time. Having no influential chemical reactions, which serves the scope of having a reliable joint that can withstand extreme conditions to be employed in industry.

REFERENCES

[1] P. L. Narayana, S.-W. Kim, J.-K. Hong, N. S. Reddy, and J.-T. Yeom, “Tensile properties of a newly developed high-temperature titanium alloy at room temperature and 650 °C,” *Materials Science and Engineering: A*, vol. 718, pp. 287–291, Mar. 2018, doi: 10.1016/j.msea.2018.01.113.

[2] B. Fu, H. Wang, C. Zou, and Z. Wei, “The influence of Zr content on microstructure and precipitation of silicide in as-cast near α titanium alloys,” *Mater Charact*, vol. 99, pp. 17–24, Jan. 2015, doi: 10.1016/j.matchar.2014.09.015.

[3] W. J. Zhang, X. Y. Song, S. X. Hui, W. J. Ye, Y. L. Wang, and W. Q. Wang, “Tensile behavior at 700°C in Ti–Al–Sn–Zr–Mo–Nb–W–Si alloy with a bi-modal microstructure,” *Materials Science and Engineering: A*, vol. 595, pp. 159–164, Feb. 2014, doi: 10.1016/j.msea.2013.11.096.

[4] M. B. Uday, M. N. Ahmad-Fauzi, A. M. Noor, and S. Rajoo, “Current Issues and Problems in the Joining of Ceramic to Metal,” in *Joining Technologies*, InTech, 2016. doi: 10.5772/64524.

[5] M. G. Nicholas and D. A. Mortimer, “Ceramic/metal joining for structural applications,” *Materials Science and Technology*, vol. 1, no. 9, pp. 657–665, Sep. 1985, doi: 10.1179/mst.1985.1.9.657.

[6] D. Palit and A. M. Meier, “Reaction kinetics and mechanical properties in the reactive brazing of copper to aluminum nitride,” *J Mater Sci*, vol. 41, no. 21, pp. 7197–7209, Nov. 2006, doi: 10.1007/s10853-006-0920-z.

[7] J.-W. Park, “A framework for designing interlayers for ceramic-to-metal joints,” MIT, 2002. Accessed: Aug. 09, 2023. [Online]. Available: http://hdl.handle.net/1721.1/29913

[8] J. L. Wiese, “Strength of Metal-to-Ceramic Brazed Joints,” Massachusetts Institute of Technology, 2001.

[9] T. Y. Yang, R. K. Shiue, and S. K. Wu, “Infrared brazing of Ti50Ni50 shape memory alloy using pure Cu and Ti–15Cu–15Ni foils,” *Intermetallics (Barking)*, vol. 12, no. 12, pp. 1285–1292, Dec. 2004, doi: 10.1016/j.intermet.2004.03.020.

[10] O. M. Akselsen, “Diffusion bonding of ceramics,” *J Mater Sci*, vol. 27, no. 3, pp. 569–579, Feb. 1992, doi: 10.1007/BF02403862.

[11] K. Morsi, “Review: reaction synthesis processing of Ni–Al intermetallic materials,” *Materials Science and Engineering: A*, vol. 299, no. 1–2, pp. 1–15, Feb. 2001, doi: 10.1016/S0921-5093(00)01407-6.

[12] Y. Miyamoto, T. Nakamoto, M. Koizumi, and O. Yamada, “Ceramic-to-metal welding by a pressurized combustion reaction,” *J Mater Res*, vol. 1, no. 1, pp. 7–9, Feb. 1986, doi: 10.1557/JMR.1986.0007.

[13] A. Krell, “Improved hardness and hierarchic influences on wear in submicron sintered alumina,” *Materials Science and Engineering: A*, vol. 209, no. 1–2, pp. 156–163, May 1996, doi: 10.1016/0921-5093(95)10155-1.

[14] L. Zeng, E. D. Case, and M. A. Crimp, “Effects of a silica spin-on interlayer and heating mode on the joining of zirconia and MaCor™,” *Materials Science and Engineering: A*, vol. 357, no. 1, pp. 67–74, 2003, doi: https://doi.org/10.1016/S0921-5093(03)00247-8.

[15] M. M. R. Howlader, T. Kaga, and T. Suga, “Investigation of bonding strength and sealing behavior of aluminum/stainless steel bonded at room temperature,” *Vacuum*, vol. 84, no. 11, pp. 1334–1340, 2010, doi: https://doi.org/10.1016/j.vacuum.2010.02.014.

[16] M. Kinsho *et al.*, “Development of alumina ceramics vacuum duct for the 3GeV-RCS of the J-PARC project,” *Vacuum*, vol. 73, no. 2, pp. 187–193, 2004, doi: https://doi.org/10.1016/j.vacuum.2003.12.043.

[17] J. X. Zhang, R. S. Chandel, and H. P. Seow, “Effect of chromium addition on brazing of copper to alumina: some microstructural aspects,” *Science and Technology of Welding and Joining*, vol. 7, no. 3, pp. 182–186, Jun. 2002, doi: 10.1179/136217102225002655.

[18] A. Kar, S. Mandal, K. Venkateswarlu, and A. K. Ray, “Characterization of interface of Al2O3–304 stainless steel braze joint,” *Mater Charact*, vol. 58, no. 6, pp. 555–562, 2007, doi: https://doi.org/10.1016/j.matchar.2006.12.001.

[19] O. Kozlova, M. Braccini, R. Voytovych, N. Eustathopoulos, P. Martinetti, and M.-F. Devismes, “Brazing copper to alumina using reactive CuAgTi alloys,” *Acta Mater*, vol. 58, no. 4, pp. 1252–1260, Feb. 2010, doi: 10.1016/j.actamat.2009.10.029.

[20] R. Asthana and M. Singh, “Joining of partially sintered alumina to alumina, titanium, Hastealloy and C–SiC composite using Ag–Cu brazes,” *J Eur Ceram Soc*, vol. 28, no. 3, pp. 617–631, Jan. 2008, doi: 10.1016/j.jeurceramsoc.2007.06.017.

[21] M. I. Barrena, L. Matesanz, and J. M. G. de Salazar, “Al2O3/Ti6Al4V diffusion bonding joints using Ag–Cu interlayer,” *Mater Charact*, vol. 60, no. 11, pp. 1263–1267, Nov. 2009, doi: 10.1016/j.matchar.2009.05.007.

[22] J. Cao, Z. J. Zheng, L. Z. Wu, J. L. Qi, Z. P. Wang, and J. C. Feng, “Processing, microstructure and mechanical properties of vacuum-brazed Al2O3/Ti6Al4V joints,” *Materials Science and Engineering: A*, vol. 535, pp. 62–67, Feb. 2012, doi: 10.1016/j.msea.2011.12.042.

[23] H.-P. Martin and A. Triebert, “Experimental investigations of TiAl- brazes for ceramic joining,” in *KMM-VIN*, 2016.

[24] P. Lourdin, D. Juvé, and D. Tréheux, “Nickel-alumina bonds: Mechanical properties related to interfacial chemistry,” *J Eur Ceram Soc*, vol. 16, no. 7, pp. 745–752, Jan. 1996, doi: 10.1016/0955-2219(95)00187-5.

[25] C. A. Calow, P. D. Bayer, and I. T. Porter, “The solid state bonding of nickel, chromium and nichrome sheets to ?-Al2O3,” *J Mater Sci*, vol. 6, no. 2, pp. 150–155, Feb. 1971, doi: 10.1007/BF00550346.

[26] F. P. Bailey and W. E. Borbidge, “Solid State Metal-Ceramic Reaction Bonding,” in *Surfaces and Interfaces in Ceramic and Ceramic — Metal Systems*, Boston, MA: Springer US, 1981, pp. 525–533. doi: 10.1007/978-1-4684-3947-2_46.

[27] C. A. Calow and I. T. Porter, “The solid state bonding of nickel to alumina,” *J Mater Sci*, vol. 6, no. 2, pp. 156–163, Feb. 1971, doi: 10.1007/BF00550347.

[28] R. G. Vardiman, “Preferred orientation of NiAl2O4 spinel grown on sapphire,” *Mater Res Bull*, vol. 7, no. 7, pp. 699–710, Jul. 1972, doi: 10.1016/0025-5408(72)90059-1.

[29] M. L. Hattali, S. Valette, F. Ropital, N. Mesrati, and D. Tréheux, “Calculation and experimental determinations of the residual stress distribution in alumina/Ni/alumina and alumina/Ni/nickel alloy systems,” *J Mater Sci*, vol. 45, no. 15, pp. 4133–4140, Aug. 2010, doi: 10.1007/s10853-010-4502-8.

[30] N. Iwamoto, N. Umesaki, M. Kamai, and K. Ohnishi, “Metal-ceramic interfaces,” *Acta-Scripta Metallurgy*, pp. 176–181, 1989.

[31] M. L. Hattali, S. Valette, F. Ropital, G. Stremsdoerfer, N. Mesrati, and D. Tréheux, “Study of SiC–nickel alloy bonding for high temperature applications,” *J Eur Ceram Soc*, vol. 29, no. 4, pp. 813–819, Mar. 2009, doi: 10.1016/j.jeurceramsoc.2008.06.035.

[32] J. Li, L. Liu, Y. Wu, W. Zhang, and W. Hu, “A high temperature Ti–Si eutectic braze for joining SiC,” *Mater Lett*, vol. 62, no. 17–18, pp. 3135–3138, Jun. 2008, doi: 10.1016/j.matlet.2008.02.024.

[33] H. Okamoto, “Ni-Zr (Nickel-Zirconium),” *J Phase Equilibria Diffus*, vol. 28, no. 4, pp. 409–409, Jul. 2007, doi: 10.1007/s11669-007-9120-z.

[34] H. T. Takeshita, S. Kondo, H. Miyamura, N. Takeichi, N. Kuriyama, and T. Oishi, “Re-examination of Zr7Ni10 single-phase region,” *J Alloys Compd*, vol. 376, no. 1–2, pp. 268–274, Aug. 2004, doi: 10.1016/j.jallcom.2004.01.064.

[35] T. Kosorukova, V. Ivanchenko, G. Firstov, and H. Noël, “Experimental Reinvestigation of Ni-Zr System,” *Solid State Phenomena*, vol. 194, pp. 14–20, Nov. 2012, doi: 10.4028/www.scientific.net/SSP.194.14.

[36] X. Tao *et al.*, “An experimental study on the interdiffusion behaviors and mechanical properties of Ni-Zr system,” *J Alloys Compd*, vol. 752, pp. 412–419, Jul. 2018, doi: 10.1016/j.jallcom.2018.04.019.

[37] Y. Lei *et al.*, “Transient liquid phase bonding of cast Al0.3CoCrFeNi high-entropy alloy using Ni/Zr/Ni laminated foils,” *J Alloys Compd*, vol. 871, p. 159504, Aug. 2021, doi: 10.1016/j.jallcom.2021.159504.

[38] D. A. Canonico, N. C. Cole, and G. M. Slaughter, “Direct brazing of ceramics, graphite and refractory metals ,” *Weld. J. (Miami); (United States)* , vol. 56, no. 8, 1977.

[39] R. Asthana and M. Singh, “Joining of ZrB2-based ultra-high-temperature ceramic composites using Pd-based braze alloys,” *Scr Mater*, vol. 61, no. 3, pp. 257–260, Aug. 2009, doi: 10.1016/j.scriptamat.2009.03.053.

[40] K. Otsuka and K. Shimizu, “Pseudoelasticity and shape memory effects in alloys,” *International Metals Reviews*, vol. 31, no. 1, pp. 93–114, Jan. 1986, doi: 10.1179/imtr.1986.31.1.93.

[41] S. Miyazaki and K. Otsuka, “Development of shape memory alloys.,” *ISIJ International*, vol. 29, no. 5, pp. 353–377, 1989, doi: 10.2355/isijinternational.29.353.

[42] C. M. Wayman, “The Growth of Martensite Since E.C. Bain (1924) - Some Milestones,” *Materials Science Forum*, vol. 56–58, pp. 1–32, Jan. 1991, doi: 10.4028/www.scientific.net/MSF.56-58.1.

[43] H. C. Lin, S. K. Wu, T. S. Chou, and H. P. Kao, “The effects of cold rolling on the martensitic transformation of an equiatomic TiNi alloy,” *Acta Metallurgica et Materialia*, vol. 39, no. 9, pp. 2069–2080, Sep. 1991, doi: 10.1016/0956-7151(91)90177-3.

[44] Y. Oshida and S. Miyazaki, “Corrosion and Biocompatibility of Shape Memory Alloys,” *Zairyo-to-Kankyo*, vol. 40, no. 12, pp. 834–844, 1991, doi: 10.3323/jcorr1991.40.834.

[45] K. Otsuka and C. M. Wayman, *Shape Memory Materials* . Cambridge University Press, 1999.

[46] L. ESPOSITO, A. BELLOSI, S. GUICCIARDI, and L. ESPOSITO, “Solid state bonding of Al2O3 with Cu, Ni and Fe: characteristics and properties,” *J Mater Sci*, vol. 33, no. 7, pp. 1827–1836, Apr. 1998, doi: 10.1023/A:1004397019927.

[47] J. P. Krugers and G. Den Ouden, “Joining of silicon carbide to austenitic stainless steel by means of diffusion welding.,” *INT J JOINING MATER.*, vol. 4, no. 3, pp. 73–78, 1992.

[48] K. Suganuma, T. Okamoto, and Y. Miyamoto, “M. Shimada and M. Koizumi,” *Mater. Sci. Technol*, vol. 2, p. 1156, 1986.

[49] R. H. Vegter and G. den Ouden, “Diffusion bonding of zirconia to silicon nitride using nickel interlayers,” *J Mater Sci*, vol. 33, no. 18, pp. 4525–4530, Sep. 1998, doi: 10.1023/A:1004400318343.

[50] Y. Zhou, W. F. Gale, and T. H. North, “Modelling of transient liquid phase bonding,” *International Materials Reviews*, vol. 40, no. 5, pp. 181–196, Jan. 1995, doi: 10.1179/imr.1995.40.5.181.

[51] I. Tuah-Poku, M. Dollar, and T. B. Massalski, “A study of the transient liquid phase bonding process applied to a Ag/Cu/Ag sandwich joint,” *Metallurgical Transactions A*, vol. 19, no. 3, pp. 675–686, Mar. 1988, doi: 10.1007/BF02649282.

[52] Y. Nakao and K. Shinozaki, “Transient liquid phase diffusion bonding of iron base oxide dispersion strengthened alloy MA 956,” *Materials Science and Technology*, vol. 11, no. 3, pp. 304–311, Mar. 1995, doi: 10.1179/mst.1995.11.3.304.

[53] G. Ceccone, M. G. Nicholas, S. D. Peteves, A. P. Tomsia, B. J. Dalgleish, and A. M. Glaeser, “An evaluation of the partial transient liquid phase bonding of Si3N4 using Au coated Ni□22Cr foils,” *Acta Mater*, vol. 44, no. 2, pp. 657–667, Feb. 1996, doi: 10.1016/1359-6454(95)00187-5.

[54] M. Paulasto, G. Ceccone, and S. D. Peteves, “Joining of silicon nitride via a transient liquid,” *Scr Mater*, vol. 36, no. 10, pp. 1167–1173, May 1997, doi: 10.1016/S1359-6462(97)00007-9.

[55] C. Zheng, H. Lou, Z. Fei, and Z. Li, “Partial transient liquid-phase bonding of Si3N4 with Ti/Cu/Ni multi-interlayers,” *J Mater Sci Lett*, vol. 16, no. 24, pp. 2026–2028, 1997.

[56] R. W. Messler Jr, “Joining of Advanced Materials, 1993.” Butterworth-Heinemann.

[57] I. E. Reimanis, J. Henager C H, and A. P. Tomsia, “Ceramic transactions: Ceramic joining. Volume 77,” United States: American Ceramic Society, Westerville, OH (United States), 1997. [Online]. Available: https://www.osti.gov/biblio/539127

[58] M. G. Nicholas, *Active metal brazing*. Chapman & Hall, 1990.

[59] S. Musikant, *What every engineer should know about ceramics*, vol. 28. CRC Press, 1991.

[60] N. Eustathopoulos, “Wetting by Liquid Metals—Application in Materials Processing: The Contribution of the Grenoble Group,” *Metals (Basel)*, vol. 5, no. 1, pp. 350–370, Mar. 2015, doi: 10.3390/met5010350.

[61] A. Passerone, M. L. Muolo, and F. Valenza, “Critical Issues for Producing UHTC-Brazed Joints: Wetting and Reactivity,” *J Mater Eng Perform*, vol. 25, no. 8, pp. 3330–3347, Aug. 2016, doi: 10.1007/s11665-016-1990-y.

[62] W. J. Boettinger, C. A. Handwerker, and U. R. Kattner, *The Mechanics of Solder Alloy Wetting and Spreading*. Boston, MA: Springer US, 1994. doi: 10.1007/978-1-4684-1440-0.

[63] S. Shu, F. Qiu, C. Tong, X. Shan, and Q. Jiang, “Effects of Fe, Co and Ni elements on the ductility of TiAl alloy,” *J Alloys Compd*, vol. 617, pp. 302–305, Dec. 2014, doi: 10.1016/j.jallcom.2014.07.199.

[64] S. Shu, C. Tong, F. Qiu, and Q. Jiang, “Effect of Mn, Fe and Co on the compression strength and ductility of in situ nano-sized TiB2/TiAl composites,” *Springerplus*, vol. 4, no. 1, p. 784, Dec. 2015, doi: 10.1186/s40064-015-1575-5.

[65] D. Astm, “1002-05. Standard test method for apparent Shear strength of single-lap-joint adhesively bonded metal specimens by tension loading (metal-to-metal),” *Annu. Book ASTM Stand*. 2005.

[66] K. Das, P. Choudhury, and S. Das, “The Al—O—Ti (Aluminum-Oxygen-Titanium) System,” *ChemInform*, vol. 34, no. 15, Apr. 2003, doi: 10.1002/chin.200315223.

[67] E. T. Turkdogan, *Physical chemistry of high temperature technology*. New York: Academic Press Inc., 1980.

[68] R. S. Wagner and A. P. Levitt, “Whisker technology,” *by AP Levitt, Wiley, New York*, pp. 47–119, 1970.

[69] R. F. Porter, P. Schissel, and M. G. Inghram, “A Mass Spectrometric Study of Gaseous Species in the Al–Al $_2$ O $_3$ System,” *J Chem Phys*, vol. 23, no. 2, pp. 339–342, Feb. 1955, doi: 10.1063/1.1741963.

[70] G. D. Botsaris, “Whiskers, C. C. Evans, M & B Monograph Me/8, Mills and Boon, Ltd., London(1972). 72 pages.£1.5,” *AIChE Journal*, vol. 18, no. 6, p. 18, Nov. 1972, doi: 10.1002/aic.690180639.

[71] N. Eustathopoulos, B. Drevet, and M. L. Muolo, “The oxygen-wetting transition in metal/oxide systems,” *Materials Science and Engineering: A*, vol. 300, no. 1–2, pp. 34–40, Feb. 2001, doi: 10.1016/S0921-5093(00)01790-1.

[72] E. Tan, P. G. Mather, A. C. Perrella, J. C. Read, and R. A. Buhrman, “Oxygen stoichiometry and instability in aluminum oxide tunnel barrier layers,” *Phys Rev B*, vol. 71, no. 16, p. 161401, Apr. 2005, doi: 10.1103/PhysRevB.71.161401.

[73] H. John and H. Hausner, “Influence of oxygen partial pressure on the wetting behaviour in the system Al/Al2O3,” *J Mater Sci Lett*, vol. 5, no. 5, pp. 549–551, May 1986, doi: 10.1007/BF01728687.

[74] R. Sui, J. Chang, and Q. Lin, “Effect of surface orientation on reactive wetting of sapphire by Al–Ti alloys at 1273 K,” *Mater Chem Phys*, vol. 285, p. 126187, Jun. 2022, doi: 10.1016/j.matchemphys.2022.126187.

[75] M. Ilatovskaia, G. Savinykh, and O. Fabrichnaya, “Thermodynamic Description of the Ti-Al-O System Based on Experimental Data,” *J Phase Equilibria Diffus*, vol. 38, no. 3, pp. 175–184, Jun. 2017, doi: 10.1007/s11669-016-0509-4.

[76] H. Okamoto, “O-Ti (Oxygen-Titanium),” *J Phase Equilibria Diffus*, vol. 32, no. 5, pp. 473–474, Oct. 2011, doi: 10.1007/s11669-011-9935-5.

[77] V. Merlin and N. Eustathopoulos, “Wetting and adhesion of Ni-Al alloys on α-Al2O3 single crystals,” *J Mater Sci*, vol. 30, no. 14, pp. 3619–3624, Jul. 1995, doi: 10.1007/BF00351875.

[78] G. Levi, C. Scheu, and W. D. Kaplan, “Segregation of aluminium at nickel-sapphire interfaces,” *Interface Science*, vol. 9, no. 3/4, pp. 213–220, 2001, doi: 10.1023/A:1015198409536.

[79] G. Levi, D. R. Clarke, and W. D. Kaplan, “Free Surface and Interface Thermodynamics of Liquid Nickel in Contact with Alumina,” *Interface Science*, vol. 12, no. 1, pp. 73–83, Jan. 2004, doi: 10.1023/B:INTS.0000012295.38485.90.

[80] F. Valenza *et al.*, “Wetting and interfacial reactivity of Ni–Al alloys with Al2O3 and ZrO2 ceramics,” *J Mater Sci*, vol. 56, no. 13, pp. 7849–7861, May 2021, doi: 10.1007/s10853-021-05769-6.

[81] E. Saiz, A. P. Tomsia, and R. M. Cannon, “Triple line ridging and attachment in high-temperature wetting,” *Scr Mater*, vol. 44, no. 1, pp. 159–164, Jan. 2001, doi: 10.1016/S1359-6462(00)00549-2.

[82] A. Gauffier, E. Saiz, A. P. Tomsia, and P. Y. Hou, “The wetting behavior of NiAl and NiPtAl on polycrystalline alumina.”

[83] K. Fritscher, C.-J. Kröder, and U. Schulz, “Adherence and Failure of an EBPVD 7YSZ Coating on a β/γ-NiCrAl Substrate: A Pilot Study,” *Oxidation of Metals*, vol. 86, no. 3–4, pp. 279–298, Oct. 2016, doi: 10.1007/s11085-016-9636-x.

[84] Y. Kang, M. Thunman, D. Sichen, T. Morohoshi, K. Mizukami, and K. Morita, “Aluminum Deoxidation Equilibrium of Molten Iron–Aluminum Alloy with Wide Aluminum Composition Range at 1 873 K,” *ISIJ International*, vol. 49, no. 10, pp. 1483–1489, 2009, doi: 10.2355/isijinternational.49.1483.

[85] B. Huneau, P. Rogl, K. Zeng, R. Schmid-Fetzer, M. Bohn, and J. Bauer, “The ternary system Al±Ni±Ti Part I: Isothermal section at 900 C; Experimental investigation and thermodynamic calculation.”

[86] C. Zhang and A. Shirzadi, “Fail-Safe Joints between Copper Alloy (C18150) and Nickel-Based Superalloy (GH4169) Made by Transient Liquid Phase (TLP) Bonding and Using Boron-Nickel (BNi-2) Interlayer,” *Metals (Basel)*, vol. 11, no. 10, p. 1504, Sep. 2021, doi: 10.3390/met11101504.

[87] S. W. Lan, “Laminated brazing filler metals for titanium assemblies,” 1982.

[88] Ming-Chi Ho, Pei Jen Lo, Wei-Liang Liu, and Ker-Chang Hsieh, “Relationship of Brazing Microstructure and Ti-Cu-Ni Phase Diagram,” *Journal of Materials Science and Engineering B*, vol. 7, no. 4, Aug. 2017, doi: 10.17265/2161-6221/2017.7-8.002.

[89] J. Hamuyuni and P. Taskinen, “Solubility of CaO and Al2O3 in Metallic Copper Saturated Molten Phase,” in *Advances in Molten Slags, Fluxes, and Salts: Proceedings of the 10th International Conference on Molten Slags, Fluxes and Salts 2016*, Cham: Springer International Publishing, 2016, pp. 937–945. doi: 10.1007/978-3-319-48769-4_100.

[90] C. T. Chang, Y. C. Du, R. K. Shiue, and C. S. Chang, “Infrared brazing of high-strength titanium alloys by Ti–15Cu–15Ni and Ti–15Cu–25Ni filler foils,” *Materials Science and Engineering: A*, vol. 420, no. 1–2, pp. 155–164, Mar. 2006, doi: 10.1016/j.msea.2006.01.046.

[91] R. K. Shiue, S. K. Wu, and Y. T. Chen, “Strong bonding of infrared brazed α2-Ti3Al and Ti–6Al–4V using Ti–Cu–Ni fillers,” *Intermetallics (Barking)*, vol. 18, no. 1, pp. 107–114, Jan. 2010, doi: 10.1016/j.intermet.2009.06.017.

[92] K. H. Hansen *et al.*, “Palladium Nanocrystals on Al2O3: Structure and Adhesion Energy,” *Phys Rev Lett*, vol. 83, no. 20, pp. 4120–4123, Nov. 1999, doi: 10.1103/PhysRevLett.83.4120.

[93] G. Ghosh, “Thermodynamics and kinetics of stable and metastable phases in the Ni–Zr system,” *J Mater Res*, vol. 9, no. 3, pp. 598–616, Mar. 1994, doi: 10.1557/JMR.1994.0598.

[94] T. B. Massalski, H. Okamoto, P. R. Subramanian, and L. Kacprzak, “Binary alloy phase diagrams, v. 1,” *ASM International*, pp. 28–29, 1990.

[95] M. Gasik, “Phase equilibria and thermal behaviour of biomedical Ti-Nb-Zr alloy,” 2009. [Online]. Available: https://www.researchgate.net/publication/215974421

[96] X. Gao *et al.*, “Diffusion bonding of Ti/Ni under the influence of an electric current: mechanism and bond structure,” *J Mater Sci*, vol. 52, no. 6, pp. 3535–3544, Mar. 2017, doi: 10.1007/s10853-016-0648-3.

[97] Y. Arai, T. Marumo, and R. Inoue, “Use of zr–ti alloy melt infiltration for fabricating carbon-fiber-reinforced ultrahigh-temperature ceramic matrix composites,” *Journal of Composites Science*, vol. 5, no. 7, Jul. 2021, doi: 10.3390/jcs5070186.

APPENDIX A


TiAl28.8Ni_Al2O3
Al_2O_3
100 µm

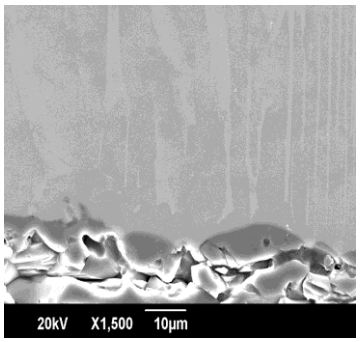
20kV X1,500 10µm

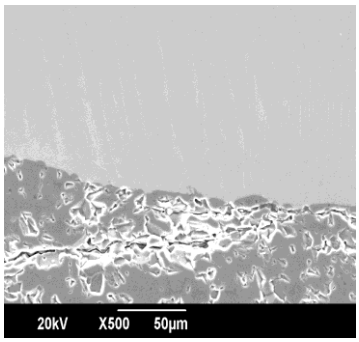
20kV X500 50µm

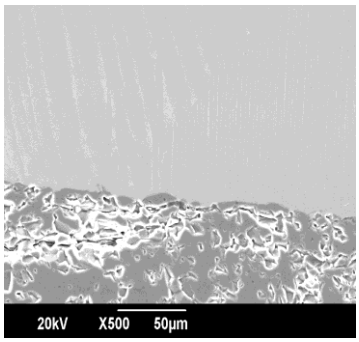
20kV X500 50µm

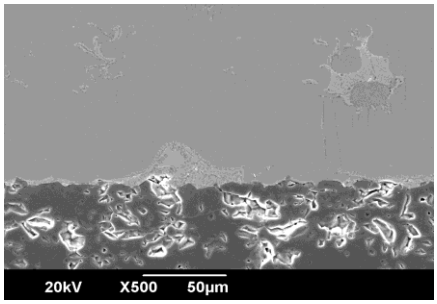

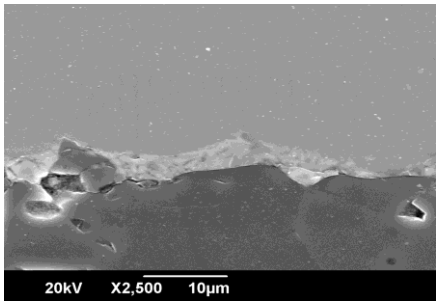

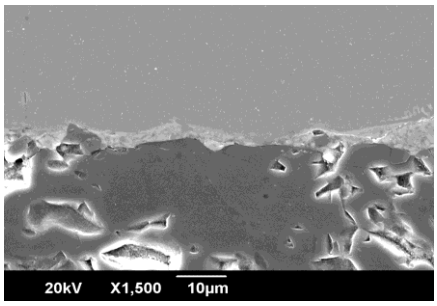

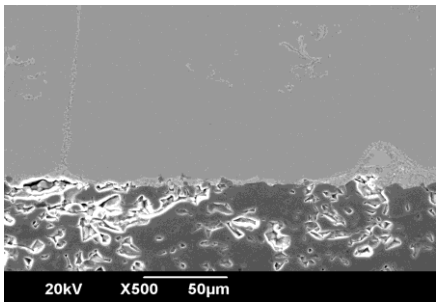

TiAl28.8Ni_Al_2O_3 (evolution of Al_2O_3 whiskers)

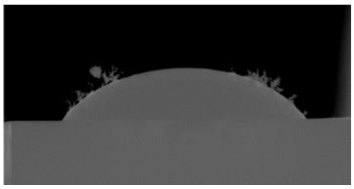

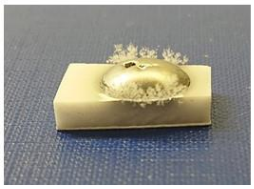

Ti50Al50_Al_2O_3